MODEL-BASED OPTIMISATION OF MIXED REFRIGERANT LNG PROCESSES

Mengyu Wang

A thesis submitted in fulfilment of
the requirements for the degree of

DOCTOR OF PHILOSOPHY

Faculty of Engineering and Information Technology
The University of Sydney, Australia
2017

DECLARATION

This is to certify that to the best of my knowledge, the content of this thesis is my own work. This thesis has not been submitted for any degree or other purposes.

I certify that the intellectual content of this thesis is the product of my own work and that all the assistance received in preparing this thesis and sources have been acknowledged.

This thesis contains materials published below:

Chapter 2 of this thesis contains material published in Wang et al.(2013), Wang et al. (2014), Wang et al. (2015), Wang et al.(2016).

Chapter 3 of this thesis contains material published in Wang et al.(2013), Wang et al. (2014).

Chapter 4 of this thesis contains material published in Wang et al. (2014).

Chapter 5 of this thesis contains material published in Wang et al.(2013).

Chapter 6 of this thesis contains material published in Wang et al. (2015), Wang et al.(2016).

The publications above have been published and are distributed throughout the thesis. As for the contributions, I designed the study, performed the whole modelling work, extracted and analysed the data, wrote the drafts of the MS, and I am also the leading author in these publications.

Publication details:

(1) WANG, M., KHALILPOUR, R. & ABBAS, A. 2014. Thermodynamic and economic optimization of LNG mixed refrigerant processes. *Energy Conversion and Management,* 88**,** 947-961.
(2) WANG, M., KHALILPOUR, R. & ABBAS, A. 2013. Operation optimization of propane precooled mixed refrigerant processes. *Journal of Natural Gas Science and Engineering,* 15**,** 93-105.
(3) WANG, M., KHALILPOUR, R. & ABBAS, A. 2015. Effect of feed natural gas conditions on the performance of mixed refrigerant LNG process. *In:* KRIST V. GERNAEY, J. K. H. & RAFIQUL, G. (eds.) *Computer Aided Chemical Engineering.* Elsevier.

(4) WANG, M. & ABBAS, A. 2016. Natural gas liquids (NGL) recovery in the liquefied natural gas production. *In:* ZDRAVKO, K. & MILOŠ, B. (eds.) *Computer Aided Chemical Engineering.* Elsevier.

Signature 

Name MENGYU WANG

ABSTRACT

Natural gas liquefaction processes are energy and cost intensive. Optimal design and operation of natural gas liquefaction processes have recently received increased attention. In addition, natural gas wellhead conditions vary over the life of a production well. These variations affect the performance, production and product quality of a liquefied natural gas (LNG) plant.

The thesis pursues the optimisation of mid-scale mixed refrigerant LNG cycles considering variations in upstream gas well conditions in order to maximise gas well life. It is primarily comprised of two sections: the design and operation optimisation, and the effect of upstream gas conditions on the process performance.

The optimisation problem was formulated with the objective to minimise energy consumption and cost owing to a trade-off between energy efficiency and capital cost. Propane precooled mixed refrigerant process is considered as the base model.

Design optimisation: Four different objective functions were selected for the thermodynamic and economic optimisation of the propane precooled mixed refrigerant and dual mixed refrigerant processes: (1) total shaft work, (2) total capital investment, (3) total annualised cost, and (4) total capital cost of both compressors and main cryogenic heat exchangers. The total capital investment is a function of two key variables: shaft work and overall heat transfer coefficient and area (*UA*) of main cryogenic heat exchangers. The LNG process optimisation therefore seeks a minimisation in process energy consumption simultaneously with the minimisation of total capital expenditure and operating expenditure. Objective function (1) results in a 45% reduction in shaft work for propane precooled mixed refrigerant process and 49% for dual mixed refrigerant process compared to their baseline values, but

infinitely high *UA* values of main cryogenic heat exchangers. Optimisation results show that objective function (4) is more effective than other objective functions for reducing both shaft work and *UA*. This leads to 15% reduction in specific shaft work for propane precooled mixed refrigerant process and 27% for dual mixed refrigerant process, while achieving lower *UA* values relative to those of the baseline. In addition, the objective functions (3) and (4) also show reasonable reductions in total shaft work at a finite increased *UA* value.

Operation optimisation: The optimisation of the operation of the propane precooled mixed refrigerant process and its split propane version was performed using four objective functions: (1) total shaft work, (2-3) two different exergy efficiency expressions, and (4) operating expenditure to identify process performance improvements. For propane precooled mixed refrigerant process, objective functions (3) results in the lowest specific shaft work 1469 MJ/tonne-LNG, followed by the objective function (4). For the split version, however, the lowest specific shaft work is found to be under objective function (1). These findings indicate that for operation optimisation of an installed LNG train, achieving the lowest specific shaft work together with the highest exergy efficiency is not possible with a fixed feed natural gas flow rate and a fixed *UA* value. In addition, the optimisation results of this work were then compared with numerous studies in the literature and were found to be impractical due to the dissimilar process conditions used, such as natural gas composition and pressure, pressure of the LNG product, and *UA* of main cryogenic heat exchangers.

The effect of upstream gas conditions: A simulation-based sensitivity analysis highlights the effects of feed natural gas conditions on performance of propane precooled mixed refrigerant process. The results are an indication of the sensitivity of the specific shaft work, and operating expenditure, towards the feed composition, flow rate, and pressure. For instance, as

LNG production decreases from its design capacity of 3 MTPA to 2.4 MTPA over time, the specific operating expenditure also increases from $128/tonne-LNG to $154/tonne-LNG.

A subsequent study was conducted focusing on the energy benefits of two configurations of integrating natural gas liquids recovery unit with propane precooled mixed refrigerant process under various gas and operating conditions. Simulation results show that specific shaft work is affected by the process configurations and feed conditions. An integrated natural gas liquids recovery unit within the natural gas liquefaction process brings about the highest energy efficient configuration, while a frontend natural gas liquids recovery unit contributes the least. Energy consumption in an integrated natural gas liquids recovery within the liquefaction unit shows an increase of 0.74% in energy consumption as the methane concentration of the feed gas decreases, however, a frontend natural gas liquids recovery unit only has a 0.18% decrease. Methane concentrations of greater than 95% in natural gas for both processes produce almost the same specific operating expenditure.

ACKNOWLEDGEMENTS

I would like to offer my most heartfelt thanks to several people who have been part of my PhD journey over the past recent years. This dissertation would not have been possible without their support.

First and foremost, I would like to express my sincere gratitude to my supervisor, A/Prof. Ali Abbas for his support, patience, motivation, and immense knowledge throughout my PhD studies. He offered me intellectual freedom in my research, supported me to attend conferences and engaged me in new ideas. I was able to benefit from his scientific insight in solving my research difficulties.

I would like to thank Dr. Rajab Khalilpour for his great support. I was fortunate to have the opportunity to work with him on publishing several papers. I learnt a lot from his ability to solve problems, his engineering knowledge, and his research curiosity. Without his passionate participation, it would have undoubtedly been much more difficult for me to accomplish.

I would like to thank my dear friend, Mouna Hamad for being the best friend ever and for giving me assistance in whatever way she could and at any time. I would to thank her for always believing in me and encouraging me and for the wonderful times we shared, especially the coffee breaks at university and the happy moments with baby Hussain.

I would like to thank our group members: Forough Parvareh, Aldric Tumilar, Huda Manaf, Alireza Shafiee, Manish Sharma, Abdul Qadir for providing a friendly atmosphere and assistance at work. And of course, my appreciation goes to the PhD students in our office, especially Mona Edrisi, and Young Hong. I would like to thank Track Changes for providing a high-quality and efficient proofreading service for this dissertation.

My sincere thanks go to the School of Chemical and Biomolecular Engineering at the University of Sydney. Thank you is not enough to let you know how much I appreciate your kindness, guidance and assistance throughout my candidature.

I would like to thank all my friends for sharing my happiness and sadness all the time. I will hold onto our happy memories forever in my heart.

Finally, I must express my very profound gratitude to my parents for all their support and encouragement throughout my life and throughout my candidature. They have always been by my side no matter what and always wiped away my tears and gave me a hug during painful and difficult moments. Thanks for being so supportive. Thanks for everything, mom and dad.

NOMENCLATURE GLOSSARY

Abbreviations

APCI	Air Products and Chemicals International
C1	Methane
C2	Ethane
C3	Propane
C4	Butane
CO_2	Carbon dioxide
CAPEX	Capital expenditure
C3MR	Propane precooled mixed refrigerant
C3MR-SP	Propane precooled mixed refrigerant with split propane
CF	Capacity factor
COP	Coefficient of performance
CWHE	Coil-wound heat exchanger
DMR	Dual mixed refrigerant
FLNG	Floating liquefied natural gas
GA	Genetic algorithm
HX	Heat exchanger
H_2S	Hydrogen sulfide
JT	Joule-Thomson
LMTD	Log mean temperature difference
LNG	Liquefied natural gas
LP	Linear programming
MCHE	Main cryogenic heat exchanger
MFC	Mixed-fluid cascade

MILP	Mixed-integer linear programming
MINLP	Mixed-integer nonlinear programming
MTA	Minimum temperature approach
MTPA	Million tonne per annum
NG	Natural gas
NGL	Natural gas liquids
NLP	Nonlinear programming
NMDS	Nelder-Mead downhill simplex
NPV	Net present value
N_2	Nitrogen
OF	Objective function
OPEX	Operating expenditure
PFHE	Plate-fin heat exchanger
PR	Peng-Robinson
PSP	Particle swarm paradigm
QLP	Quadratic lagrangian programming
SMR	Single mixed refrigerant
SQP	Sequential quadratic programming
SRK	Soave-Redlich-Kwong
SWHE	Spiral-wound heat exchanger
TCF	Trillion cubic feet
TS	Tabu search
VBA	Visual Basic for Applications
VBC	Visual Basic Code

Greek

α	Percentage of the equipment cost of an LNG value chain
β	Percentage of the component cost of an LNG plant over the total capital cost of an LNG plant
λ	Percentage of capital cost of an LNG plant over total capital cost of an LNG value chain
x	Mole fraction of mixed refrigerant
ε	Exergy efficiency
Δ	Difference

Roman

C	Equipment cost, $
E	Exergy
F	Flow rate, kg/h
e	Specific exergy
H	Enthalpy, J/mol
HPA	Hours per annum, h
h	Specific enthalpy, J/ mol^2
I	Exergy loss
m	Production capacity, tonne
P	Pressure, kPa
Q	Cooling duty, MW
R	Gas constant, 8.314 J/ (mol.K)
S	Entropy, J/K
s	Specific entropy, J/K/kg
T	Temperature, K or °C

TCI	Total capital investment, $
TAC	Total annualised cost
UA	Overall heat transfer coefficient and area of MCHE, MW/°C
W	Shaft work, MW
X	Plant capacity, MTPA

TABLE OF CONTENTS

LIST OF FIGURES

LIST OF TABLES

CHAPTER 1. THESIS INTRODUCTION

The thesis will firstly introduce the reader to the current standing of the natural gas market alongside a brief overview and existing trends in LNG technology. This chapter will then be followed by the thesis aims and a detailed outline of the subsequent chapters.

1.1 Background in brief

1.1.1 Natural gas market

Natural gas has become widely recognised in recent years as a clean and economical energy source, due to its low carbon intensity and relatively low price compared with other fossil fuels. Figure 1-1 below shows the share distribution of energy consumption from the BP Statistical Review of World Energy. Natural gas is the fastest emerging fuel in the market from 1965 up until today. It undergoes a gradual increase of 1.6% of total energy consumption per annum and is predicted to become the second-largest fuel source by 2035, accounting for one-quarter of total energy consumption (BP, 2017).

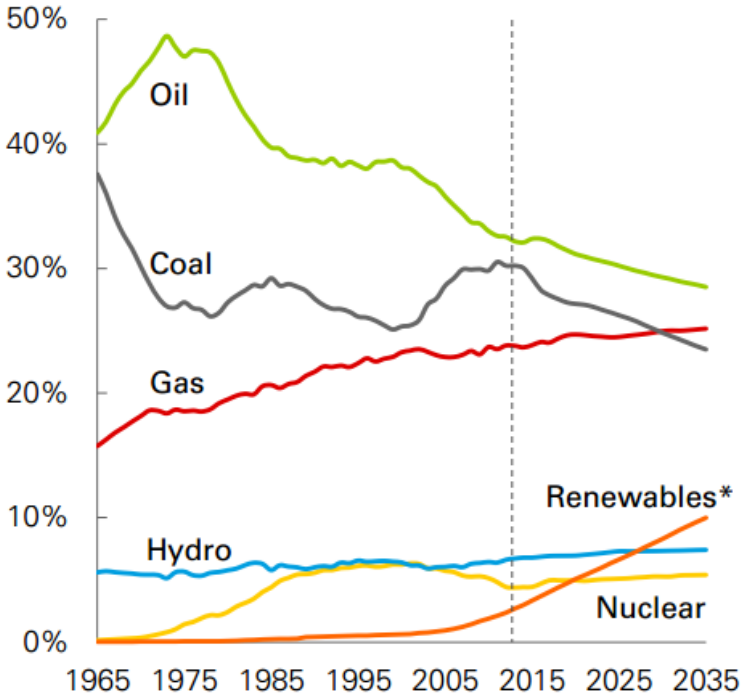

Figure 1-1 Energy consumption of natural gas from 1965 to 2035 (BP, 2017).

1.1.2 Overview of LNG value chain

LNG is a natural gas that has been converted to liquid form thereby reducing its volume to about 1/600th of its gaseous volume. It is the second feasible option for natural gas utilisation and monetisation after pipeline. This allows the natural gas to be more efficiently and economically stored and transported across long distances to market (Department of Resources, 2011).

An LNG value chain is composed of four independent segments: gas exploration, liquefaction, LNG transportation and regasification. The natural gas liquefaction process is the heart of the natural gas supply chain. This process constitutes a significant capital cost. The typical capital cost breakdown for an LNG plant ranges from 20% to 50% of the total LNG value chain (Avidan et al., 1997, Jensen et al., 2004, Hirschhausen et al., 2008, Humphrey, 2011). The capital cost of the liquefaction process accounts for around 30-45% of the total capital cost of an LNG plant. It is concurrently an energy intensive process. Due to these elevated capital and operating costs, the design and operation optimisation of LNG plants has received significant attention from both industry and research works, as reviewed in Chapter 2.

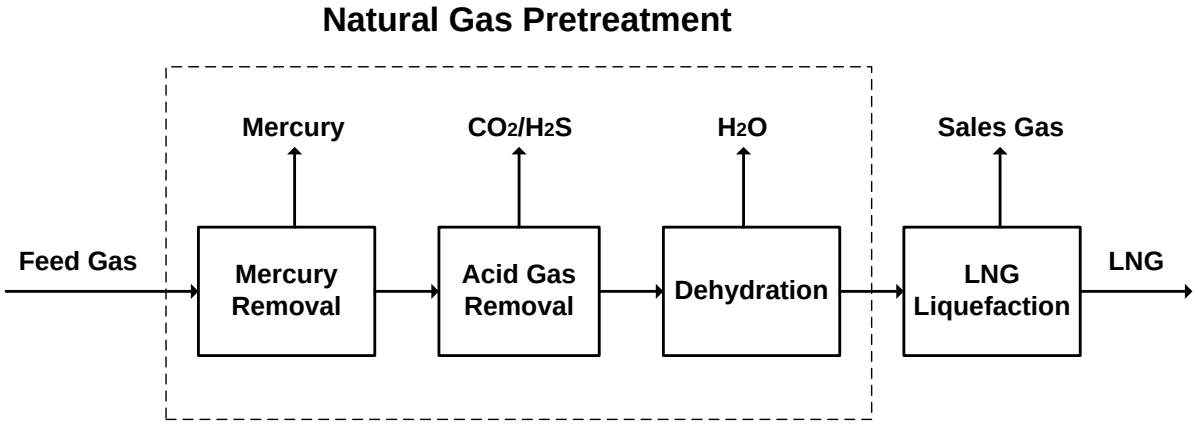

Figure 1-2 Flow diagram of an LNG process.

A typical LNG process consists of pretreatment and liquefaction processes, as shown in Figure 1-2. Raw natural gas is extracted from an upstream gas field predominantly consisting of methane with low concentrations of heavier hydrocarbons. It also contains nitrogen, carbon dioxide, and trace contaminants, such as water and hydrogen sulphide. However, these contaminants found in raw natural gas may freeze at lower temperatures, thus resulting in blockages of liquefaction equipment and pipelines (Klinkenbijl *et al*., 1999). Therefore, they must be removed to sufficiently lower levels prior to liquefaction in order to meet the specifications of LNG products (Finn *et al*., April 1999). The treated gas is liquefied in the liquefaction cycles and then distributed to the LNG receiving terminals by ship or trucks.

1.1.3 Trends in gas liquefaction technology

The first LNG plant started operation in Algeria and had a capacity of 1.2 MTPA. Since then, the proven technologies have evolved from small capacities of around one million tonne per annum (MTPA) in the 1970s to the current so-called "mega trains" with capacities above 7.8 MTPA (Wang *et al*., 2013). Figure 1-3 illustrates the historical development of LNG production technologies from 1965 to 2012. The details of these LNG plants are provided in Appendix A.

The main LNG technology providers are Black & Veatch, ConocoPhillips, Air Products and Chemicals Inc. (APCI), Shell, and Statoil/Linde (Lim *et al*., 2012). The current existing onshore liquefaction technologies include:

- ConocoPhillips Optimised Cascade®
- PRICO® Single Mixed Refrigerant (PRICO® SMR)
- APCI Propane Precooled Mixed Refrigerant (AP-C3MR™)
- Shell® Dual Mixed Refrigerant (DMR)

- Statoil/Linde Mixed-Fluid Cascade (MFC®)
- AP-X® LNG Process (Shukri, 2004, Venkatarathnam, 2010).

These technologies have been reviewed in more details in Chapter 2.

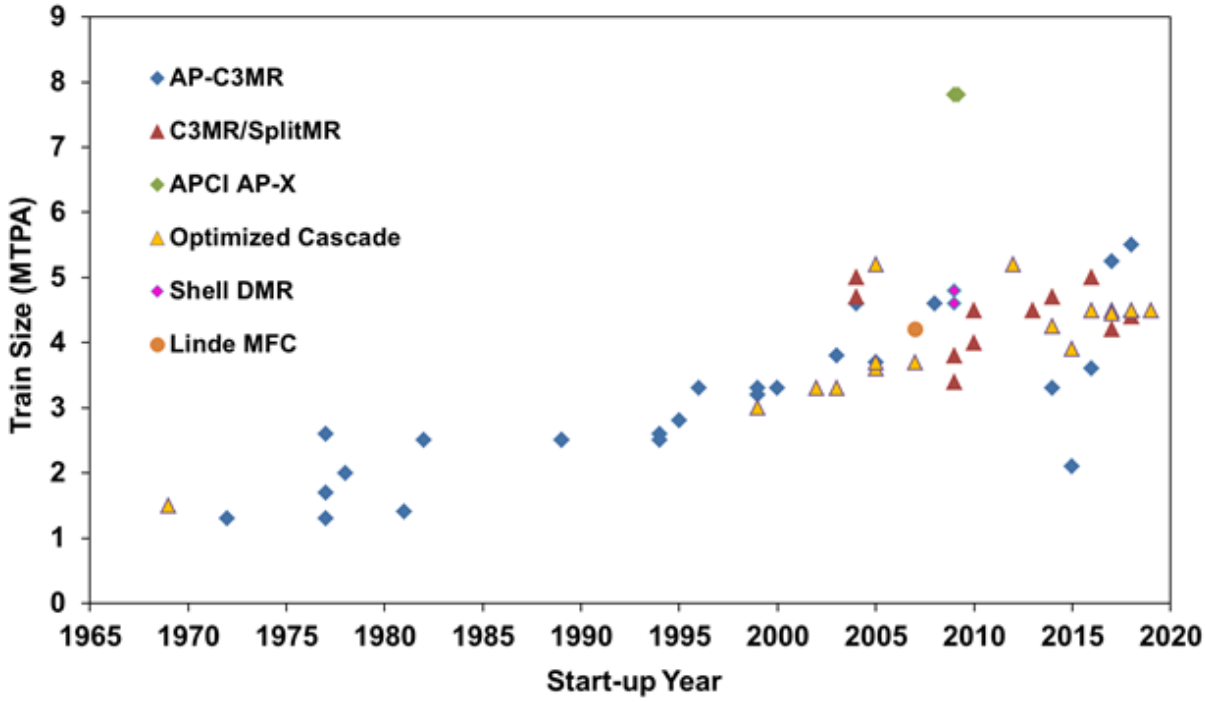

Figure 1-3 A general trend in LNG train size from year 1965 to 2015.

The LNG industry has primarily made significant effort on the development of the liquefaction technologies for various size of LNG plants over the past 50 years. The trend in LNG train size is expected to be toward larger plants. As the liquefaction train capacity increases, the LNG processes become more complex in terms of energy management and investment decision making. The current studies in the literature have been concerned on improving energy efficiency. However, the main challenges for LNG industry are associated with the lack of systematic and effective design and optimisation approaches to enhance the economic benefits of large plants.

1.2 Aims and objectives

The aim of this research is to maximise the energy efficiency of an LNG liquefaction process in order to minimise the associated plant costs. To achieve this aim, the following objectives were undertaken:

1) To develop an optimisation framework and present a techno-economic optimisation analysis considering design and operation;
2) To investigate the relationship between mixed refrigerant compositions and power consumption and uncover the optimal mixed refrigerant composition; and
3) To understand the effects of upstream upsets on energy consumption of LNG processes.

1.3 Thesis statement

1.3.1 Thesis structure

This thesis is divided into seven chapters.

Chapter 2 reviews the basic refrigeration and liquefaction technologies and the current literature standing on the optimisation of the LNG processes, alongside the effect of upstream gas well conditions on process performance.

Chapter 3 introduces the methodology of the modelling and optimisation of two-stage mixed refrigerant cycles, followed by a detailed description of the selected cycles. It also portrays in detail the general equations involved in calculating the required energy consumption, as well as exergy efficiency of individual equipment.

Chapter 4 summarises the key results for the design optimisation of C3MR and DMR processes. The economic functions were proposed as a function of two key variables: shaft work and overall heat transfer coefficient and area of main cryogenic heat exchanger

(MCHE). Sensitivity analysis for these functions are carried out to better understand the effect of varying the objective-function coefficient of variables on the optimal results

Chapter 5 recapitulates the key results for operation optimisation of C3MR and its split propane version (C3MR-SP). It presents four objective functions used for optimisation which includes shaft work, two exergy efficiency functions and OPEX. The optimal results are then compared with those of the literature.

Chapter 6 investigates the effects of variation in feed natural gas conditions on process performance of C3MR through a sensitivity analysis. It also discusses the benefits of integrating NGL with C3MR under such conditions.

Chapter 7 makes relevant conclusions and future recommendations in terms of steady-state optimisation and dynamic modelling studies for LNG plants.

Appendix A lists the global LNG plants in details, e.g. location, start-up year, and train capacity.

Appendix B presents the derivative of the economic objective function used in Chapter 4 and an example for the cost calculation.

1.3.2 Publications

This thesis contains four published papers listed in Table 1-1. These papers are distributed in Chapter 3-6.

Table 1-1 Contributions of this thesis.

Paper	Title and authors	Contributions
1	*Journal of Energy Conversion and Management* as: Thermodynamic and economic optimisation of LNG mixed refrigerant processes, WANG, M., KHALILPOUR, R. & ABBAS, A.	Chapter 3 Chapter 4
2	*Journal of Natural Gas Science and Engineering* as: Operation optimisation of propane precooled mixed refrigerant processes, WANG, M., KHALILPOUR, R. & ABBAS, A.	Chapter 3 Chapter 5
3	*Computer Aided Chemical Engineering* as: Effect of feed natural gas conditions on the performance of mixed refrigerant LNG process , WANG, M., ABBAS, A.	Chapter 6
4	*Computer Aided Chemical Engineering* as: Natural gas liquids (NGL) recovery in the liquefied natural gas production, WANG, M., ABBAS, A.	Chapter 6

CHAPTER 2. LITERATURE REVIEW

This chapter reviews the fundamental principles of the refrigeration cycle and key features of LNG liquefaction technologies, followed by a review of the literature in regards to the current research challenges.

2.1 Fundamental principles of the refrigeration cycle

Refrigeration cycles have been widely used in gas liquefaction processes. The most common refrigeration cycles for commercial use are Brayton refrigeration cycles and vapour compression cycles. The Brayton refrigeration cycle dominates the small- to medium-scale LNG trains and floating liquefied natural gas (FLNG) applications. Most of these cycles use the non-flammable working fluids which have low impact on FLNG vessel motions. The vapour compression cycle is suitable for medium- to large-scale LNG trains. The efficiency of this cycle is dependent on not only equipment design but also refrigerant candidate.

The vapour compression cycle is a cooling system that use a working fluid to transfer heat from a low temperature reservoir to a high temperature one (Çengel et al., 2011). It mainly consists of a compressor, a condenser, an expansion valve, and an evaporator. Its working principle is based on the second law of thermodynamics. The typical vapour compression cycle and its corresponding pressure-enthalpy diagram are shown in Figure 2-1 (Winnick, 1997, Narayanan, 2004). This cycle undergoes the following steps:

1) Compression (point 1 to 2) – When a saturated vapour enters the compressor, it is isentropically compressed to a high pressure and becomes a superheated vapour.
2) Condensation (point 2 to 3) – The superheat of the refrigerant vapour is removed through a condenser and condensed into a saturated liquid at constant pressure.

3) Expansion (point 3 to 4) – The high pressure of the saturated liquid is regulated through an expansion valve to form a partial vapour at low pressure, which is an isenthalpic process.

4) Evaporation (point 4 to 1) – The last step of the vapour compression refrigeration cycle is evaporation. The process starts with evaporation of the refrigerant in the evaporator at constant pressure. (Winnick, 1997, Narayanan, 2004).

The coefficient of performance (COP) is the ratio of heat supplied or removed from the reservoir (Q) to the power consumption (W) and is defined by Eq. 2-1. COP provides the measures of performance efficiency for refrigeration systems. This can be also used to monitor the system performance and identify the system faults (Çengel et al., 2011).

$$COP = \frac{Q}{W} \qquad \text{Eq. 2-1}$$

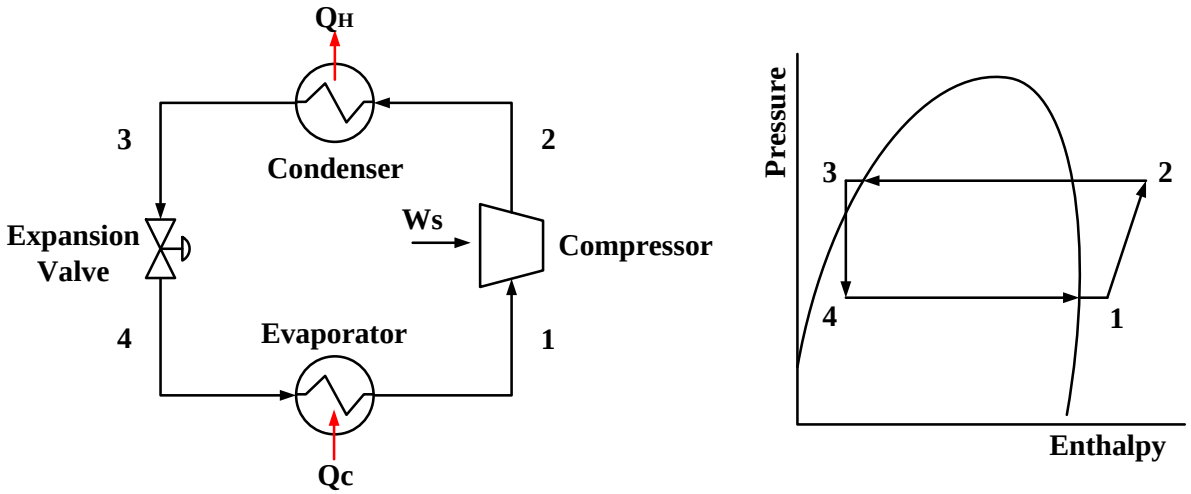

Figure 2-1 Vapour compression cycle (left) and its corresponding pressure-enthalpy diagram (right).

2.2 Technology review of natural gas liquefaction

There are a number of existing liquefaction technologies licensed that are available for various capacities of the LNG plants. Generally, they are classified into two groups depending on the type of refrigerants: pure refrigerant cycles and mixed-refrigerant cycles.

2.2.1 Pure refrigerant cycles

Pure refrigerant cycles use pure component refrigerants to achieve the desired temperature. Pure refrigerant has a constant evaporating temperature at various pressure levels. These cycles have been applied in classical cascade process and ConocoPhillips Optimised Cascade® process. Both processes are suitable for large train capacity.

2.2.1.1 Classical cascade process

The classical cascade process, developed by Phillip Petroleum Company, was applied in the first LNG plant with a capacity of 1.2 MTPA. This plant was built in Algeria and started operation in 1964. (Venkatarathnam, 2008).

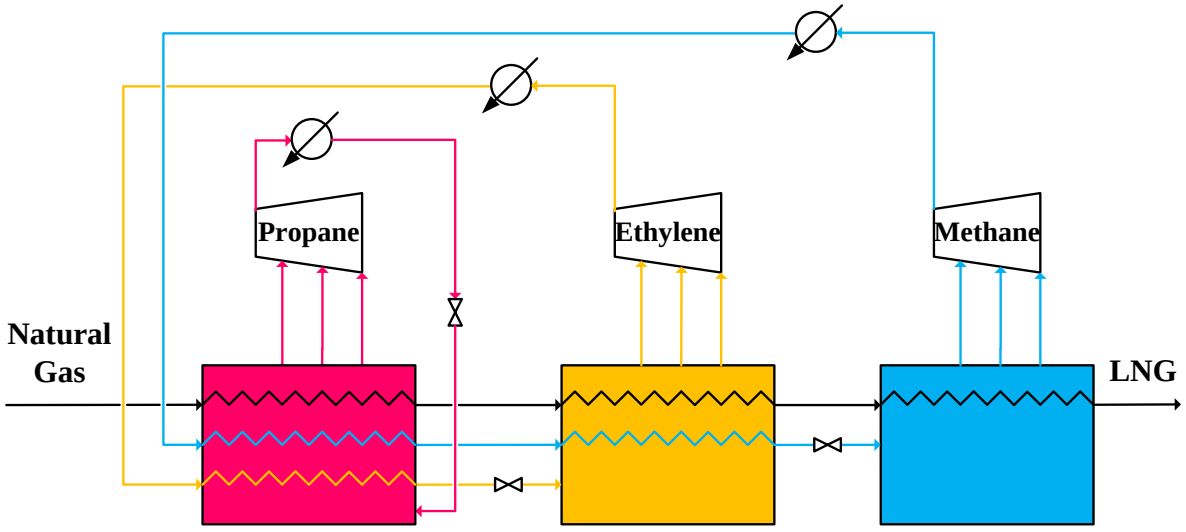

Figure 2-2 A simplified flowsheet of the classical cascade process.

The classical cascade process consists of three pure refrigerant cycles, as shown in Figure 2-2. Each refrigeration cycle operates at multiple pressure levels. Three pure component refrigerants are sequentially used in each cycle: propane, ethylene, and methane The treated feed gas is cooled to about -30 °C in a propane cycle followed by an ethylene cycle. The ethylene cycle cools the feed gas and methane to about -100 °C. at the high pressure. It is

finally liquefied in the methane cycle to achieve the desired temperature (Tusiani et al., 2007, Fountain, 2011). The propane cycle uses a plate-fin heat exchanger (PFHE) in each cycle.

The advantages of such processes are ease of operation and control. However, these processes have a complex system which requires a large amount of equipment, leading to elevated capital and operating costs.

2.2.1.2 Optimised cascade cycles

The ConocoPhillips Optimised Cascade® process is an advancement of the classical cascade process. This technology is owned and licenced by ConocoPhillips Company. It was first applied in the Kenai LNG plant in Alaska and started operation in 1969. Similar to the classical cascade cycle, the ConocoPhillips Optimised Cascade® process involves three steps in gas liquefaction. Nevertheless, several modifications have been made to this process in order to increase the operational efficiency, train capacity, and LNG production. One modification is the use of an open methane cycle instead of an original closed cycle. Another modification is the use of brazed aluminium heat exchangers, aeroderivative gas turbines, and waste heat recovery integration.

There are several advantages of the ConocoPhillips Optimised Cascade® process. Firstly, it is a proven technology with more than 45 years of operation. Secondly, it can operate flexibly under a broad range of operating conditions. Finally, it has high thermal efficiency and low emissions (Tusiani et al., 2007).

2.2.2 Mixed refrigerant cycles

The mixed refrigerant cycle uses a mixture of hydrocarbons (methane, ethane, ethylene and propane etc.) and nitrogen as refrigerant to provide the cooling duty for natural gas. Compared to the cascade cycle, the mixed refrigerant cycle has greater flexibility in operation

and requires lower energy consumption The energy efficiency of this cycles can be improved by optimising the mixed refrigerant composition to match the natural gas cooling curve as closely as possible (see Section 2.3.1) (Bronfenbrenner *et al*., 2009).

2.2.2.1 Single mixed refrigerant

The single mixed refrigerant (SMR) process was firstly licenced by Pritchard Companyand used in 1981 in Skikda, Algeria. This process has a single closed loop which use mixed refrigerant to liquefy natural gas over a broad temperature range. It is suitable for small-scale LNG plants with a capacity up to 1 MTPA. The advantages of using this process are simple design operational simplicity and low equipment count for offshore LNG plants (Mokhatab et al., 2012).

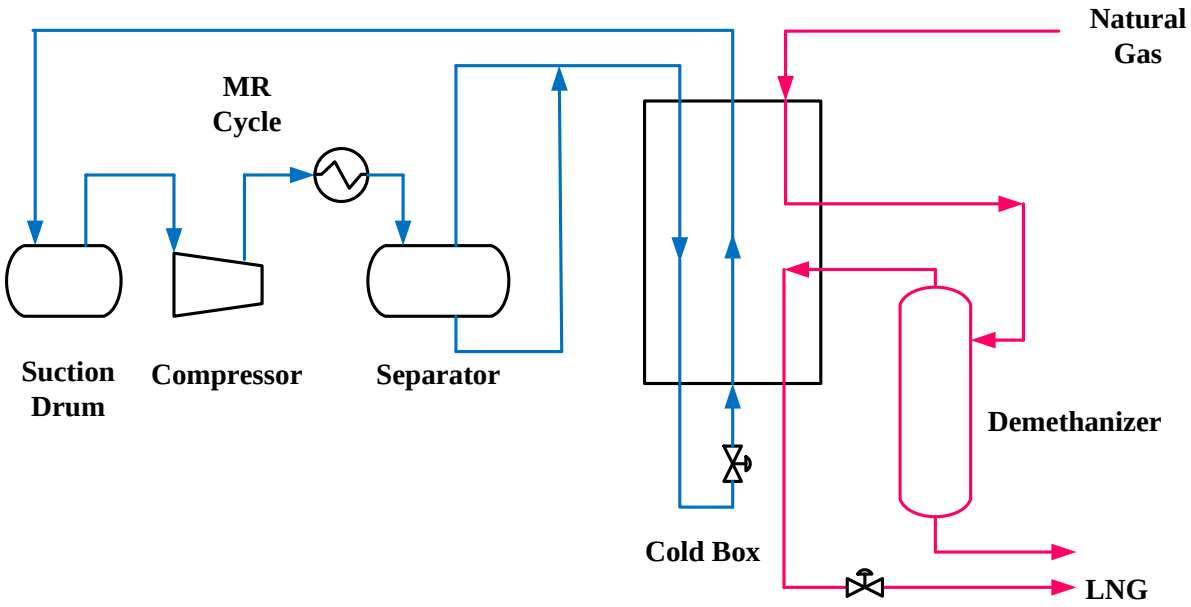

Figure 2-3 A simplified flowsheet of the SMR process.

Figure 2-3 shows a simplified flowsheet of the SMR process. A warm and low pressure mixed refrigerant steam enters the suction drum and is then compressed into two levels of evaporating pressures. After condensation in the aftercooler, the mixed refrigerant is partially vapourised. Both vapour and liquid are separated and flow into the spiral-wound heat

exchanger (SWHE) to provide the cooling for natural gas. If ethane and heavier hydrocarbons recovery from natural gas stream are required, then a demethaniser is used.

2.2.2.2 Propane precooled mixed refrigerant

The C3MR process is currently the most desirable process, amongst other liquefaction technologies, due to the fact that the majority of world's natural gas reserves have medium or small capacities (< 5 TCF). This technology accounts for more than three-quarter of the installed natural gas liquefaction plants (Barclay *et al*., 2005). For more details, refer to Figure 1-3.

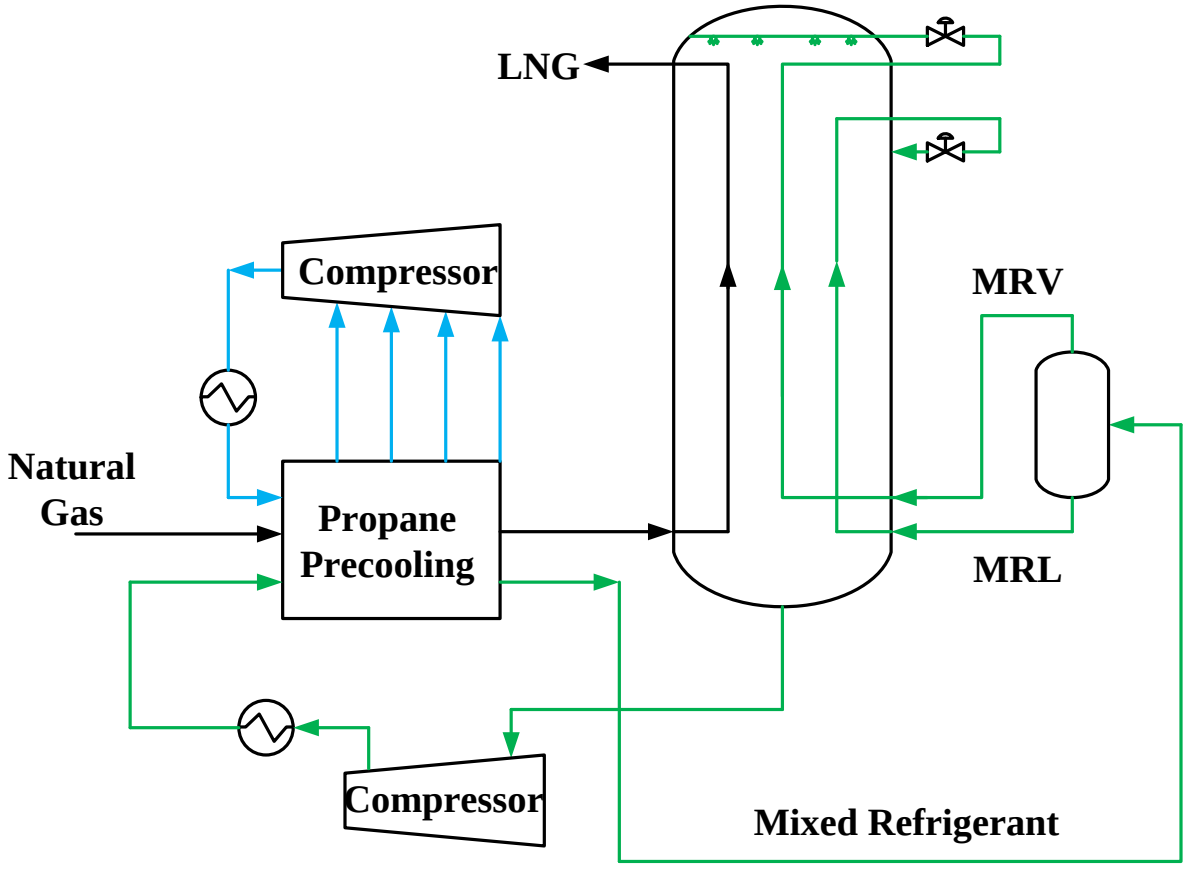

Figure 2-4 A simplified flowsheet of the C3MR process.

Figure 2-4 shows a simplified flowsheet of the C3MR process. It involves two refrigerant cycles: a propane precooling cycle and a mixed refrigerant cycle. The propane cycle precools natural gas at three or four different pressure levels and uses kettle-type heat exchangers.

These heat exchangers are suitable for pure refrigerant as they are more reliable and of lower energy consumption. Afterwards, the precooled gas is liquefied in a mixed refrigerant cycle using a coil-wound heat exchanger (CWHE) (Smaal, 2003, Bronfenbrenner *et al*., 2009).

The main advantage of the mixed refrigerant cycles is that this technology is safe and has not imposed any serious issues in terms of the start-up or the facilities' operation over the past 30 years. Furthermore, the C3MR process is a simple process with a reduced power requirement and high thermodynamic efficiency, leading to a commercial process. The limitation of the C3MR process is less flexibility in terms of shifting the refrigeration load between the propane and the mixed-refrigerant cooling cycles (Tariq et al., 2004).

2.2.2.3 Dual mixed refrigerant

Dual mixed refrigerant (DMR) is an alternative C3MR process which was licenced by Shell companies, APCI and Axens-IFP alliance. This technology encompasses two mixed refrigerant cycles. Both cycles are very flexible to use PFHEs or SWHEs. Figure 2-5 is a simplified flowsheet of the DMR process.

The major difference between C3MR and DMR processes is associated with the refrigerant in the precooling cycle. The mixture of hydrocarbons (propane and ethane) is used as the refrigerant in the precooling cycle of DMR processes. In some regions, there is a wide seasonal variation throughout the year. The fluctuation in ambient temperature affects the refrigeration requirement. By adjusting the composition of precooling refrigerant, DMR can provide a broader temperature range than propane precooling cycle. Therefore, the DMR is more preferable than the C3MR for cold climates. For instance, the refrigerant composition is preferable to have a higher concentration of propane in summer and ethane in winter.

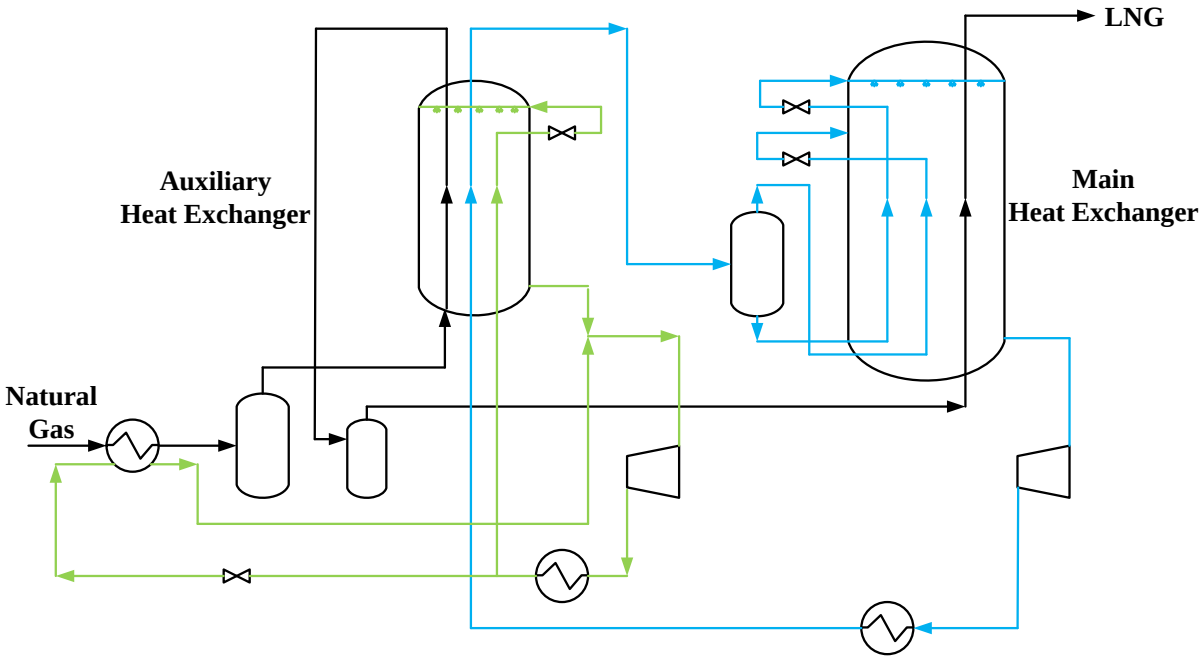

Figure 2-5 A simplified flowsheet of the DMR process.

2.2.2.4 Mixed-fluid cascade process

The mixed fluid cascade (MFC) process was developed by Linde and was constructed in the Snohvit LNG plant with a capacity of 4 MTPA. This process comprises three cooling cycles which are a precooling cycle, a subcooling cycle, and a liquefaction cycle. It is similar to the classic cascade process but utilises different mixed refrigerants in each cycle. PFHEs are used for precooling cycle and CWHE for subcooling and liquefaction cycles. The train capacity of this technology ranges from 3 to 12 MTPA. Figure 2-6 shows the simplified flowsheet of an MFC process.

The MFC process has more advantages than that of the cascade process. The major advantage of the MFC process is associated with higher energy efficiency and operational flexibility due to the use of mixed refrigerants. It also allows larger single compressor to handle refrigerant over a broader temperature range. However, this process requires numerous equipment and a hydrocarbon inventory.

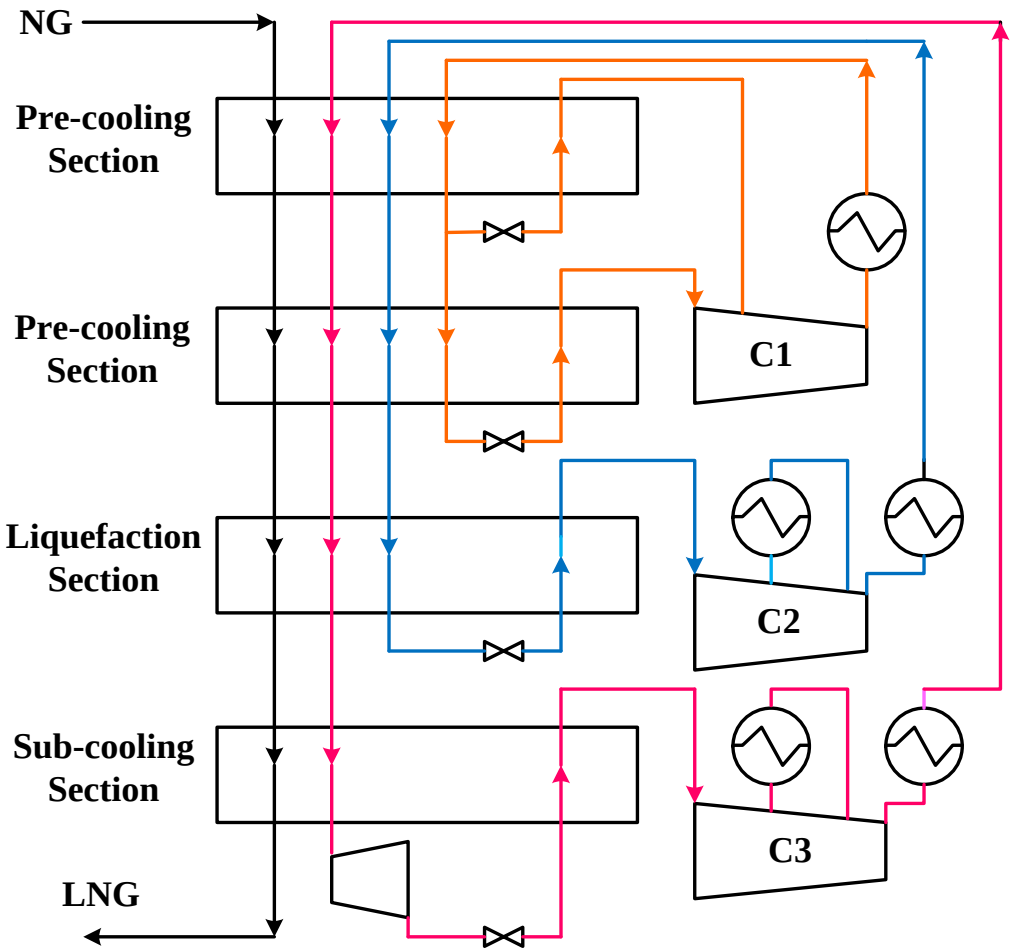

Figure 2-6 A simplified flowsheet of the MFC process.

2.2.2.5 AP-X® LNG Process

The AP-X® LNG process is an evolution of the C3MR technology which was developed by APCI in 2002. This technology involves three refrigeration cycles, which include a propane precooling cycle, a mixed refrigerant cycle and a nitrogen expander cycle. Natural gas is cooled to about -30 °C in the propane cycle and is further cooled to -120 °C in the mixed refrigerant cycle. The nitrogen expander cycle provides the subcooling duty for cooled natural gas. This design reduces the refrigeration loads on the propane and mixed refrigerant cycles, enabling an increased train capacity up to 8 MTPA (Susan et al., 2010). Figure 2-7 shows a simplified flowsheet of the AP-X® LNG process.

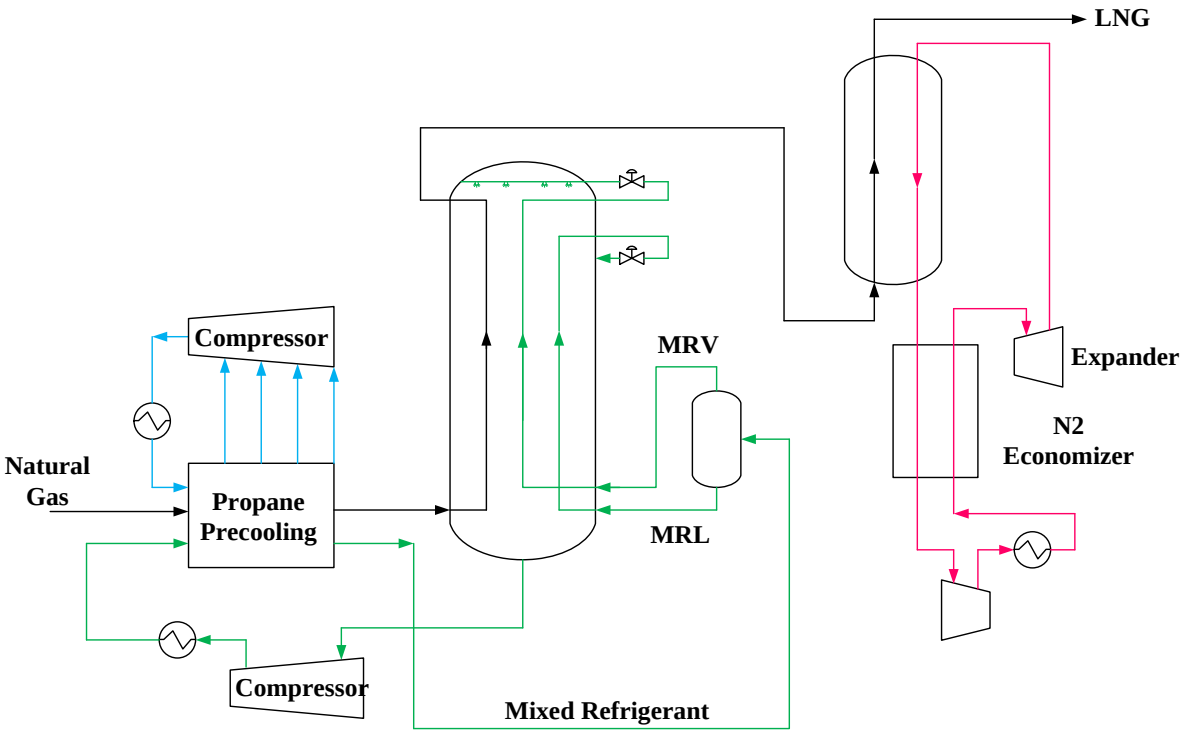

Figure 2-7 A simplified flowsheet of the AP-X® LNG process.

2.3 Thermodynamic analysis of an LNG process

Pinch and exergy analyses have been successfully used for reducing energy consumption of chemical processes.

2.3.1 Pinch analysis

Hot and cold composite curves are a graphical tool used to determine the minimum energy consumption of gas liquefaction processes by calculating feasible energy target. Hot composite curves illustrate the availability of process heat and cold composite curves represent the process heat required. These curves are a function of heat flow versus temperature (see Figure 2-8). The gap between the two curves indicates the thermodynamic inefficiency of liquefaction processes.

The closest approaching point between hot and cold composite curves relates to the minimum temperature difference (ΔT_{min}) in heat exchangers. It represents a trade-off between the energy savings and capital cost. A typical temperature-enthalpy diagram showing the hot and

cold composite curves for a pure refrigerant and a mixed component refrigerant are illustrated in Figure 2-9.

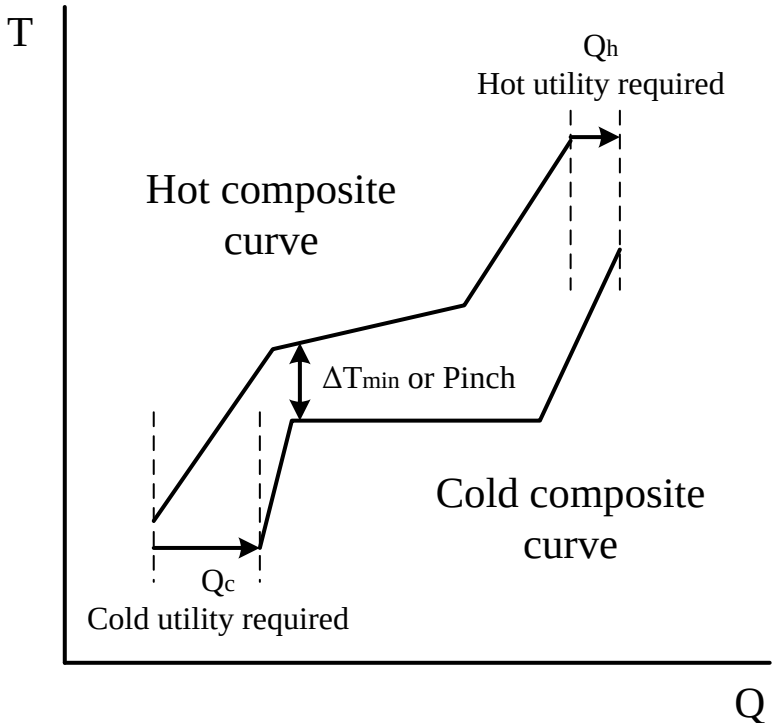

Figure 2-8 Typical hot and cold composite curves.

Mixed refrigerant evaporates over a broad range of temperatures owing to the various boiling points of the pure components; nevertheless, pure refrigerant has a constant evaporating point. The use of various refrigerant compositions potentially reduces the refrigerant mass flow and pressure. This leads to an improved emerging between the hot and cold composite curves than does pure refrigerant. Therefore, mixed refrigerant cycles are of lower energy demand and higher thermodynamic efficiency than cascade cycles for the same LNG production. They also allow economically-feasible size design of major equipment such as the cold box and compressors (Venkatarathnam, 2008, Mokhatab *et al*., 2013).

The issue with using mixed refrigerant is that its composition is very sensitive to the composition of the feed gas. The most favourable refrigerant composition can reduce thermodynamic irreversibility (Tusiani et al., 2007).

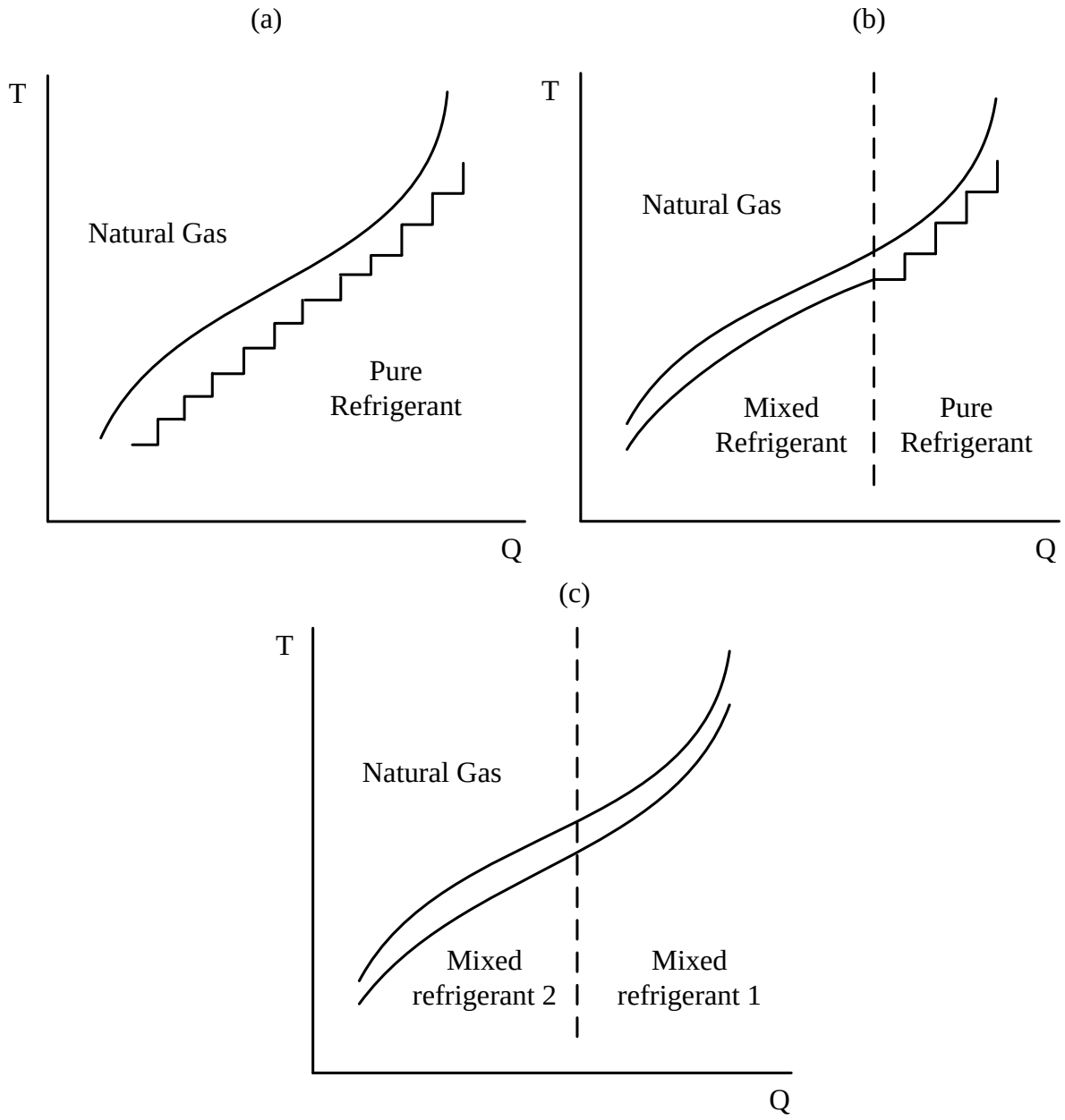

Figure 2-9 Typical hot and cold composite curves for (a) a cascade process (b) a C3MR process (c) a DMR process.

2.3.2 Energy and exergy analyses

According to the second law of thermodynamics, the shaft work and cooling duty cannot be completely converted into useful energy in practice. Exergy is useful for evaluating the utilities consumed in the system in order to reveal the potential for minimising energy consumption. It can be classified into physical exergy, kinetic exergy, potential exergy, and chemical exergy. The total exergy of a system is expressed as:

$$E_{total} = E_{phy} + E_{kinetic} + E_{potential} + E_{chem} \quad \text{Eq. 2-2}$$

where, E_{total} is total exergy, E_{phy} is physical exergy, $E_{kinetic}$ is kinetic exergy, $E_{potential}$ is potential exergy, E_{chem} is chemical exergy.

For gas liquefaction, kinetic exergy and potential exergy are not being considered. Chemical exergy is also neglected due to the absence of chemical reactions. The chemical composition of streams is assumed to remain constant (Çengel et al., 2011). Therefore, energy and materials are only denoted by the physical resources. Physical exergy represents the maximum amount of work obtained from the pressure and temperature of the surroundings to its dead state. According to Çengel et al. (2011), physical exergy of a stream at steady state can be expressed as shown in Eq. 2-3.

$$E_{phy} = (H - H_0) - T_0(S - S_0) \quad \text{Eq. 2-3}$$

where, H and S are enthalpy and entropy, H_0 and S_0 are enthalpy and entropy at the temperature T_0 and pressure P_0 of the environment, respectively.

The specific physical exergy of the stream on a mass basis can be expressed as:

$$e_{phy} = (h - h_0) - T_0(s - s_0) \quad \text{Eq. 2-4}$$

where, h and s denote the specific enthalpy and entropy, h_0 and s_0 are the specific enthalpy and entropy at the temperature T_0 and pressure P_0 of the environment.

Exergy balance is generally expressed equivalent to that of energy balance. Exergy balance equations for each section of the liquefaction system are defined in Eq. 2-5.

$$\sum Q\left(1-\frac{T_0}{T}\right)-W+\sum_{in} m_{in}e_{in}-\sum_{out} m_{out}e_{out}=E_D \qquad \text{Eq. 2-5}$$

where, E_D is the exergy loss, e_{in} is the physical exergy of an inlet stream, e_{out} is the physical exergy of an outlet stream.

2.4 Introduction to optimisation

Optimisation is a technique that solves the problem of minimising or maximising an objective function to find the most suitable solution for a chemical process. It is applicable to all engineering areas such as modelling, design and synthesis, process control and real-time optimisation of chemical processes.

2.4.1 Mathematical formulation of the optimisation problem

The optimisation problem can be formulated into mathematical form. It consists of objective functions, design variables, and constraints. Each optimisation problem has been handled using an objective function which is to be optimised. The general form of the optimisation problem is:

minimise $f(x)$

with respect to $x=(x,x,...,x_n)$

subject to $g_i(x)\le 0$ for $i=1,...,m$

$h_j(x)=0$ for $i=1,...,n$

where, $f(x)$ is the objective function, $g_i(x)$ is equality constraint function i, $h_j(x)$ is inequality constraint function j, x are the vector of m design variables, m and n are the number of inequality (g) and equality (h) constraints, respectively.

Objective function, $f(x)$, is a function of the design variables to be optimised. It is used to optimise design and operating variables of process systems in order to improve their performance, costs, and profitability.

Design variables, x, are the inputs to a model that can be manipulated and controlled. However, not all variables are equally important during the optimisation process; the optimisation results are sensitive to the selection of key design variables.

Constraints, $g_i(x)$ and $h_i(x)$, are additional functions to define the limit of any design variables and process parameters. As stated above, the constraints can represent an equality and/or inequality. The limit range of any variable affects the feasible area of the solution. In chemical processes, the equality constraints represent the material and energy balance and the inequality constraints represent the operating conditions.

2.4.2 Optimisation algorithms in process simulators

The optimisation problems are commonly found in engineering applications. According to the nature of the objective function, they are classified into

- Linear programming (LP)
- Mixed-integer linear programming (MILP)
- Nonlinear programming (NLP)
- Mixed-integer nonlinear programming (MINLP)

There are many well-known optimisation algorithms utilised to solve these optimisation problems. The main purpose of the optimisation study in this dissertation was related to the formulation of the objective function for the constrained optimisation problem. Thus, the optimisation algorithm used was selected from five available optimisation algorithms in the

optimisation tool-box in Aspen HYSYS®. This simulator is the common simulation tool used in current literatures. Five optimisation algorithms are available in the optimiser. The major difference amongst these optimiser algorithms are summarised in Table 2-1 (AspenTech, 2004).

Table 2-1 Five optimisation algorithms available in the Aspen HYSYS Optimiser.

Method	**Unconstrained**	**Constrained**		**Objective function**	
		Equality	**Inequality**	**Linear**	**Nonlinear**
Fletcher-Reeves	✓				
Quasi Newtown	✓				
BOX	✓		✓		✓
SQP	✓	✓	✓	✓	✓
Mixed	✓		✓		✓

BOX method is a sequential search technique which handles nonlinear objective function with inequality constraints. It is a robust method if the optimisation can converge with a large number of iterations.

Sequential quadratic programming (SQP) is the most efficient method for constrained optimisation problems. It is suitable for both linear and nonlinear objective functions.

Mixed method is a mixed scheme of BOX and SQP and has the advantages of both methods. It starts the minimisation with the BOX method using low tolerance and then uses SQP method to finalise the solution with the desired tolerance.

Fletcher-Reeves method is the Polak-Ribiere modification of the Fletcher-Reeves conjugate gradient scheme. It is efficient for unconstrained optimisation.

Quasi-Newtown method is similar to the Fletcher-Reeves method and refers to the Broyden-Fletcher-Goldfarb-Shanno (BFGS) method.

2.5 Current research challenges in LNG processes

Natural gas liquefaction processes are energy intensive. The main contribution to the energy consumption is the compressor power. Therefore, the majority of recent optimisation studies have focused on the minimisation of total shaft work of the liquefaction system. They have encompassed the different optimisation techniques, objective functions, and design variables. The selection of appropriate design variables, at any given condition, can maximise the overall performance of the liquefaction process.

2.5.1 Design and operation optimisation

There have been extensive studies conducted on improving the energy efficiency of the natural gas liquefaction processes. The studies which have provided optimisation of such processes will be subsequently reviewed. The optimisation formulation involves different techniques, objective functions, and selected variables. The first step in any optimisation task is to define the goal or technically the "objective function". Objective functions are the mathematical expression of design variables. The effects of these design variables on the overall performance are identified by thermodynamic analysis. Table 2-2 lists the objective functions formulated in various studies.

Lee *et al*. (2002) presented a synthesis method to optimise a PRICO process with an objective of shaft work reduction. Their method was a combination of NLP techniques and a thermodynamic approach. A variety of design variables were included: condensing and evaporating pressure levels, refrigerant flow rate, and refrigerant composition. Their proposed NLP techniques were to optimise the refrigerant composition at given refrigerant flow rate and pressures. New refrigerant flow rate and pressures were proposed based on heuristics, judgment, or optimisation.

Table 2-2 Objective functions found in literature.

Reference	Process	Objective function
Lee *et al*. (2002)	SMR	Minimise the single largest ΔT_{min} violation Minimise the sum of the overall ΔT_{min} violation Minimise the shaft work requirement
Vaidyaraman et al. (2002)	MRC	Minimise shaft work required
Shah et al. (2007)	SMR	Minimise CAPEX Maximise energy efficiency
Nogal *et al*. (2008)		Minimise the size of heat exchanger
Bauck Jensen et al. (2009)	SMR	Minimise operation cost Minimise shaft work required Maximise the production of LNG
Mokarizadeh Haghighi Shirazi et al. (2010)	SMR	Minimise shaft work required
Wang et al. (2011)	C3MR	Minimise shaft work required
Alabdulkarem *et al*. (2011)	C3MR	Minimise shaft work required
Khan *et al*. (2012)	SMR	Minimise shaft work required
Wang *et al*. (2012)	C3MR	Minimise shaft work required
Hatcher *et al*. (2012)	C3MR	Minimise shaft work required Minimise heat duty Minimise pressure differential and mixed refrigerant flow rate using sensitivity analysis Minimise pressure differential and mixed refrigerant flow rate Maximise the net present value (NPV) Minimise both heat duty and UA Minimise shaft work and UA Minimise heat duty, shaft work, and UA
Jacobsen et al. (2013)	SMR	Minimise the cost of compression work
Hwang *et al*. (2013)	DMR	Minimise shaft work required

Vaidyaraman et al. (2002) focused on the optimal synthesis of MFC cycles considering the design objective to reduce the total work required. They formulated an optimisation model as a non-convex NLP. The selected variables included mixed refrigerant composition,

temperature, pressure, vaporisation fraction, and compressor pressure ratios. However, only the temperature approach at the end of each refrigeration stage was constrained. This cannot guarantee no temperature cross in the heat exchangers. Shah et al. (2007) carried out a multi-objective optimisation study on an SMR process. The optimal parameters included the minimum-temperature-difference and compression ratio, and the number of refrigeration stages. The capital cost and the energy efficiency were optimised simultaneously as two different objective functions. Nogal *et al*. (2008) presented an optimal design methodology for an SMR cycle to reduce the compression work. They built a mathematical model based on a genetic algorithm (GA) to search for the optimal solution for the objective functions. They considered the capital cost in their objective function and selected the mixed refrigerant flow rate and composition, the inlet and outlet pressures of the compressor, and the intermediate temperatures between stages as design variables.

Aspelund *et al*. (2010) performed an optimisation study of PRICO process using a combination of Tabu Search (TS) and Nelder-Mead Dowhill Simplex (NMDS) method in Aspen HYSYS® and Microsoft® Visual Basic for Applications (VBA). They defined three objective functions for optimisation: fixed minimum temperature difference in cryogenic heat exchanger, fixed area of heat exchanger, and the effect of changing heat exchanger area on power consumption and cost. They employed a mixture of C1-C4 and N_2 as mixed refrigerant fluid and set each refrigerant component, refrigerant flow rate, suction, and condenser pressures as an optimisation variable. Wahl *et al*. (2013) conducted similar optimisation work to the case studies on the PRICO process in Aspelund *et al*. (2010) using NLP by quadratic lagrangian programming (NLP-QLP) for process simulation and optimisation. In comparison to the previous work of Aspelund *et al*. (2010), the NLP-QLP was more robust and efficient in solving the optimisation problems.

Shirazi et al. (2010) developed a GA based mathematical model using MATLAB for the optimisation of the liquefaction process in a peak shaving plant. They combined all chosen variables in the objective function of the shaft work. The set of variables were condensation, evaporation and intermediate pressures, flow rate and composition of mixed refrigerant. They found that the compressors and LNG heat exchangers made a significantly energy-saving improvement to the liquefaction process.

Alabdulkarem *et al*. (2011) carried out a simulation and optimisation study of the C3MR process with the application of the GA model in Aspen HYSYS and MATLAB programs. They ran four different pinch temperatures (0.01 K, 1.00 K, 3.00 K, and 5.00 K) in two stages of optimisation. The first stage was to optimise the mixed refrigerant cycle followed by optimisation of the propane cycle. Their results showed that a pinch temperature of 1 K brought out a significant improvement in power consumption.

Wang *et al*. (2012) performed the optimal design and operation of the mixed refrigerant system. They used a MINLP methodology with an objective function of power consumption. Although the complexity of optimisation was simplified by a thermodynamic function on the basis of rigorous simulation regression, it was still comparatively complex to find the optimal solution. Based on their optimisation results, their overall conclusion agreed with that of Hasan *et al*. (2009b) in that the high operational flexibility of heat exchangers depends on the processing capacity.

Hatcher *et al*. (2012) determined the most appropriate formulation of the C3MR process. They formulated four objective functions for operation optimisation and four objective functions for design optimisation. They used a mixed refrigerant flow rate, outlet pressures of expansion and compression, outlet temperatures of heat exchangers for natural gas stream as variables. Their results indicated that the most effective objective functions were: the

minimisation of shaft work for operation optimisation and minimisation of shaft work and *UA* for design optimisation.

Khan *et al.* (2012) optimised the SMR process with NLP along with an exergy efficiency analysis. The process efficiency was improved by using refrigerant composition and flow rate, suction and evaporation pressures, and refrigerant vaporisation as design variables. Khan et al. (2013a) applied the particle swarm paradigm (PSP) to optimise the SMR process. The objective function was to minimise the compression energy requirement using the same variables as Khan *et al*. (2012). Their results illustrated that the improvement of the gap between the composite curves resulted in a decreased energy requirement. The stochastic features of PSP are more beneficial in avoiding the local optima and in finding the more feasible solution.

Khan et al. (2013b) developed a knowledge-based algorithm for the optimisation of the SMR and C3MR processes. They used a function of maximum heat exchanger exergy efficiency as the optimisation objective. It was found that the flow fractions of propane and ethane have a noticeable impact on the performance of the SMR and C3MR processes respectively.

Hwang *et al*. (2013) studied the operation optimisation of the DMR process. They used a hybrid optimisation method of the GA and SQP for the minimisation of the power consumption. The design variables for the optimisation were refrigerant flow rate, mole fraction of refrigerant, suction and evaporation pressures, temperature, and flow rate ratio of the tee.

Several other optimisation studies exist which have not presented their objective functions. Paradowski *et al*. (2004) addressed a parametric study on the C3MR process where they studied the influence of selected variables on the increasing LNG train capacity of the

propane precooling cycle. They used mixed refrigerant composition, mixed refrigerant vaporisation pressure, propane precooling temperature, propane compressor speed, and outlet temperature of MCHE as variables. They concluded that the increase in train capacity of the C3MR process could potentially be achieved by rearranging the propane compressors.

Remeljej et al. (2006) performed exergy analyses for four different liquefaction processes including: a single-stage mixed refrigerant, a two-stage expander nitrogen refrigerant, and two open-loop expander processes. Their specific shaft work and energy efficiency were compared.

Hasan *et al*. (2009a) performed an operation optimisation of compressors in two refrigeration cycles of the C3MR process in aim of reducing the energy consumption. They presented a mathematical model for the compressor optimisation in a propane precooling cycle. The suction pressure of the refrigerant compressors was the main design variable considered in their study.

Jensen et al. (2007a), Jensen et al. (2007b), and Jacobsen and Skogestad (2013) worked on an operation optimisation of the SMR cycle. They focused primarily on determining the degree of freedom, the disturbances, as well as the selection of the control variables, rather than focusing solely on optimisation studies and thermodynamic analysis.

Aspelund *et al*. (2010) developed a non-deterministic search technique for the optimisation of the PRICO cycle. They used three different formulations for optimisation: (i) fixed minimum temperature difference in a cryogenic heat exchanger, (ii) fixed area of heat exchanger, and (iii) the effect of changing heat exchanger area on power consumption and cost. They combined a TS with the NMDS method to find the optimal solution. The optimisation

variables included refrigerant flow, composition, the compressor suction pressure, and the condenser pressure.

2.5.2 Economic analysis of the LNG process

LNG plants are capital intensive. Liquefaction processes involve relatively high capital costs of equipment required (MCHE, massive compressors, and other cryogenic equipment) and high operating cost of energy consumed. However, few studies have developed the objective functions associating with both CAPEX and OPEX.

The main objective of an economic optimisation is to minimise cost, including OPEX and CAPEX. It is well known that there is a trade-off between the OPEX and CAPEX. The OPEX is primarily dependent on the power consumption. The power consumption of the compressors can be reduced by using larger sized heat exchangers or additional cooling cycles. However, this increases the complexity of the process resulting in higher capital costs.

An earlier study by Barnés et al. (1974) attempted to minimise the cost of pure refrigeration and gas liquefaction systems. They employed a dynamic programming method with heuristics to identify the process configuration using minimal equipment and operating costs. This method was capable of handling the detailed equipment cost correlations and thermodynamic properties. However, it had a limitation in determining the number of stages and their operating temperature ranges. Later on, Cheng et al. (1980) developed an interactive synthesis of a cascade refrigeration system. They incorporated all the refrigeration features and the cost functions identified by Barnés and King (1974). Vaidyaraman et al. (1999) suggested a systematic methodology to design the refrigeration system and to select pure refrigerants for each refrigeration cycle simultaneously. They used MILP to minimise a weighted sum of investment and operating costs.

Numerous studies have dealt with a simple economic objective function to optimise either CAPEX or OPEX. Nogal *et al*. (2008) developed a GA-based model for the optimal design of an SMR cycle in order to reduce the compression work. They built a mathematical model based on GA to determine the optimal solution for the objective functions. They considered the capital cost in their objective function and selected the mixed refrigerant flow rate and composition, the inlet and outlet pressures of the compressor, and intermediate temperature between stages as design variables. Jensen et al. (2008) proposed a simple *TAC* equation as the cost function. They only considered the capital cost of heat exchangers, while the capital cost of compressors was included in the operating cost of the shaft work.

Castillo et al. (2012) presented a decision-making approach based on a game theory. This approach addresses multiple levels and multi-objective problems simultaneously. An SMR process was used as an example to examine the robustness and practicality of this approach via a binary GA. They focused on cost optimisation while simultaneously considering the market cost, power consumption and heat transfer area.

Shah et al. (2007) and Shah *et al*. (2009) addressed a multi-objective optimisation study on an SMR process. An approach was proposed to solve the multi-objective optimisation for a mixed refrigerant process. The objective functions considered were the CAPEX and the energy efficiency. The optimisation variables included the minimum temperature difference and pressure ratio, and the number of refrigeration stages. Jensen et al. (2009a) used total annualised cost as an objective function. Jensen et al. (2006), and Jensen et al. (2009b) implemented the optimal operation of a mixed refrigerant process to optimise OPEX.

In our previous works, Hatcher *et al*. (2012) introduced the basic NPV function so as to maximise the profit of design and operation. However, it is favoured where the area of MCHE can be infinitely large.

The energy efficiency is dependent on the size of heat exchangers, and refrigerant composition. The key factor to affect the energy consumption is associated with a *UA* value of MCHE. Aspelund *et al*. (2010), Alabdulkarem *et al*. (2011), and Castillo et al. (2013a) concluded in their studies that *UA* is a function of varying refrigerant flows and log mean temperature difference (LMTD). An increase in refrigerant flow resulted in the elevation of both power consumption and *UA* and also contributes to the overall capital cost. However, there is a trade-off between capital cost and operational cost. A few studies revealed their power consumption with the *UA* value of MCHE. Aspelund *et al*. (2010) concluded that the higher the *UA* value, the more improved the thermal performance of the heat exchangers for the same LNG production. *UA* is a function of varying refrigerant flows and LMTD. An increase in refrigerant flow results in elevation of both power consumption and *UA* (Aspelund et al., 2010, Alabdulkarem et al., 2011, Castillo et al., 2013a, Wang et al., 2013, Wahl et al., 2013, Hatcher et al., 2012).

Another key factor is the mixed refrigerant composition. Mixed refrigerant consists of a mixture of hydrocarbons and nitrogen. The appropriate selection of refrigerant composition, at any given condition, can maximise the overall performance of the liquefaction process. However, the importance of mixed refrigerant composition on the overall process performance of the liquefaction process has been addressed in a limited number of studies.

Lee *et al*. (2002) determined a method for the selection of the refrigerant composition via a combination of NLP and thermodynamic approach. The refrigerant composition in their study was C1-C4 and N_2. They revealed that the optimal refrigerant composition can reduce the efficiency of the refrigeration system, however, these variables are unable to be optimised simultaneously.

Nogal *et al*. (2008) and Aspelund *et al*. (2010) also used a mixture of C1-C4 and N_2 as mixed refrigerant fluid and set each refrigerant component as an optimisation variable. The variable refrigerant composition from Alabdulkarem *et al*. (2011) and Khan *et al*. (2012) were C1-C3 and N_2. These studies established the optimal refrigerant composition that significantly reduces the total power consumption.

2.5.3 Upstream gas well conditions

The natural gas well conditions vary over the life of a production well. The variations in the upstream gas conditions (feed compositions, pressure and temperature) influence process performance, production and product quality over time (Mokhatab et al., 2012). For the most natural gas wellhead, raw natural gas primarily contains methane but may also contains small amounts of heavier hydrocarbons, and other contaminants such as water, acidic gases (CO_2 and H_2S), and/or mercury. Many licensed technologies can be independently selected to remove these contaminants prior to liquefaction in order to avoid blockages and damage to the process equipment and to also meet pipeline specifications (Kidnay et al., 2006).

Castillo et al. (2013b) evaluated the performance of different LNG precooling cycles in cold and warm climates. Their results showed that a three-stage propane precooled mixed refrigerant cycle is more suitable for warmer climates, while a two-stage mixed refrigerant cycle is the most efficient technology for colder climates. Clementino *et al*. (2014) studied the sensitivity analysis of C3MR process in aim of determining the specific shaft work required at various temperatures and pressures of the feed natural gas.

In addition, hydrocarbons heavier than methane may be required to recover as NGLs. The NGL recovery system has the ability to lower the heating value of the LNG product and to minimise the impact of the gas composition variation on process operation over time. Getu *et al*. (2013) compared the economic performances of several NGL recovery schemes under a

range of feed compositions known as lean and rich feeds. Khan *et al*. (2014) determined the benefits of three proposed integrated schemes of NGL recovery with natural gas liquefaction. Park *et al*. (2014) evaluated a proposed configuration of the NGL recovery process and nine patented schemes for offshore applications.

2.6 Literature conclusions

The optimal design and operation of natural gas liquefaction processes has gained increasing interest in recent years. A major gap still exists in the literature in terms of the optimisation problem formulation.

- The majority of recent studies have been concerned about reducing the power consumption of compressors in terms of design and operation via minimising the temperature difference of the MCHE. This brings about an increase in heat exchange area which constitutes the highest proportion of the capital cost. Therefore, the size of the heat exchangers is the key design variable to be considered in the optimisation study of minimising both capital cost and operation cost. Only a limited number of studies have assigned both capital cost and size of heat exchangers to the objective functions.
- For operation optimisation, the majority of studies have used total shaft work as the objective function (Table 2-2). Not many studies have included exergy efficiency and OPEX as objective functions to identify the performance improvement. In some works, optimal results were compared with previous studies but key factors affecting the power consumption were overlooked.
- Few studies have addressed the impact of variations in feed natural gas composition and flow rate on the process performance of mixed refrigerant processes. Beside optimisation, an integration of NGL recovery and LNG liquefaction has been

introduced to offer maximum economic benefits. There are various patented configurations and methods for extracting the NGL from a natural gas stream. Nevertheless, in the open literature little attention has been given to the benefits of these process integration configurations under different feed conditions and operating conditions.

CHAPTER 3. METHODOLOGY AND MODELLING FRAMEWORK

This chapter illustrates the methodology employed throughout the research work, including process simulation, optimisation framework, performance analysis, and sensitivity analysis.

3.1 Introduction

The C3MR model was considered a primary model of the entire study. C3MR-SP and DMR, which are modified C3MR processes, were also simulated in Aspen HYSYS. The proposed methodology for the improvement of the process performance was outlined in Figure 3-1. The first section of this study involved the formulation of the optimisation problems combined with an economic model for design and operation. This was consequently followed by a sensitivity analysis conducted on the effect of the variations of upstream gas conditions on the process performance of C3MR.

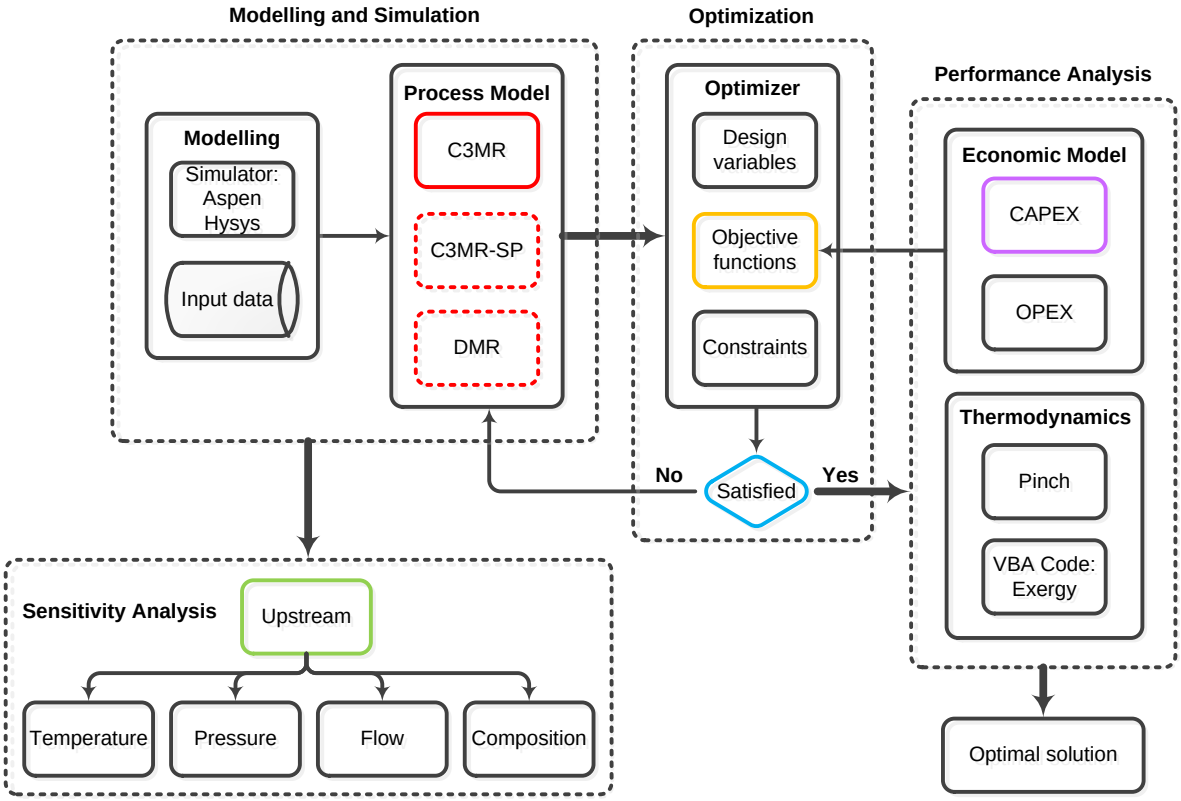

Figure 3-1 An overview of the proposed methodology.

3.2 Modelling basis and assumptions

3.2.1 Process modelling tool

Aspen HYSYS® is the most popular process simulator used for modelling oil and gas processes. This software was first developed by Hyprotech and commercialised in 1996. It is used for both steady state and dynamic simulation, process design, and optimisation. It can be also used for economics analyses and environmental evaluations.

In this study, Aspen HYSYS® V.8.8 is used to perform the process simulation and optimisation of the selected LNG processes. The main-flowsheet of the C3MR model consists of three sub-flowsheets which are: precooling, compression, and liquefaction. These sub-flowsheets have the same basis as the main-flowsheet. The details for modelling the unit operations within the sub-flowsheets are illustrated in Section 3.4.

The fluid package used is Peng-Robinson (PR) equation of state (EOS). This is an adequate thermodynamic package for simulation of hydrocarbon systems. The PR package solves for the physical properties of hydrocarbon systems with phase change over a broad range of conditions.

The Aspen HYSYS® flowsheet is customised with Visual Basic (VB) code for calculating the physical exergy of material streams built in the flowsheets. The exergy values of the material streams are derived from the VB code and are then obtained via User Properties tab of the Simulation Basis Manager of Aspen HYSYS. These values are exported into Spreadsheet and subsequently used for the calculation of the exergy loss and exergy efficiency within the HYSYS environment.

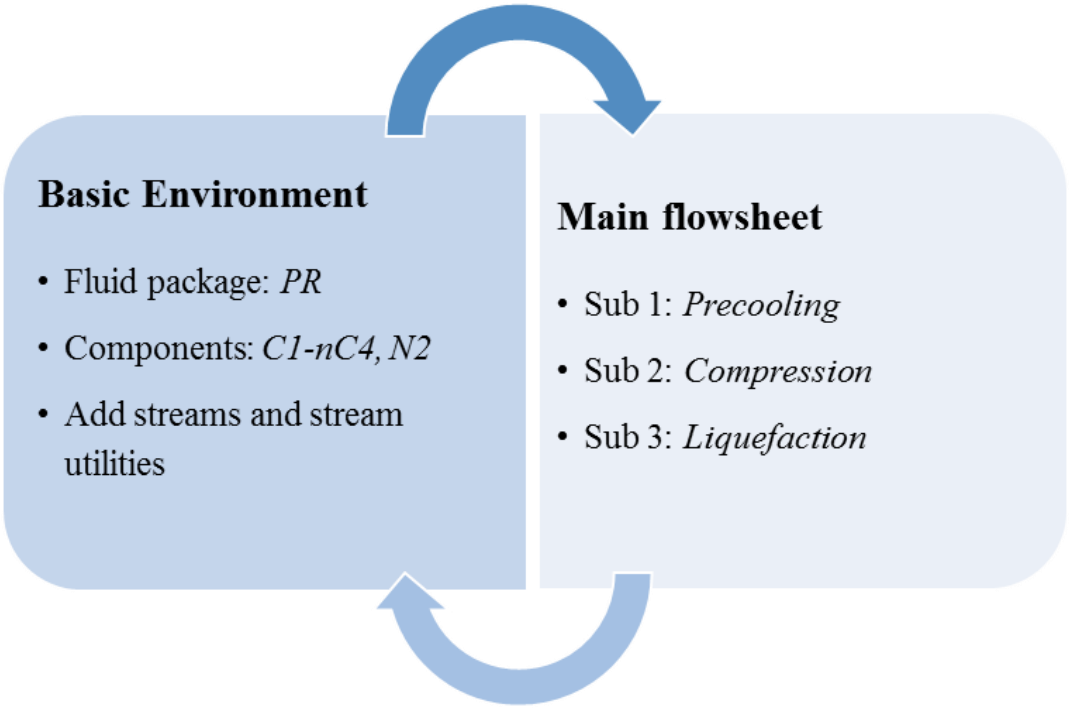

Figure 3-2 The simulation environment of the selected processes in Aspen HYSYS.

3.2.2 Assumptions

C3MR, C3MR-SP and DMR processes were simulated under equivalent conditions. The latter included feed gas conditions and several other specifications listed below:

1) The feed natural gas was assumed to be a dry sweet gas prior to processing and treatment, i.e. the contaminants (including acid gas, water, mercury, and heavier hydrocarbons) have been removed. Table 3-1 lists the feed natural gas composition used throughout this study.

Table 3-1 Feed natural gas composition.

Components	Mole fraction (%)
Methane	96.92
Ethane	2.94
Propane	0.06
n-butane	0.01
Nitrogen	0.07

2) Natural gas enters the liquefaction process at a temperature of 25 ºC and a pressure of 5000 kPa.
3) The plant produces 3 MTPA of LNG at a temperature of -161.3 °C and a pressure of 101.3 kPa.
4) The ambient temperature is 25 °C at 101.3 kPa.
5) All processes operate at steady state. The potential and kinetic energy effects of steady flow are negligible.
6) The throttle valve and compressors were considered adiabatic. The adiabatic efficiency of all compressors is assumed to be 75%.
7) Water coolers are used to provide the cooling of the system.

For operating cost:

8) The price of the pre-treated feed natural gas is $2/MMBtu.
9) The price of the electricity is $10.99/GJ (Turton *et al*., 2009).
10) The price of the cooling water is $0.40/GJ (Turton *et al*., 2009).

3.3 Process description

3.3.1 Process 1: The C3MR process

The C3MR process consists of two refrigeration cycles: the propane precooling cycle and the mixed refrigerant subcooling cycle. Figure 3-3 is the flow diagram of the C3MR process. Natural gas is cooled to -35 °C in the propane cycle, and then subcooled and liquefied in the mixed refrigerant cycle. Finally, the liquefied gas is reduced in pressure through the end flash unit.

In the propane precooling cycle, the liquid propane refrigerant is expanded to lower pressure through Joule-Thomson (J-T) valves and is completely vaporised to precool both natural gas

and mixed refrigerant streams. The propane vapour is compressed to a high pressure. It is then fully condensed into liquid phase before being recycled back to the heat exchangers.

In the mixed refrigerant cycle, the high pressure mixed refrigerant is partially cooled in the precooling cycle. The precooled mixed refrigerant flow is then separated into gaseous and liquid streams. Both MR liquid and MR vapour enter the MCHE to provide the cooling for the natural gas. The vapourised mixed refrigerant, exits the MCHE, is then compressed by a series of compressors to its initial inlet conditions.

3.3.2 Process 2: The C3MR-SP process

Figure 3-4 is the flow diagram of the C3MR-SP process which is a modification of the C3MR process. The extra equipment are added to the propane precooling cycle of the C3MR process. The latter include the compressors of C-204 and C-205, the heat exchangers of HX-207 and HX-208, the splitters of T-205 and T-206, and the valves of V-207 and V-208.

3.3.3 Process 3: The DMR process

DMR process is an alternative for the C3MR process. They differ mainly in their precooling cycles that the C3MR uses pure propane as a refrigerant, while the DMR uses a mixture of hydrocarbons. In addition, the precooling cycle of DMR process has less equipment than the C3MR (such as, mixed refrigerant compressors, mixed refrigerant heat exchangers, and valves). Figure 3-5 represents the flow diagrams of the DMR process.

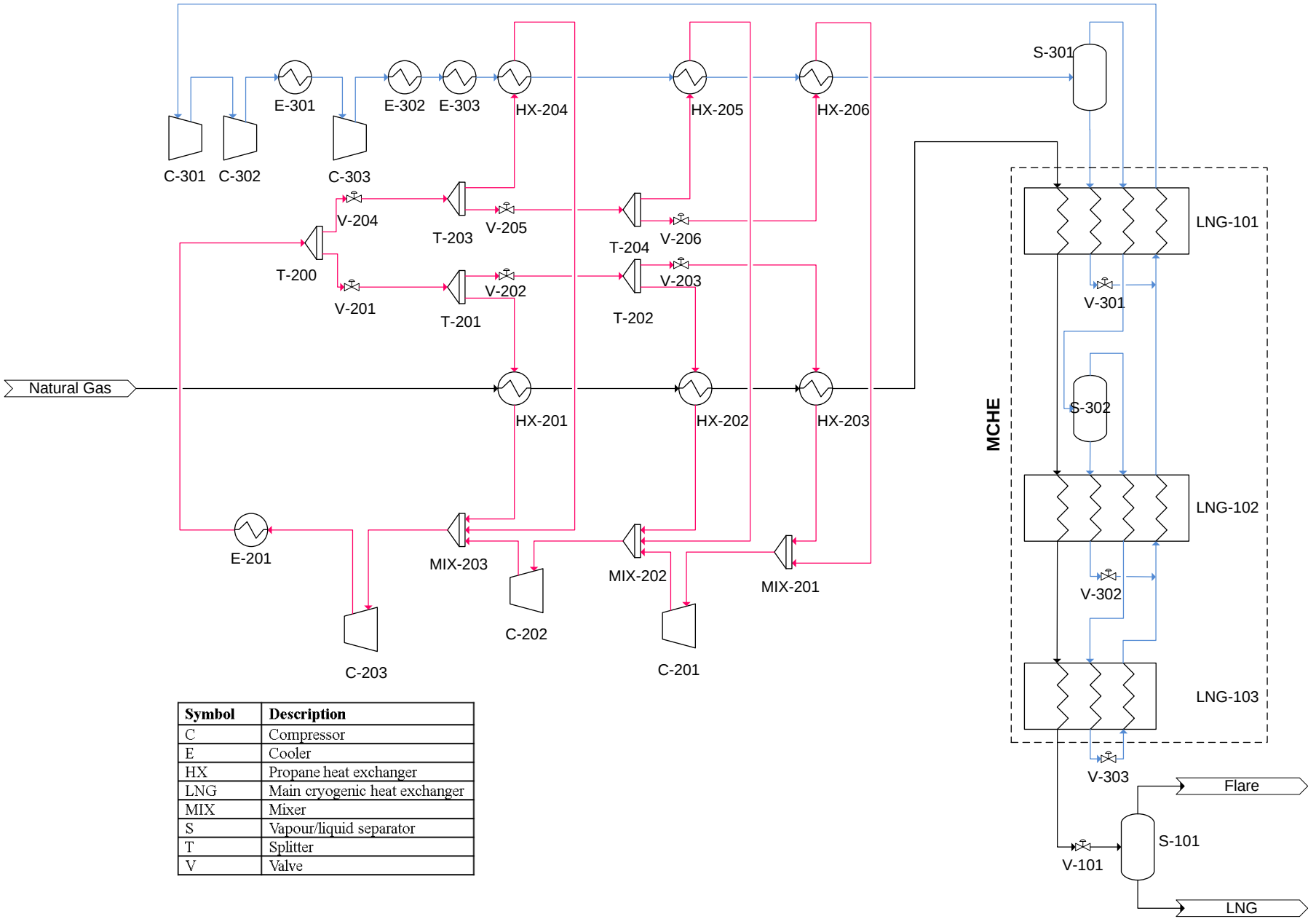

Symbol	Description
C	Compressor
E	Cooler
HX	Propane heat exchanger
LNG	Main cryogenic heat exchanger
MIX	Mixer
S	Vapour/liquid separator
T	Splitter
V	Valve

Figure 3-3 The flow diagram of the C3MR process (red lines represent propane precooling cycle and blue lines mixed refrigerant subcooling cycle).

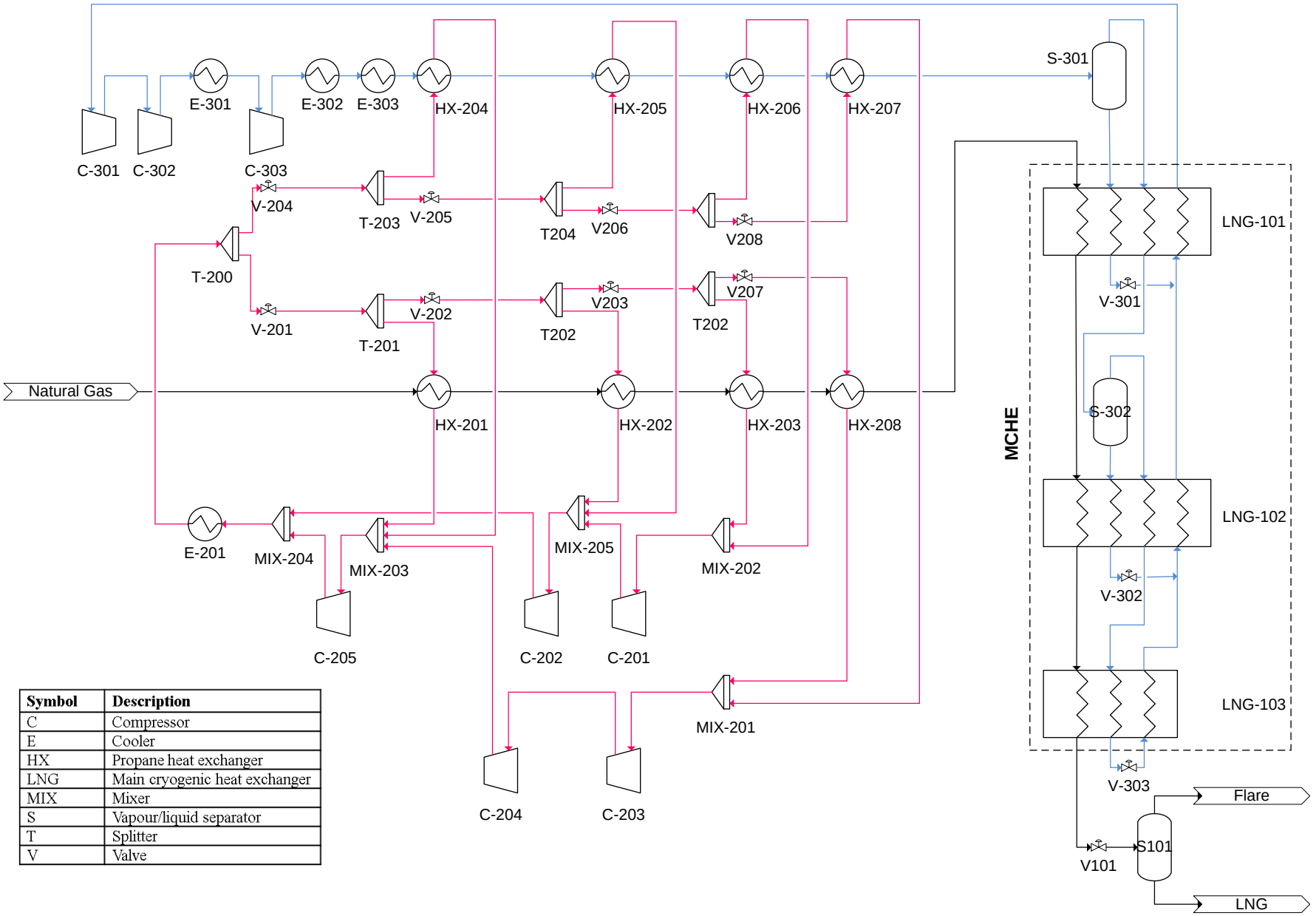

Symbol	Description
C	Compressor
E	Cooler
HX	Propane heat exchanger
LNG	Main cryogenic heat exchanger
MIX	Mixer
S	Vapour/liquid separator
T	Splitter
V	Valve

Figure 3-4 The flow diagram of the C3MR-SP process (red lines represent propane precooling cycle and blue lines mixed refrigerant subcooling cycle).

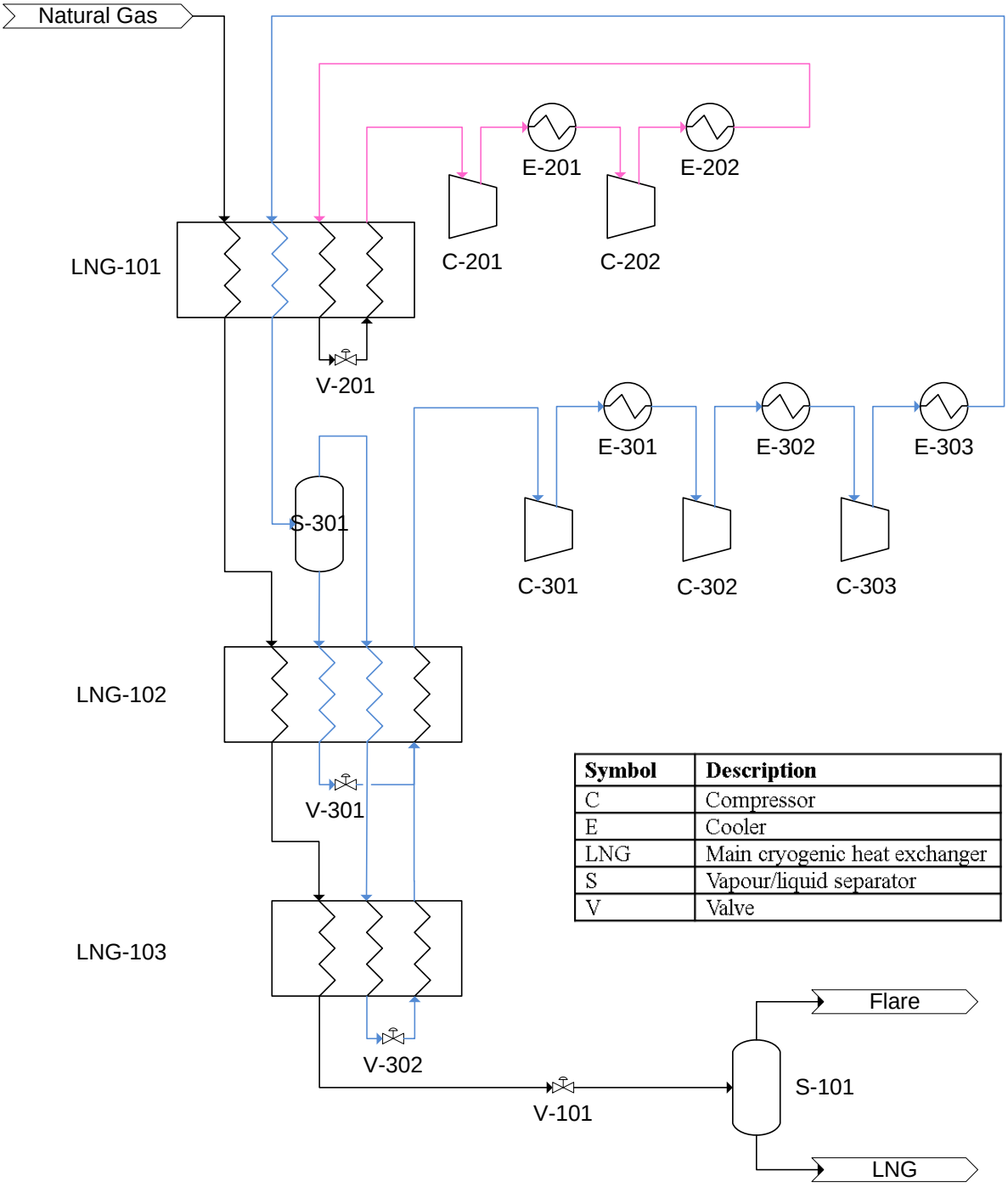

Symbol	Description
C	Compressor
E	Cooler
LNG	Main cryogenic heat exchanger
S	Vapour/liquid separator
V	Valve

Figure 3-5 The flow diagram of the DMR process (red lines represent mixed refrigerant precooling cycle and blue lines mixed refrigerant subcooling cycle.

3.4 Modelling of unit operations

The HYSYS model was built by introducing the unit operations, such as cold box, compressors and heat exchanges. These unit operations were connected with material or energy streams. The key unit operations of the C3MR processes are described in this section. For the C3MR-SP and DMR processes, the desired specifications of their unit operations are equivalent to those described below.

3.4.1 The precooling cycle

The primary step was to model the precooling cycle of the C3MR process. The Aspen HYSYS flowsheet of the precooling cycle is shown in Figure 3-6. The key unit operations are heat exchangers, propane compressors, and propane condenser; their specifications are listed in Table 3-2.

The heat exchangers were used to cool the feed natural gas and mixed refrigerant streams separately to the desired temperature. They were modelled as counter-current shell and tube heat exchangers, requiring specifying the temperature of the outlet streams and the pressure drop.

The propane compressors were employed to increase the pressure of the propane streams. Since the pressure of outlet streams of the compressors were specified, the compression work was calculated by Aspen HYSYS. The adiabatic efficiency of the compressors was assumed to be 75%. Moreover, the inlet stream of the compressors must be superheated, thus ensuring no liquid entering the compressor suction.

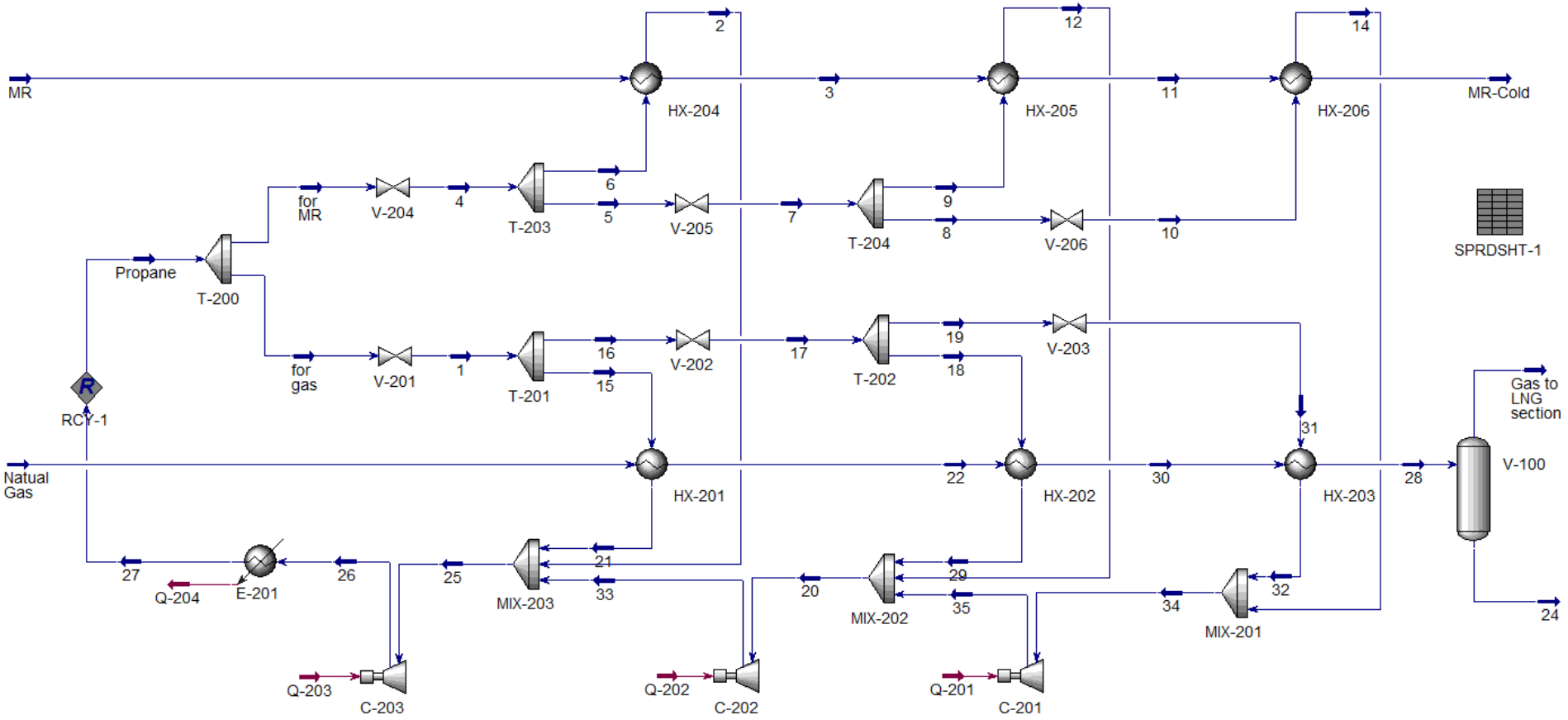

Figure 3-6 The flowsheet of the precooling cycle of C3MR process in Aspen HYSYS.

The propane condenser was modelled as a cooler with no heat loss. The temperatures of the outlet stream and pressure drop were specified. The cooling duty required by the condenser was calculated by Aspen HYSYS.

Table 3-2 The specifications of unit operations in the precooling cycle.

Unit operation	Aspen HYSYS model	Specifications
Propane heat exchangers Mixed refrigerant heat exchangers	Heat exchanger	Tube-side ΔP = 1.7kPa Shell-side ΔP = 30kPa
Propane compressors	Compressor	Adiabatic efficiency =75%
Propane condenser	Cooler	Pressure drop ΔP = 30kPa

3.4.2 The compression cycle

The second step was to model the compression cycle of C3MR. It elevated the mixed refrigerant stream to higher pressures. The flowsheet of the compression cycle in Aspen HYSYS is shown in Figure 3-7. This cycle consists of a series of mixed refrigerant compressors and mixed refrigerant condensers. The specifications of the mixed refrigerant compressors are equivalent to those of the propane compressors and are listed in Table 3-3. The mixed refrigerant condenser was modelled as cooler which has the same specification as the propane condenser.

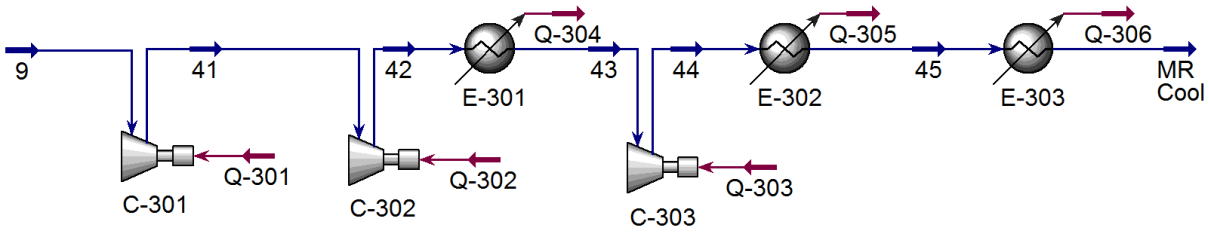

Figure 3-7 The flowsheet of the compression cycle of C3MR process in Aspen HYSYS.

Table 3-3 The specifications of unit operations in the compression cycle.

Unit operation	Aspen HYSYS model	Specifications
Mixed refrigerant condenser	Cooler	Pressure drop ΔP = 30kPa
Mixed refrigerant compressor	Compressor	Adiabatic efficiency = 75%

3.4.3 The liquefaction cycle

The liquefaction cycle was modelled to liquefy natural gas down to -160 °C at atmospheric pressure. The flowsheet of the liquefaction cycle in Aspen HYSYS is shown in Figure 3-8. The key unit operations are the cold box and J-T valves, and their specifications are listed in

Three LNG exchangers (multi-stream heat exchangers) were added to the simulation of the liquefaction cycle. The hot stream is natural gas and the cold streams are mixed refrigerant. In steady state, no detailed geometric information of the LNG exchangers was required for the thermodynamic calculation and optimisation; thus, it was unnecessary to model the streams inside the layers of the LNG exchangers in any particular order.

Various parameters of the LNG exchangers can be specified. In this study, the pressure drop across each layer of the LNG exchangers was specified. In order to converge the LNG exchanger, the temperature of outlet streams needed to be defined and was considered the manipulated variables of the optimisation. Under these specifications, the overall LMTD in the exchangers was calculated by Aspen HYSYS. The heat loss was assumed to be zero.

The J-T valves expand the natural gas pressure to low pressure at constant enthalpy. The pressure drop was specified and frictional losses are assumed to be negligible.

Table 3-4 The specifications of unit operations in the liquefaction cycle.

Unit operation	**Aspen HYSYS model**	**Specifications**
Cold box	LNG exchanger	Hot stream ΔP = 200kPa Cold stream ΔP = 30kPa
J-T valve	Valve	Pressure drop

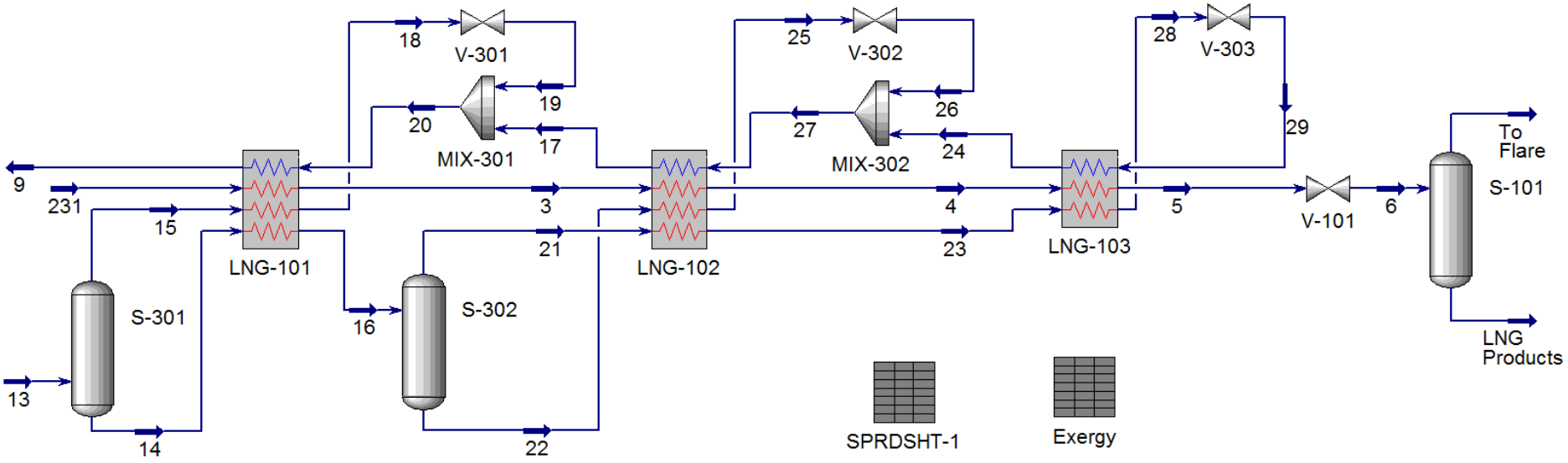

Figure 3-8 The flowsheet of the subcooling cycle of C3MR process in Aspen HYSYS.

3.5 Optimisation

The optimisation problem was solved using the optimiser in Aspen HYSYS®. BOX method was employed to solve this nonlinear problem. It is a sequential search technique built-in within Aspen HYSYS® and is capable of handling nonlinear inequality constraints (AspenTech, 2004).

The optimisation formulation requires design variables, objective functions and constraints. The optimiser provides the optimisation framework for optimising the flowsheet at steady state. The Optimiser-Spreadsheet was set up within the main-flowsheet where the objective functions were defined within the different cells of the Spreadsheet. These objective functions were formulated based on the design variables described in Section 4.2.4 and Section 5.2.3. These variables are distributed in the main-flowsheet and sub-flowsheets which are summarised in Table 3-5.

Table 3-5 Key design variables required for optimisation.

Flowsheet name	Design variables
Main flowsheet	Mixed refrigerant composition Mixed refrigerant pressure Mixed refrigerant flow rate
Sub 1: Precooling	Propane flow rate* Propane pressure* Outlet pressure of compressors Mass split ratio of propane
Sub 2: Compression	Outlet pressure of compressors
Sub 3: Liquefaction	Outlet temperature of MCHE

*For DMR, mixed refrigerant flow rate, pressure and composition in precooling are selected as design variables instead of propane flow rate and pressure.

3.6 Thermodynamic analyses

Thermodynamic analysis was performed for the selected LNG processes and evaluated by the energy and exergy analyses discussed in Section 2.3.

3.6.1 Energy analysis

A heat exchanger is a device that transfers heat from one medium to another. It is widely used in cryogenic systems. The heat transfer rate across a heat exchanger is defined by:

$$\dot{Q} = UA \cdot LMTD \qquad \text{Eq. 3-1}$$

where, *UA* is the heat exchange area of the cold box, *LMTD* is the temperature driving force for the heat transfer in the cold box.

The heat exchanger includes the hot and cold streams. The *LMTD* is a logarithmic average of the temperature differences between the hot and cold streams and is expressed as:

$$LMTD = \frac{\Delta T_1 - \Delta T_2}{\ln\left(\frac{\Delta T_1}{\Delta T_2}\right)} \qquad \text{Eq. 3-2}$$

where, ΔT_1 and ΔT_2 are the temperature difference between the two streams on either side of the heat exchanger.

The total shaft work (W_{total}) supplied to the liquefaction process is given by:

$$W_{total} = \sum_{i=1}^{n} W_i \qquad \text{Eq. 3-3}$$

where, W_i is the shaft work used at compressor *i* (MW).

The specific shaft work ($W_{specific}$) is the compression work required to produce a unit of LNG (MJ/tonne-LNG). It is represented as

$$W_{specific} = \frac{W_{total}}{m_{LNG}} \qquad \text{Eq. 3-4}$$

where, W_{total} is the total shaft work required (MW), m_{LNG} is LNG production capacity (tonne).

3.6.2 Exergy analysis

As aforementioned in Section 2.3.2, kinetic exergy, potential exergy and chemical exergy were ignored. Therefore, energy and materials are only denoted by the physical resources.

Based on the overall exergy balance equation (Eq. 2-4), the exergy loss and efficiency equations related to the individual components of the liquefaction process are given as below:

(1) Compressors

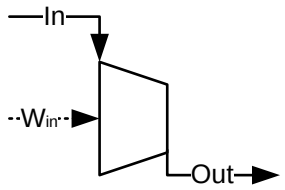

Exergy loss: $$I_C = E_{in} - E_{out} = \sum(m_C e_C)_{in} + W_{in} - \sum(m_C e_C)_{out}$$ Eq. 3-5

Exergy efficiency: $$\varepsilon_C = \frac{\sum(m_C e_C)_{out} - \sum(m_C e_C)_{out}}{W_{in}}$$ Eq. 3-6

(2) Cold box

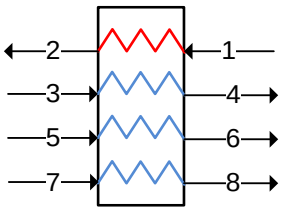

Exergy loss: $$I_E = E_{in} - E_{out} = \sum(m_E e_E)_{1,3,5,7} - \sum(m_E e_E)_{2,4,6,8}$$ Eq. 3-7

Exergy efficiency: $$\varepsilon_E = \frac{\sum(m_E e_E)_{2,4,6,8}}{\sum(m_E e_E)_{1,3,5,7}}$$ Eq. 3-8

(3) Propane heat exchanger

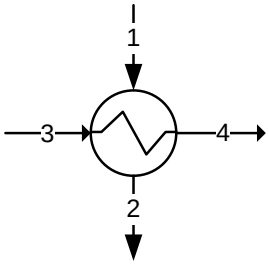

Exergy loss: $$I_E = E_{in} - E_{out} = \sum (m_E e_E)_{1,3} - \sum (m_E e_E)_{2,4}$$ Eq. 3-9

Exergy efficiency: $$\varepsilon_E = \frac{\sum (m_E e_E)_{2,4}}{\sum (m_E e_E)_{1,3}}$$ Eq. 3-10

(4) Throttle valve

Exergy loss: $$I_V = E_{in} - E_{out} = (m_V e_V)_{in} - (m_V e_V)_{out}$$ Eq. 3-11

Exergy efficiency: $$\varepsilon_V = \frac{\sum (m_V e_V)_{out}}{\sum (m_V e_V)_{in}}$$ Eq. 3-12

(5) Phase separator

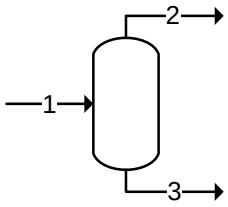

Exergy loss: $$I_S = E_{in} - E_{out} = (m_S e_S)_1 - \sum (m_S e_S)_{2,3}$$ Eq. 3-13

Exergy efficiency: $$\varepsilon_S = \frac{\sum (m_S e_S)_{2,3}}{(m_S e_S)_1}$$ Eq. 3-14

CHAPTER 4. THERMODYNAMIC AND ECONOMIC OPTIMISATION OF MIXED REFRIGERANT PROCESS

4.1 Introduction

This chapter focuses on the optimisation of two mid-scale processes, namely C3MR and DMR. We investigated the merits of C3MR and DMR processes with a capacity of 3 MTPA and evaluated their performances with a focus on minimisation of both energy consumption and cost. A new preliminary economic objective function was formulated to reduce both shaft work and equipment size. This objective function combines the design variable *UA* of MCHE and the operating variable shaft work. Subsequently, the optimisation results of the C3MR and DMR processes were compared with that of the literature based on process configuration, performance, and cost. Future potential enhancement of the optimised process was then evaluated by exergy analysis. The descriptions of the selected LNG processes are presented in Sections 3.3.1 and 3.3.3.

4.2 Optimisation formulation

4.2.1 Assumptions

Natural gas enters the liquefaction process at a temperature of 25 ºC and a pressure of 5000 kPa. The flow rate of feed natural gas is 3.99×10^5 kg/h (equivalent to 2.421×10^4 kmol/h). C3MR and DMR processes are simulated under the same conditions, including the feed gas condition described in Section 3.2, and several other specifications for economic analysis listed below:

1) For consistency, the CAPEX breakdown of the C3MR and DMR processes is the same, including pretreatment, liquefaction, LNG storage, and loading facilities.
2) The cost distribution of the main equipment is estimated according to Yin *et al*. (2008).

3) The *TCI* of a C3MR plant is expected to be around $3 billion for a capacity of 3 MTPA. The capital cost index of the DMR to the C3MR is 1.05 (Vink et al., 1998).
4) For LNG plants, the typical operating capacity factor (CF) lies within a range of 0.85 and 0.9. The annual operation hours are 8760×CF h/year.
5) No loan is made for the total plant investment.

4.2.2 Preliminary cost model

The preliminary cost equations below are applied for formulating economic objective functions in Section 4.2.3.

4.2.2.1 Capital cost

The natural gas liquefaction process mainly consists of condensers, evaporators, compressors and other equipment. MCHE and compressors constitute the major cost of liquefaction processes. However, limited economic values have been found regarding the facility costs of the liquefaction processes. A non-rigorous approach was therefore developed to calculate the cost of compressors and MCHE. The equation for total capital investment is represented in Eq. 4-1.

$$TCI = \sum_{f=1}^{m} C_f \left(\frac{X}{X_0} \right) \qquad \text{Eq. 4-1}$$

where, *TCI* is total capital investments ($), X is plant capacity of this study (MTPA), X_0 is the basis reference of plant capacity (MTPA), C_f is the equipment cost of an LNG plant for equipment type f ($).

Eq. 4-2 is derived from Eq. 4-1 for the capital cost of each equipment.

$$C_f = \alpha_f \left(\frac{X}{X_0} \right) TCI_0 \qquad \text{Eq. 4-2}$$

where, TCI_0 is the baseline value for total capital investment of an LNG plant, α_f is the percentage of the equipment cost of the LNG value chain which is expressed in Eq. 4-3.

$$\alpha_f = \lambda \beta_f \qquad \text{Eq. 4-3}$$

where, λ is the percentage of capital cost of an LNG plant over total cost of an LNG value chain, β_f is the percentage of the component cost of an LNG plant over the total capital cost of an LNG plant, β_f values are presented in Table 4-1.

Table 4-1 Capital cost distribution of an LNG plant (Yin et al., 2008).

Item	**Million RMB**	**β_f (%)**
Cold box (include pipeline, heat exchangers)	2.30	37.70
Compression system	1.50	24.59
Instrument and control system	1.40	22.95
Assistant equipment (include water, boiler, fire protection	0.70	11.48
Mixed refrigerant confection system	0.20	3.28
Sum	6.1	100

For an LNG plant, the size of MCHE (*UA*) contributes to the CAPEX; shaft work (*W*) contributes to the OPEX which determines the required compressor size. In turn, this results in CAPEX variation. According to the equipment cost for mixed refrigerant cycles given by Yin *et al*. (2008) in Table 4-1, the equation for capital cost of MCHE (C_{MCHE}) is defined as a function of design variable *UA* as shown below:

$$C_{MCHE} = \left(\alpha_1 \frac{\sum_{t=1}^{k} UA_t}{UA_0} \right) \left(\frac{X}{X_0} \right) TCI_0 \qquad \text{Eq. 4-4}$$

where, UA_t is the overall heat transfer coefficient and area at $MCHE_t$ in this study (MW/°C), UA_0 is the reference value for MCHE obtained from the patent given by Jager et al. (2009), α_1 is the ratio of the capital cost of cold box to that of the LNG value chain.

The derivation of the capital cost equation for compressors (C_{comp}) is similar to that shown above; it is a function of the operating variable W:

$$C_{comp} = \left(\alpha_2 \frac{\sum_{i=1}^{n} W_i}{W_0} \right) \left(\frac{X}{X_0} \right) TCI_0 \qquad \text{Eq. 4-5}$$

where, W_0 is the referenced shaft work obtained from the patent given by Jager et al. (2009), α_2 is the ratio of the capital cost of compressors to that of the LNG value chain.

From the above, the new equation for the total capital investment consisting of the key operating variable (W) and the design variable (the overall UA of MCHE) is represented below:

$$TCI = \left(\alpha_1 \frac{\sum_{t=1}^{k} UA_t}{UA_0} + \alpha_2 \frac{\sum_{i=1}^{n} W_i}{W_0} + \alpha_3 + \alpha_4 + \alpha_5 + \alpha_6 \right) \left(\frac{X}{X_0} \right) TCI_0 \qquad \text{Eq. 4-6}$$

where, TCI is the total capital investment ($), α_3, α_4, α_5, and α_6 are the proportion of the capital cost of instrument and control system, assistant equipment, construction engineering, and mixed refrigerant confection system in the LNG value chain, respectively.

4.2.2.2 Operating cost

The operating cost includes the costs of natural gas and utility (cooling water and electricity). The equation for the cost of natural gas is displayed below:

$$C_{NG} = F_{NG} P_{NG} HPA \qquad \text{Eq. 4-7}$$

where, F_{NG} is the flow rate of the feed natural gas (kg/h), P_{NG} is the price of the feed natural gas ($/MMBtu), HPA is hours per annum (h).

The equation for the cost of utilities is

$$C_{UT} = P_{electricity} \sum_{i=1}^{n} W_i HPA + P_{cooling} \sum_{j=1}^{m} Q_j HPA \qquad \text{Eq. 4-8}$$

where, $P_{electricity}$ is the price of the electricity ($/GJ), $P_{cooling}$ is the price of the cooling water ($/GJ), Q_j is the cooling duty at heat exchanger j (MW).

4.2.3 Objective functions

There are four objective functions formulated for design optimisation. Objective function 1 (OF1) is the minimisation of total shaft work. It is a well-known objective function found throughout the literature for design and operation optimisation and is represented below:

$$\min W_{total} = \sum_{i=1}^{n} W_i \qquad \text{Eq. 4-9}$$

where, W_i is the shaft work used at the compressor i (MW).

Objective function 2 (OF2) is the minimisation of the total capital cost of the main equipment in the gas liquefaction process. The expression for this objective function is equivalent to that of Eq. 4-6.

$$\min TCI = \left(\alpha_1 \frac{\sum_{t=1}^{k} UA_t}{UA_0} + \alpha_2 \frac{\sum_{i=1}^{n} W_i}{W_0} + \alpha_3 + \alpha_4 + \alpha_5 + \alpha_6 \right) \left(\frac{X}{X_0} \right) TCI_0 \qquad \text{Eq. 4-10}$$

where, TCI is the total capital investment ($).

The OF2 is then substituted into the total annualised cost (*TAC*) equation given in Eq. 4-11 below:

$$\min TAC = f(CAPEX + OPEX) \quad \text{Eq. 4-11}$$

$$\min TAC = \frac{1}{X}\left(0.1TCI + C_{NG} + C_{UT}\right) \quad \text{Eq. 4-12}$$

$$\min TAC = \frac{1}{X}\left[0.1\left(\alpha_1 \frac{\sum_{t=1}^{k} UA_t}{UA_0} + \alpha_2 \frac{\sum_{i=1}^{n} W_i}{W_0} + \alpha_3 + \alpha_4 + \alpha_5 + \alpha_6\right)\left(\frac{X}{X_0}\right)TCI_0 + C_{NG} + C_{UT}\right] \quad \text{Eq. 4-13}$$

where, *0.1TCI* is the depreciation cost ($/year), *TAC* is the total annual cost per tonne LNG ($/tonne-LNG), C_{NG} is the cost of natural gas ($/year), C_{UT} is the cost of utilities ($/year).

To simplify the expression of OF2, α_3, α_4, α_5, α_6 are eliminated since capital costs of the equipment remain constant during optimisation. These include the costs of the instrument and control system, assistant equipment (including cycle water, boiler, fire protection, etc.), construction engineering, and the mixed refrigerant confection system. The following simplified function is called objective function 4 (OF4); it is a minimisation of MCHE and compressors cost:

$$\min(C_{MCHE}, C_{comp}) = \left(\alpha_1 \frac{\sum_{t=1}^{k} UA_t}{UA_0} + \alpha_2 \frac{\sum_{i=1}^{n} W_i}{W_0}\right)\left(\frac{X}{X_0}\right)TCI_0 \quad \text{Eq. 4-14}$$

4.2.4 Optimisation variables

DMR has more manipulated variables than C3MR since mixed refrigerant is used in the precooling cycle of DMR. The baseline values of variables are stated in Table 4-2. For the subcooling cycle, a mixture of potential hydrocarbons and nitrogen is used as a candid

refrigerant for C3MR and DMR processes. The subcooling mixed refrigerant consists of methane, ethane, propane, i-butane, and nitrogen. The optimal composition of any refrigerant must be of non-zero value to ensure feasibility of that specific refrigerant.

Table 4-2 Optimisation variables and their baseline values for precooling and subcooling cycles of C3MR and DMR processes.

Variables	**Unit**	**C3MR**	**DMR**
	Precooling cycle		
Type of refrigerant		Propane	Mixed
Refrigerant molar flow rate	kmol/h	40,139	41,200
Refrigerant pressure	kPa	1100	1320
Refrigerant composition			
Ethane	mol%	0.0	45.5
Propane	mol%	100.0	4.9
n-Butane	mol%	0.0	49.6
Outlet pressure of C-201	kPa	268	850
Outlet pressure of C-202	kPa	528	1350
Outlet pressure of C-203	kPa	1130	-
Mass split ratio to T-201		0.127	-
Mass split ratio to HX-201		0.256	-
Mass split ratio to HX-202		0.379	-
Mass split ratio to HX-204		0.213	-
Mass split ratio to HX-205		0.153	-
	Subcooling cycle		
Type of refrigerant		Mixed	Mixed
Refrigerant molar flow rate	kmol/h	73,600	59,700
Refrigerant pressure	kPa	2630	3400
Refrigerant composition			
Nitrogen	mol%	8.5	8.5
Methane	mol%	50.5	50.5

Ethane	mol%	33.8	33.8
Propane	mol%	7.1	7.1
i-Butane	mol%	0.1	0.1
Outlet pressure of C-301	kPa	454	445
Outlet pressure of C-302	kPa	1212	1245
Outlet pressure of C-303	kPa	2690	3430
Outlet temperature of LNG-101	°C	-87.2	-36.0
Outlet temperature of LNG-102	°C	-124.0	-105.0
Outlet temperature of LNG-103	°C	-155.9	-155.9

4.2.5 Optimisation constraints

The following represents the optimisation constraints for C3MR and DMR processes.

1) The sum of mixed refrigerant mole fraction must be one.

   For precooling cycle of DMR,

$$\sum_{i=1}^{3} x_i = 1 \qquad \text{Eq. 4-15}$$

   For subcooling cycle of C3MR and DMR,

$$\sum_{i=1}^{5} x_i = 1 \qquad \text{Eq. 4-16}$$

   where x_i is the mole fraction of mixed refrigerant flow.

2) The mixed refrigerant flowing into the compressor must be in the vapour phase. To prevent any liquid entering compressors, the following constraints are used:

$$\frac{F_i^V}{F_i^V + F_i^L} = 1 \qquad \text{Eq. 4-17}$$

   where F_i^V and F_i^L represent the flow rates of refrigerant in its vapour phase and liquid phase, respectively, entering compressor *i*.

3) For a feasible heat transfer, the minimum temperature difference between hot and cold composite curves must be above zero.

4) The range of the compression ratio is 1.5 to 4 in order to achieve adequate thermal efficiency (Finlayson, 2006).

$$1.5 < \frac{P_i^{out}}{P_i^{in}} < 4 \qquad \text{Eq. 4-18}$$

where, P_i^{out} is the outlet pressure of the compressor *i* and P_i^{in} is the inlet pressure of the compressor *i*.

5) The temperature of all outlet streams in MCHE must be the same (Hasan *et al*., 2007).

$$\begin{aligned} T_{LNG101}^{out1} &= T_{LNG101}^{out2} = T_{LNG101}^{out3} \\ T_{LNG102}^{out1} &= T_{LNG102}^{out2} = T_{LNG102}^{out3} \\ T_{LNG103}^{out1} &= T_{LNG103}^{out2} \end{aligned} \qquad \text{Eq. 4-19}$$

where T^{out} is the temperature of the outlet stream in MCHE for LNG.

6) All inlet streams of the mixer must remain at the same pressure.

7) The outlet temperature of the cooler must be lower than that of the inlet.

$$T_j^{out} \le T_j^{in} \qquad \text{Eq. 4-20}$$

where T_j^{out} is the outlet temperature of the cooler *j* and T_j^{in} is the inlet temperature of the cooler *j*.

8) For the precooling cycle of C3MR, the propane flow splitter divides the flow by a split ratio of:

$$0 < \frac{F_1^{out}}{F_1^{out} + F_2^{out}} < 1 \qquad \text{Eq. 4-21}$$

where F_1^{out} and F_2^{out} represent the propane flow of the outlet streams of the splitter.

4.3 Optimisation results

The optimisation study with 3 MTPA C3MR and DMR processes using energy and cost objective functions under numerous decision variables and constraints was carried out. The *UA* of MCHE is allowed to be changed while LNG production remains constant. The DMR process uses the same optimisation and cost estimation methodologies as that applied for the C3MR process.

Table 4-3 Baseline values of energy consumption and cost for C3MR and DMR processes.

Variables	**Unit**	**C3MR**	**DMR**
Energy consumption			
Total shaft work required	MW	245.1	231.5
Specific shaft work	MJ/tonne-LNG	2319.1	2190.2
Total cooling duty	MW	336.2	322.6
Specific cooling duty	MJ/tonne-LNG	3181.2	3052.4
LMTD	°C	18.82	19.06
Precooling *UA*	MW/°C	-	27.39
Subcooling *UA*	MW/°C	16.39	12.83
Cost			
OPEX	$million/year	453.0	448.0
Specific OPEX	$/tonne-LNG	135.8	134.4
CAPEX	$million	2944	3005
Specific CAPEX	$/tonne-LNG	981	1002
Annual cost	$million/year	3397	3453
Specific annual cost	$/tonne-LNG	1116.8	1136.4

Table 4-3 presents the baseline values of the energy consumption and cost for C3MR and DMR processes. The optimal operating conditions of C3MR and DMR processes obtained from four objective functions are summarised in Table 4-4 and Table 4-6, respectively. The

optimal cost of both processes is shown in Table 4-5 and Table 4-7. The hot and cold composite curves are presented in Figure 4-2 and Figure 4-4.

4.3.1 C3MR process

The optimal results of the C3MR process were compared with its baseline values (see Figure 4-1). The specific shaft work of the C3MR process from OF1 was found to be of lowest energy consumption. Total shaft work decreased from its baseline value of 2319.1MJ/tonne-LNG to 1288.2 MJ/tonne-LNG, together with a yield of the highest exergy efficiency of 35.8%; however, there was a significant increase in the *UA* value of MCHE from its baseline value of 16.4 MW/°C to 113.5 MW/°C, which exceeded its baseline value of 97.1 MW/°C. The specific CAPEX decreases from $981/tonne-LNG to $972/tonne-LNG. From an economic viewpoint, the relative lower specific CAPEX was obtained through OF2-4 amongst the four objective functions. For OF3, the specific shaft work of 1547.3MJ/tonne-LNG and the exergy efficiency of 29.8% were the second best results. The overall optimal results for the C3MR process are illustrated in Table 4-4.

The process performance can be represented by the composite curves shown in Figure 4-2. In Figure 4-2 (a), the base C3MR process has a temperature difference of more than 10 °C between hot and cold composite curves, hence offering more room for energy improvement. Clearly, the average temperature difference between the composite curves in Figure 4-2 (b) is more closely approaching 3 °C within the temperature range of -30 °C and -163 °C while having the largest *UA* value of MCHE. Figure 4-2 (d) depicts the optimised composite curves with a LMTD value of 11.56 °C, which is the second smallest temperature difference amongst all optimal results. In Figure 4-2 (c) and (e), the gap between the optimised composite curves obtained through the optimisation via OF2 slightly increases to 21.77 °C

and then decreases to 18.15 °C with OF4. However, they have relatively the lowest *UA* value of 12.8 MW/°C for the C3MR process.

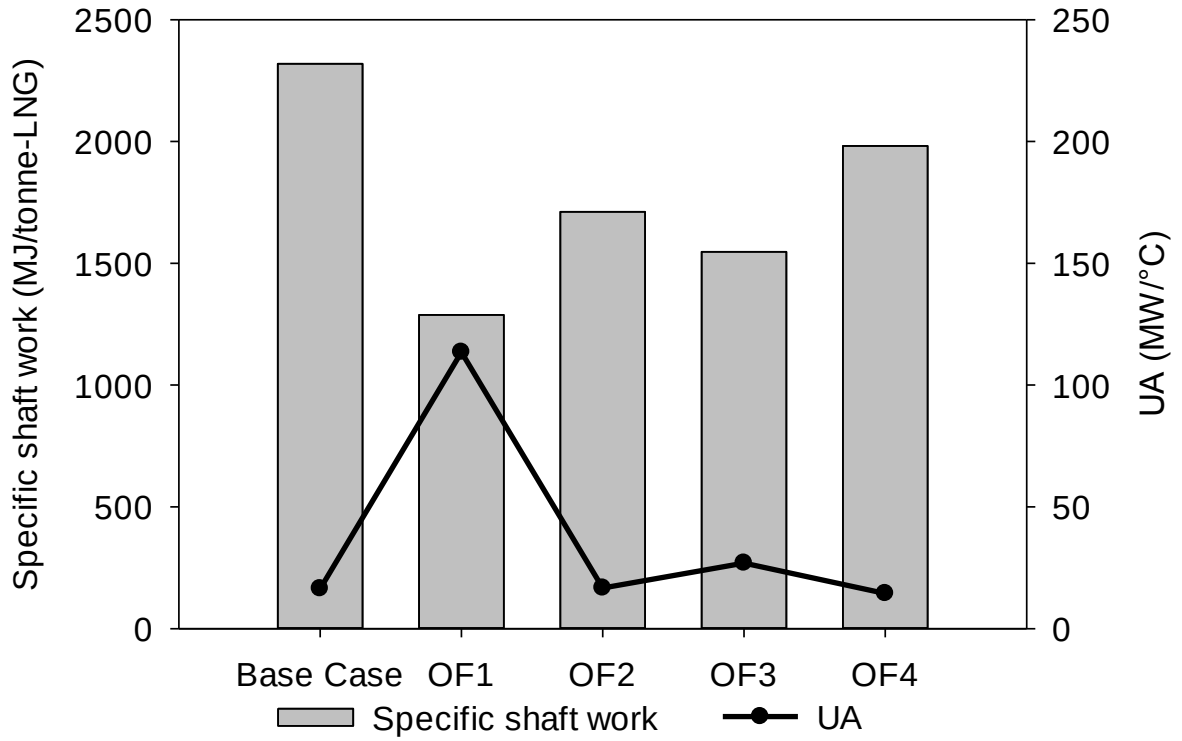

Figure 4-1 Baseline values and optimal results of C3MR process.

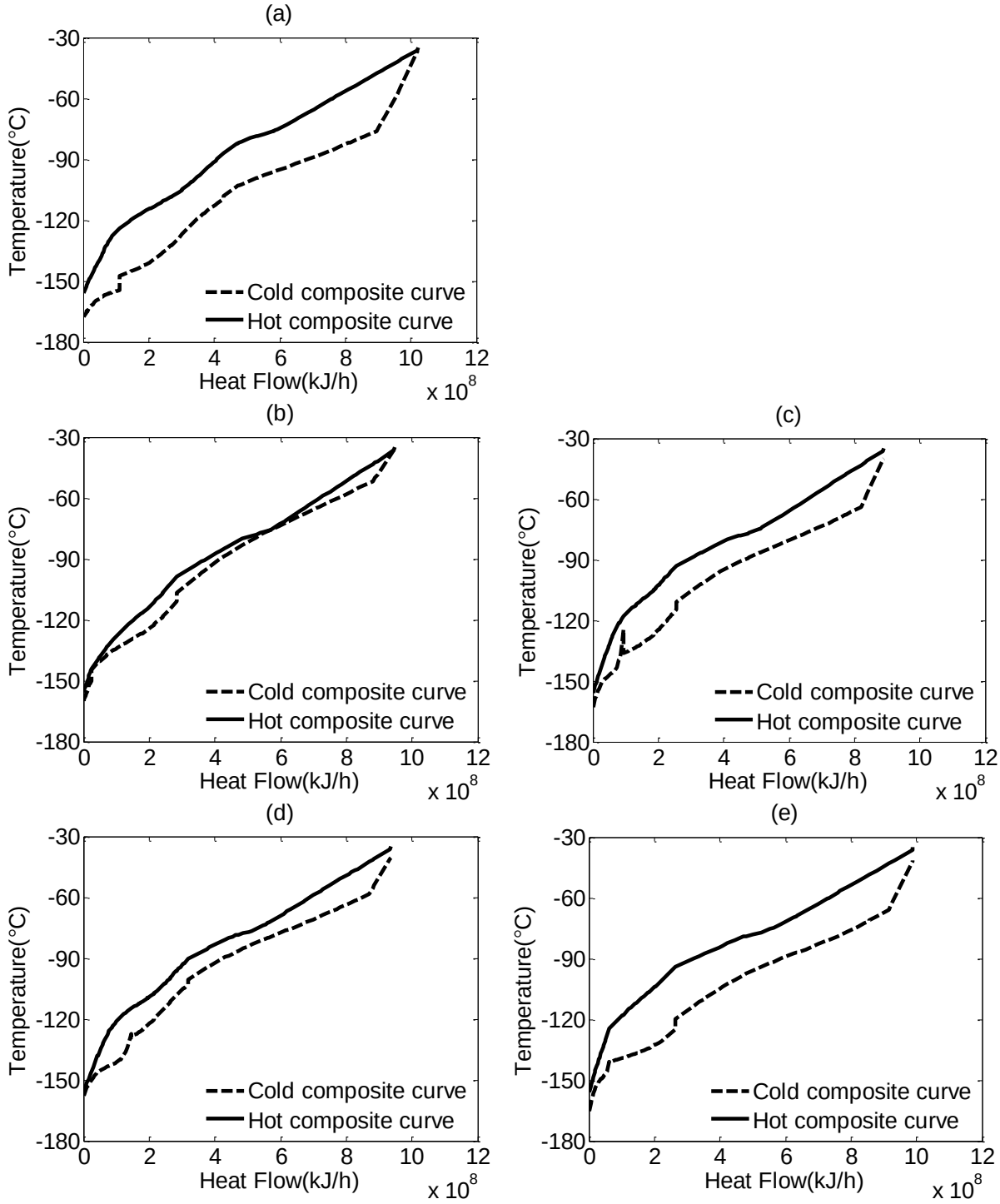

Figure 4-2 Composite curves for the C3MR process (a) Base Case (b) OF1 (c) OF2 (d) OF3 (e) OF4.

Table 4-4 Optimal results for the C3MR process using four objective functions.

Variables	**Unit**	**OF1**	**OF2**	**OF3**	**OF4**
Precooling refrigerant		Propane	Propane	Propane	Propane
Refrigerant flow	kmol/h	40,791	40,019	41,741	39,630
Refrigerant pressure	kPa	1086	1110	1085	1125
Subcooling refrigerant		Mixed	Mixed	Mixed	Mixed
Refrigerant flow	kmol/h	63,773	65,323	66,149	74,319
Refrigerant pressure	kPa	2547	2877	2352	3194
Refrigerant composition					
Nitrogen	mol%	7.42	5.66	4.33	6.40
Methane	mol%	47.98	51.55	49.47	55.04
Ethane	mol%	35.64	35.82	37.44	32.95
Propane	mol%	8.65	6.80	8.37	5.17
i-Butane	mol%	0.32	0.18	0.39	0.44
MCHE					
Outlet temperature of LNG-101	°C	-98.6	-92.9	-90.5	-94.2
Outlet temperature of LNG-102	°C	-144.3	-117.9	-114.8	-124.6
Energy consumption					
Total shaft work required	MW	136.1	180.9	163.5	209.5
Specific shaft work	MJ/tonne-LNG	1288.2	1711.3	1547.3	1982.0
Total cooling duty	MW	227.3	272.0	254.6	300.6
Specific cooling duty	MJ/tonne-LNG	2150.4	2573.5	2409.4	2844.2
Exergy efficiency	%	35.8	27.0	29.8	23.3
LMTD	°C	3.19	14.76	9.54	18.40
UA	MW/°C	113.5	16.7	26.9	14.4

Table 4-5 Optimal results for the cost of C3MR process using four objective functions.

Variables	Unit	OF1	OF2	OF3	OF4
OPEX	$million/year	414	430	423	440
Specific OPEX	$/tonne-LNG	124.1	128.9	127.0	132.0
CAPEX	$million/year	3240	2904	2929	2914
Specific CAPEX	$/tonne-LNG	972.0	871.2	878.8	874.4
Annual cost	$million/year	3654	3334	3352	3354
Specific annual cost	$/tonne-LNG	1096.1	1000.1	1005.8	1006.4

4.3.2 DMR process

The optimal results of the DMR process in Figure 4-3 and Table 4-6 illustrate the similarity of this process to the C3MR process. For OF1, both processes display the most significant improvement in energy consumption. The specific shaft work decreases from its baseline value of 2190.2 MJ/tonne-LNG to 1125.8 MJ/tonne-LNG. The large shaft work reduction was a result of an increase in the *UA* value of MCHE. The *UA* value of MCHE in the subcooling cycle increases from its baseline value of 12.83 MW/°C to 113.5 MW/°C.

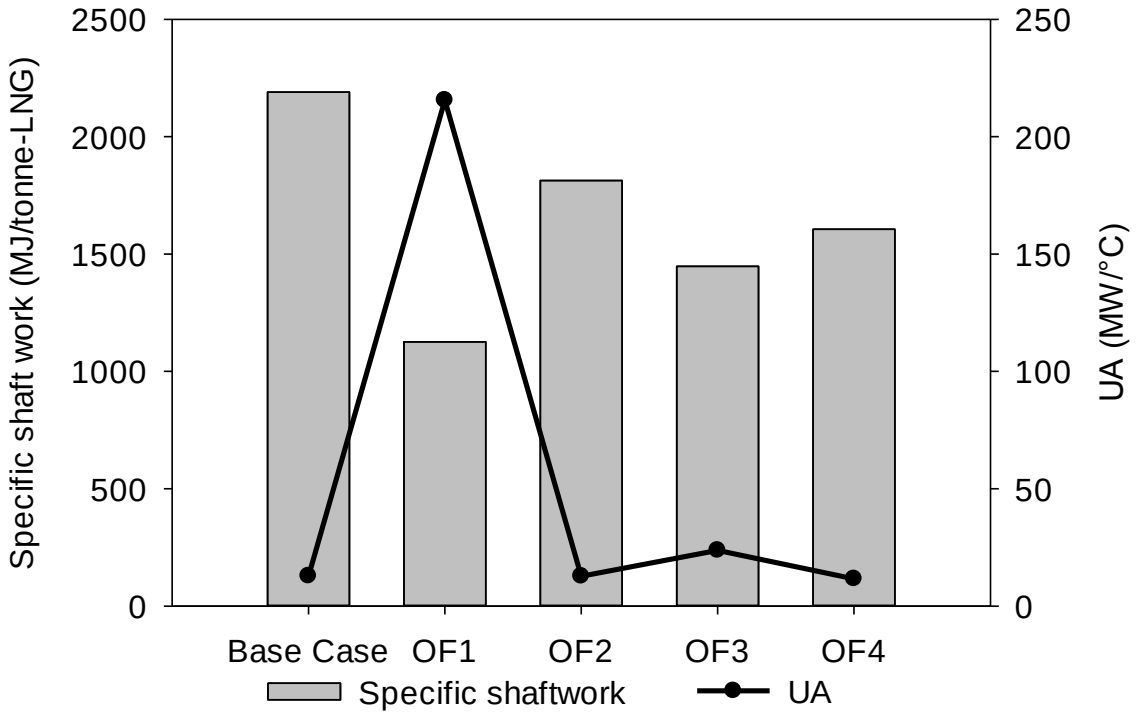

Figure 4-3 Baseline values and optimal results of the DMR process.

Table 4-6 Optimal results for the DMR process using four objective functions.

Variables	**Unit**	**OF1**	**OF2**	**OF3**	**OF4**
Precooling refrigerant		Mixed	Mixed	Mixed	Mixed
Refrigerant flow	kmol/h	39,955	32,364	36,062	28.224
Refrigerant pressure	kPa	1283	2073	1366	1990
Nitrogen	mol%	0.40	1.97	0.75	0.18
Methane	mol%	2.07	0.30	0.26	0.21
Ethane	mol%	33.85	30.74	33.70	36.82
Propane	mol%	24.08	32.18	25.16	39.03
i-Butane	mol%	1.61	5.07	3.15	3.91
n-Butane	mol%	37.99	29.74	36.98	19.86
Subcooling refrigerant		Mixed	Mixed	Mixed	Mixed
Refrigerant flow	kmol/h	47,936	38,256	40,050	31,041
Refrigerant pressure	kPa	3386	3944	3793	3598
Refrigerant composition					
Nitrogen	mol%	7.29	8.11	7.05	2.73
Methane	mol%	42.44	37.12	40.39	39.62
Ethane	mol%	44.35	46.58	45.55	43.36
Propane	mol%	0.10	7.24	5.87	7.30
i-Butane	mol%	5.81	0.94	1.14	6.99
MCHE					
Outlet temperature of LNG-101	°C	-33.0	-35.0	-34.6	-35.2
Outlet temperature of LNG-102	°C	-115.9	-109.9	-104.2	-115.8
Energy consumption					
Total shaft work required	MW	119.0	175.1	143.4	169.7
Specific shaft work	MJ/tonne-LNG	1125.8	1656.6	1356.5	1605.9
Total cooling duty	MW	210.1	266.2	234.5	260.9
Specific cooling duty	MJ/tonne-LNG	1988	2519	2219	2468
Exergy efficiency	%	41.0	27.9	31.9	28.7
LMTD	°C	1.00	13.27	6.66	11.91
UA	MW/°C	215.5	12.0	25.9	11.6

The specific CAPEX of OF1 is $1238.2/tonne-LNG which is higher than its baseline value of $23/tonne-LNG (see Table 4-7), although the lowest specific shaft work of 1125.8 MJ/tonne-LNG was obtained through OF1. For OF3, the specific shaft works of 1356.5 MJ/tonne-LNG is the second lowest value, together with compression energy of 1356.5 MJ/tonne-LNG and an exergy efficiency of 31.9%. This, in turn, enabled the reduction in the specific CAPEX to $885.7/tonne-LNG.

Table 4-7 Optimal results for the cost of DMR process using four objective functions.

Variables	**Unit**	**OF1**	**OF2**	**OF3**	**OF4**
OPEX	$million/year	407	428	416	426
Specific OPEX	$/tonne-LNG	122.2	128.3	124.9	127.7
CAPEX	$million/year	4127	2898	2952	2880
Specific CAPEX	$/tonne-LNG	1238.2	869.4	885.7	864.0
Annual cost	$million/year	4534	3326	3368	3306
Specific annual cost	$/tonne-LNG	1360.4	997.7	1010.6	991.7

The composite curves of the DMR process are shown in Figure 4-4. In Figure 4-4 (a), the composite curves of the base DMR process have a similar gap to that of the base C3MR process. The smaller temperature difference seen in the composite curves of Figure 4-4 (b) reached less than 3°C within the temperature range of -60 °C and -70 °C, hence resulting in a high thermodynamic efficiency. Figure 4-4 (c), (d), (e), enabled us to make equivalent conclusion to those presented in the C3MR process. It was noticed that the optimised composite curves of the DMR process displayed a smaller gap, accompanied by a higher heat transfer efficiency.

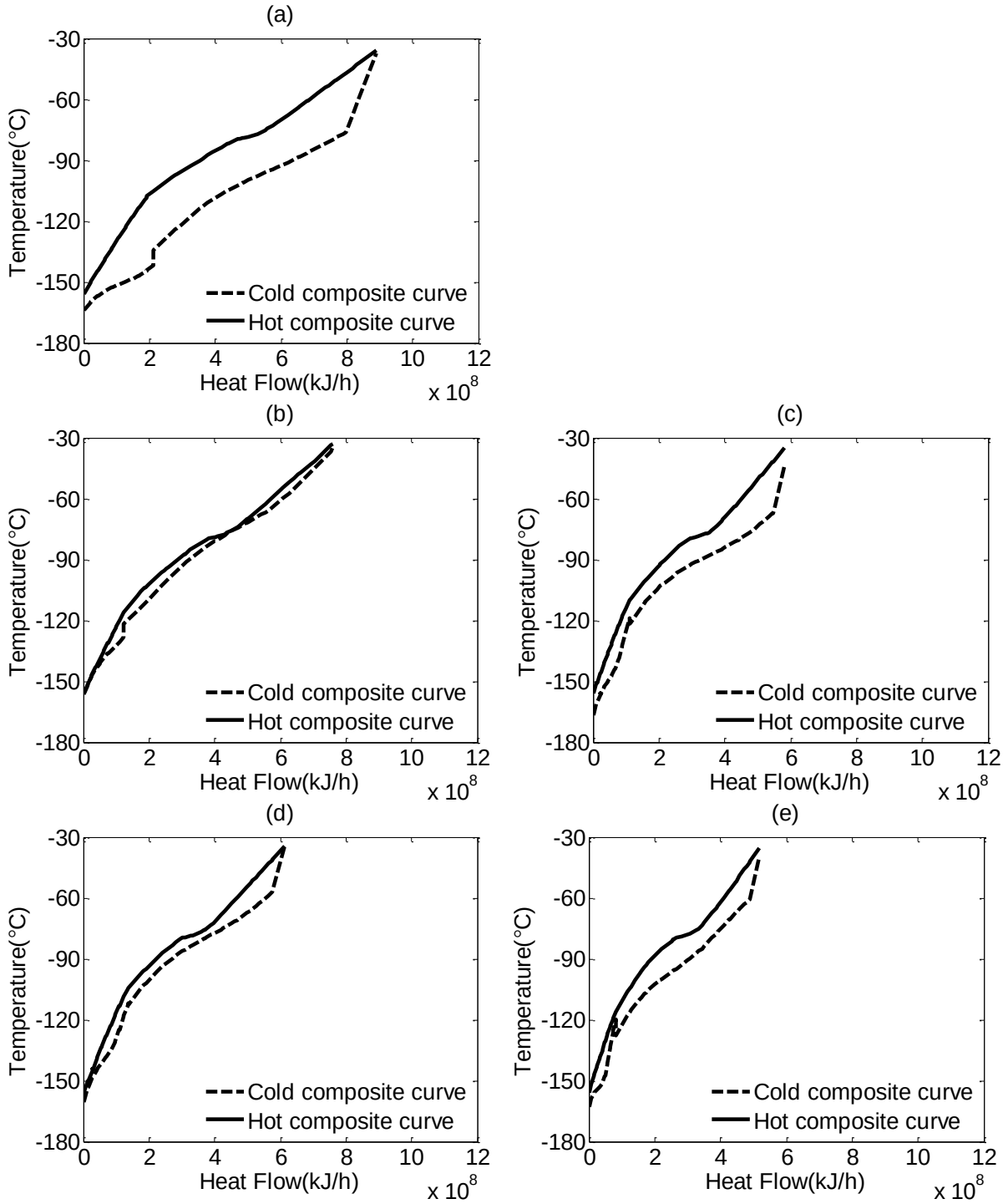

Figure 4-4 Composite curves for the DMR process (a) Base Case (b) OF1 (c) OF2 (d) OF3 (e) OF4.

4.4 Sensitivity analysis and discussion

In general, the problems formulated using the different techniques, such as energy and cost minimisation, had an impact on the optimal results. Two types of optimisation formulations were proposed. The formulation of OF1 presented an optimisation problem in terms of

energy consumption. Although OF1 revealed the greatest improvement of energy consumption, the size of MCHE was consequently finitely large. The formulation of the cost functions (OF2, OF3 and OF4) denoted an optimisation problem with regards to energy consumption and the size of MCHE. We achieved our predicted objectives through the preliminary cost functions which comprise the conflicts of the total energy consumption (W) and the size of MCHE (UA). This formulation, however, imposes restrictions on the size of MCHE. Nevertheless, OF4 was revealed to be the most efficient in the optimization of shaft work and UA; it was capable of reducing the size of MCHE and power consumption.

Next, sensitivity analysis was performed to identify the effect of varying the objective-function coefficient of variables on the optimal results. Two scenarios were explored using the simplified objective function of OF4 as an example.

Table 4-8 Key equipment count.

Equipment	**C3MR**		**DMR**	
Precooling cycle	Number	Type	Number	Type
Mixed refrigerant/Propane compressor	3	Centrifugal	2	Centrifugal
Precooler	1	Kettle	1	CWHE
Subcooling cycle				
Mixed refrigerant compressor	3	Centrifugal	3	Centrifugal
LNG exchanger	3	CWHE	2	CWHE

4.4.1 Sensitivity of component cost (λ) and equipment cost (β_f) to optimisation

The effects of varying alpha values on the optimal results were conducted. Alpha value (α_f) corresponds to the percentage of capital cost of an LNG plant in an LNG value chain (λ) and the percentage of the component cost of an LNG plant (β_f). However, accurate data on plant and equipment costs is currently unavailable. The cost variation depends on a number of

uncertainties, such as manufacture location, equipment types (see Table 4-8), as well as whether it is a greenfield or a brownfield plant. If either of the λ or β_f values changes, the α_f value will subsequently change. It results in a proportional change amongst the cost items of cost functions. There are two scenarios concerning the adjustment of the α_f values using OF4; for each scenario, we estimated the λ and β_f values under a set of values presented in Table 4-9 and Table 4-10.

Table 4-9 Varying α and λ values for Scenario 1 at constant β_f values.

λ (%)	β_1	β_2	α_1	α_2
25	0.227	0.349	0.0871	0.0568
35	0.227	0.349	0.122	0.0796
45	0.227	0.349	0.157	0.102

Table 4-10 Varying α and β_f values for Scenario 2 at a constant λ value of 25%.

λ (%)	Compressor cost	β_1	β_2	α_1	α_2
	50% decrease	0.128	0.393	0.0983	0.0321
	40% decrease	0.150	0.383	0.0958	0.0375
25	30% decrease	0.171	0.374	0.0935	0.0427
	20% decrease	0.191	0.365	0.0913	0.0476
	10% decrease	0.209	0.357	0.0892	0.0523
25	Baseline value	0.227	0.346	0.0871	0.0568
	10% increase	0.244	0.341	0.0852	0.0611
	20% increase	0.261	0.333	0.0833	0.0652
25	30% increase	0.277	0.326	0.0816	0.0692
	40% increase	0.292	0.319	0.0799	0.0729
	50% increase	0.306	0.313	0.0782	0.0765

Scenario 1: The effects of varying the percentage of the liquefaction plant cost to the total cost of the entire LNG value chain (λ) on optimal results

To determine the effects of alternative α_f values on the optimal results, a sensitivity analysis was carried out by varying the percentage cost of an LNG plant in an LNG value chain (λ) within a range of 25% and 50%. In the base case, the liquefaction plant accounts for 25% of the total capital cost of the LNG value chain. Another two cases were run under a cost assumption of 35% and 45%, respectively.

Based on the optimal results of sensitivity shown in Figure 4-5, it was found that the percentage of the liquefaction plant cost (λ) increases linearly with a consistent increase in all alpha values via all cost objective functions. As expected, OF2 and OF4, associating with the capital cost of major equipment, enabled the reduction of shaft work and *UA* of MCHE for the C3MR process. The optimal results observed from OF4 remain constant regardless of any changes in λ values. Total annualised cost (OF3) as objective function brought out a higher energy saving than that of OF2 and OF4; however, their optimal *UA* values increase by more than double of their baseline values. As the percentage of an LNG plant cost increases, this objective function can limit the *UA* value of MHCEs from being infinitely large.

Scenario 2: The effects of varying the percentage of equipment cost of the liquefaction plant (β_f) on optimal results.

Scenario 2 attempts to determine the effect of varying the equipment cost of the liquefaction plant (β_f) on optimal results. Alongside the capital cost of a liquefaction plant, the equipment cost of a liquefaction plant is yet another important factor influencing plant cost. The key pieces of equipment in the liquefaction system are the refrigerant compressors and the main cryogenic exchangers.

For example, if the variation of the compressor cost for the C3MR process is to be considered, it ranges from a 50% decrease of the original cost estimate to a 50% increase. A 10% proportional change is assumed in compressor costs for each attempt as shown in Table 4-10. Figure 4-6 illustrates cost and sizing optimisation results using the β values from Table 4-10. As evident in Figure 4-6, the specific cost of the compressors is \$40.6/tonne-LNG for the base case with a β_1 value of 0.227. At a lower extreme condition of β_1 = 0.128, the specific cost of compressors declines to \$26.5/tonne-LNG, however, this value increases to \$57.3/tonne-LNG at an upper extreme value of β_1 = 0.306. Interestingly, although the specific cost of compressors increases as the compressor's price rises (β_2), specific size of the compressors declines to reach a minimum point of a β_1 value of around 0.244 after which it then increases. As the size of the compressors approaches its minimum value, the sizes of the other unit operations, such as the cold box, tend to increase (See *UA* line in Figure 4-7). However, the size of the compressors is limited to a minimum (1988.3 MW/tonne-LNG). An increase in the cost of other equipment, which outweighs the benefits of savings in the cost of the compressors, is limited. This implies that there is a limit to the level of benefits in the saving cost of compressors. This is clearly evident via Figure 4-7 which shows the optimal operation results with variation of the β_1 value; the increase of the β_1 value results in a subsequent increase in the *UA* value of MCHE and a decline in LMTD until optima is reached.

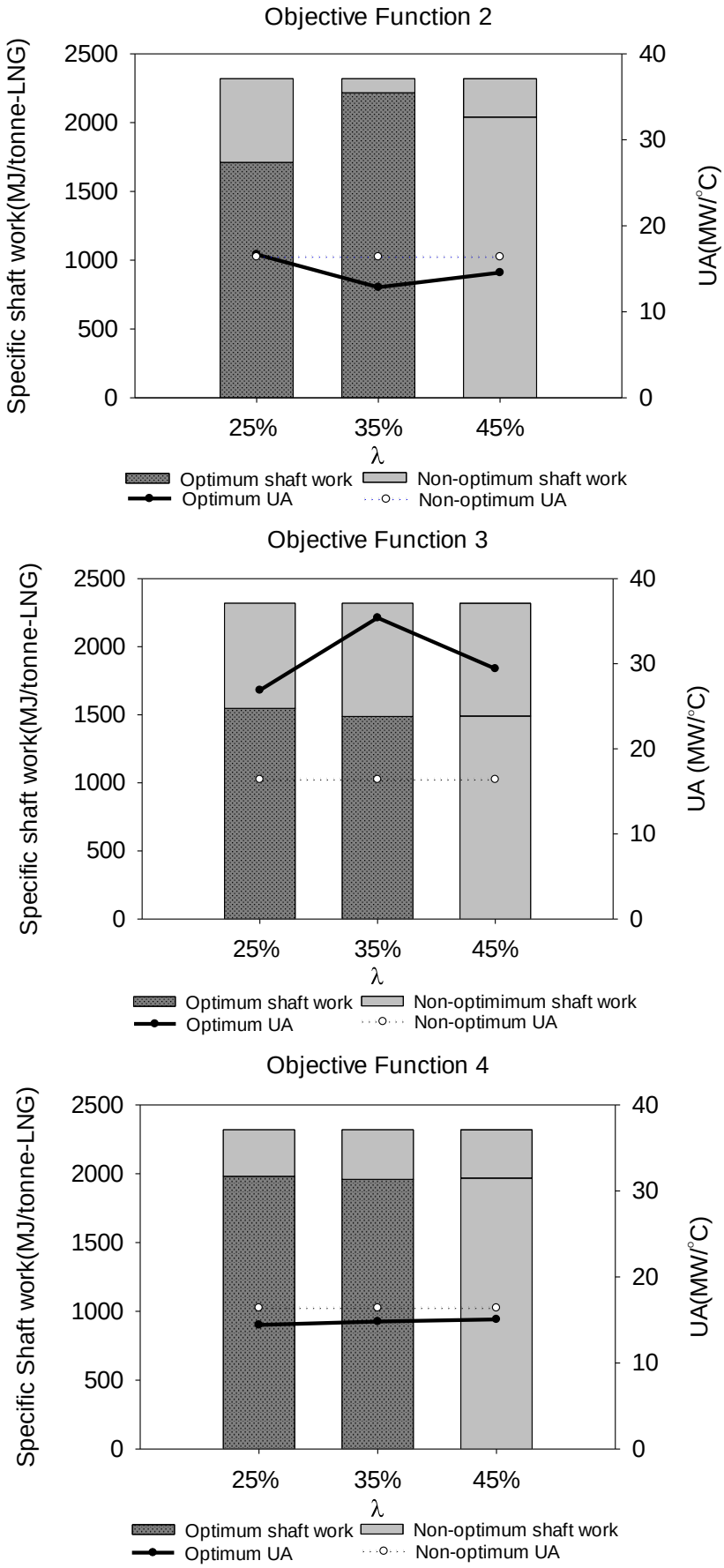

Figure 4-5 The effect of varying λ value on the optimal results of the C3MR process.

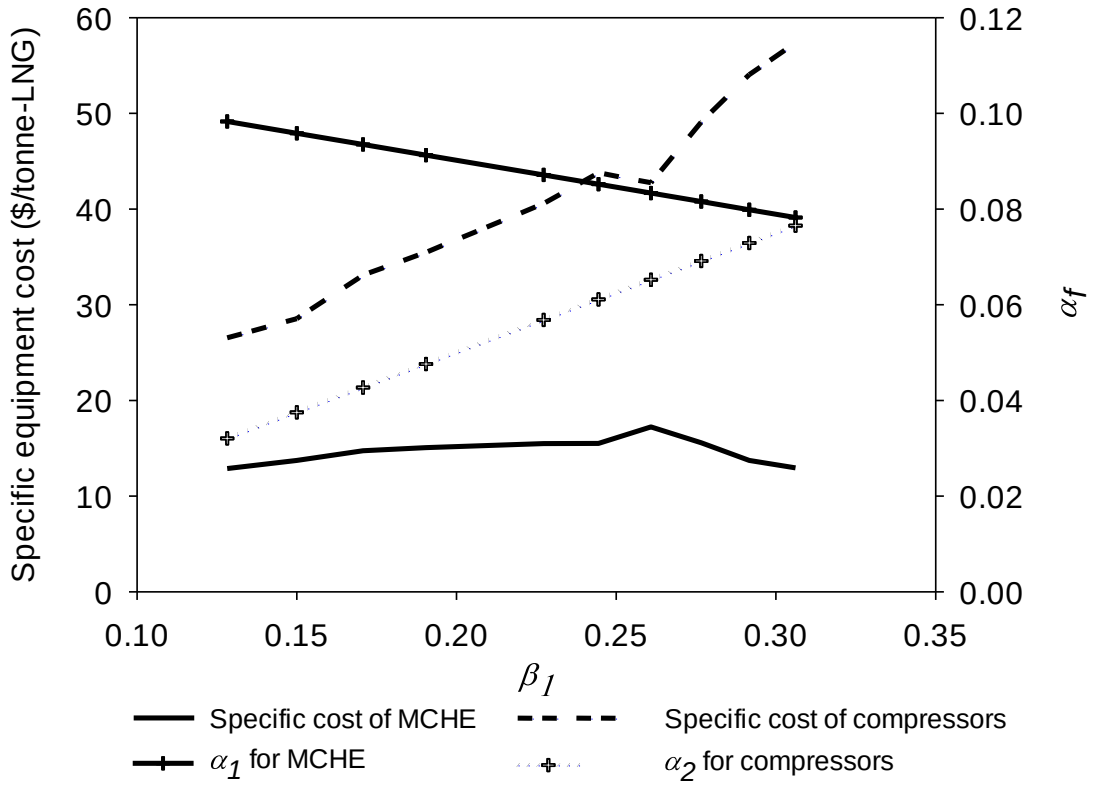

Figure 4-6 The effect of varying β values on α values and specific equipment cost of the C3MR process.

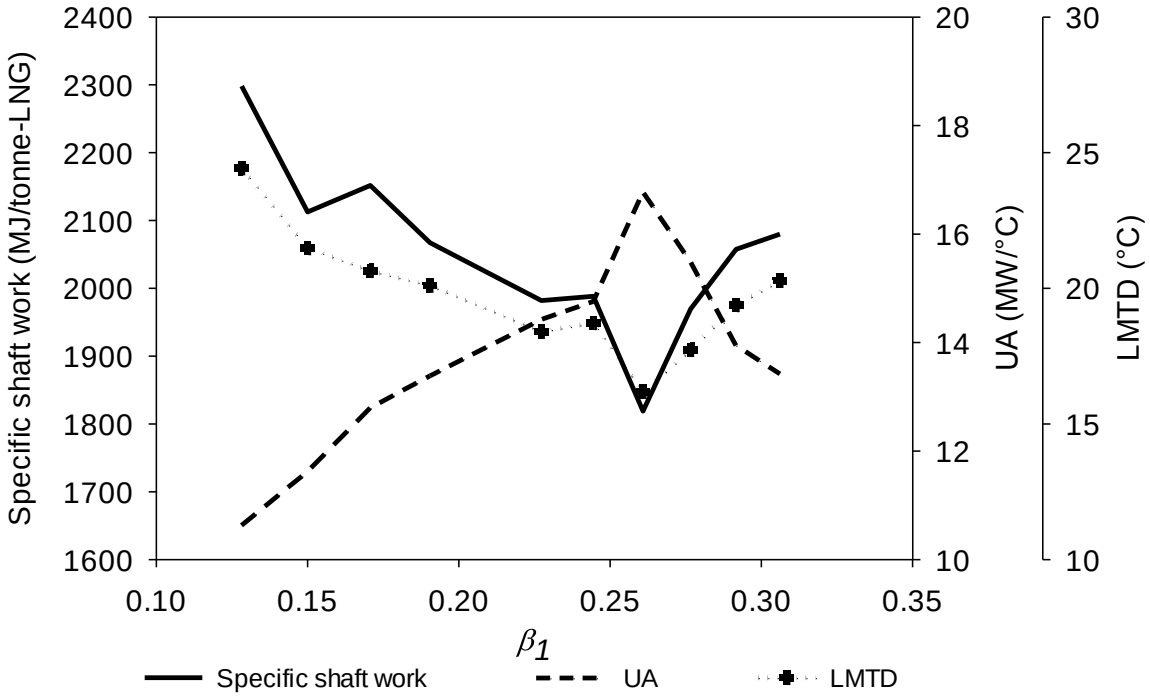

Figure 4-7 The effect of varying β_1 values on the optimal results of the C3MR process.

4.4.2 Comparison of C3MR and DMR processes

The comparison of C3MR and DMR processes can be identified in terms of process configuration, performance, and capital cost. To conduct a fair comparison, both processes were simulated and optimised using the same feed gas condition, same refrigerant mixture for subcooling, and same LNG production.

For the process configuration comparison, the main differences between C3MR and DMR processes are the types of precooling equipment. The C3MR process is more complex than the DMR process. The C3MR process has a considerably large number of equipment included, a precooling step using a single large CWHE for the DMR process would be considerably more cost-prohibitive than the multiple kettle type exchangers for the propane precooling cycle utilised in the C3MR process.

In comparing performance, both C3MR and DMR processes require a large amount of energy. The optimal results of OF1 show that the specific shaft work required by DMR is lower than that required by C3MR; nonetheless, both processes almost have the same *UA* value of MCHE. As displayed in Figure 4-2 and Figure 4-4, the option of using mixed refrigerant in the precooling cycle narrows the temperature difference between the natural gas curve and the refrigerant curve of a typical natural gas liquefaction process; this, in turn, enables us to achieve increased high refrigeration efficiency and reduced energy consumption; an option which also provides additional flexibility in the optimisation.

As for the cost comparison, the size and count of the equipment are the main factors influencing the capital cost. The equipment cost of an LNG plant increases depending on that plant’s manufacture location(s), construction years, and the project's specific requirements. In addition, only limited data is available throughout the literature regarding the facility costs of the liquefaction process. Using the cost consideration aforementioned, the cost evaluation can

be deduced by comparing the relative cost of the two processes rather than the accurate estimates. The DMR process is assumed to be more costly due to the use of MHCEs in the precooling cycle.

The optimal results reveal that the capital costs are similar in both processes via the cost function; however, the capital cost of DMR is slightly higher than that of C3MR via the energy function. For the energy function (OF1), there is no restriction on the *UA* of MCHE. It leads to a significant increase in the *UA* value, especially in the DMR process. This additional cost is compensated for partially by saving more energy. In contrast, precooling *UA* of the DMR process is included in the cost functions. Cost functions can be sensitive to the overall *UA* value of DMR, yet only the subcooling *UA* of the C3MR process is available. It is noticeable from cost functions OF2 and OF4 that the DMR process has more potential in the minimisation of the equipment size and the energy consumption.

Figure 4-8 and Figure 4-9 shows the distribution patterns of exergy loss for the C3MR and the DMR processes, respectively. It is noticeable that the exergy distribution of the two processes is similar. For OF1, the compression system is the major source of exergy loss; it accounts for 35% and 38% for the C3MR process and the DMR process, respectively. MCHE is accountable for the second largest exergy loss: 20% of the overall exergy loss for C3MR and 25% for DMR. In contrast, the MCHE is accountable for the largest exergy loss when using OF4 which is 37% for both the C3MR process and the DMR process. The optimisation objective for OF4 is to reduce both shaft work and *UA*. The smaller the size of the heat exchangers, the larger the temperature difference between the hot and cold composite curves. This yields a higher exergy loss of the heat exchangers. Additionally, the compression system caused a higher exergy loss of 29% for the C3MR and DMR processes.

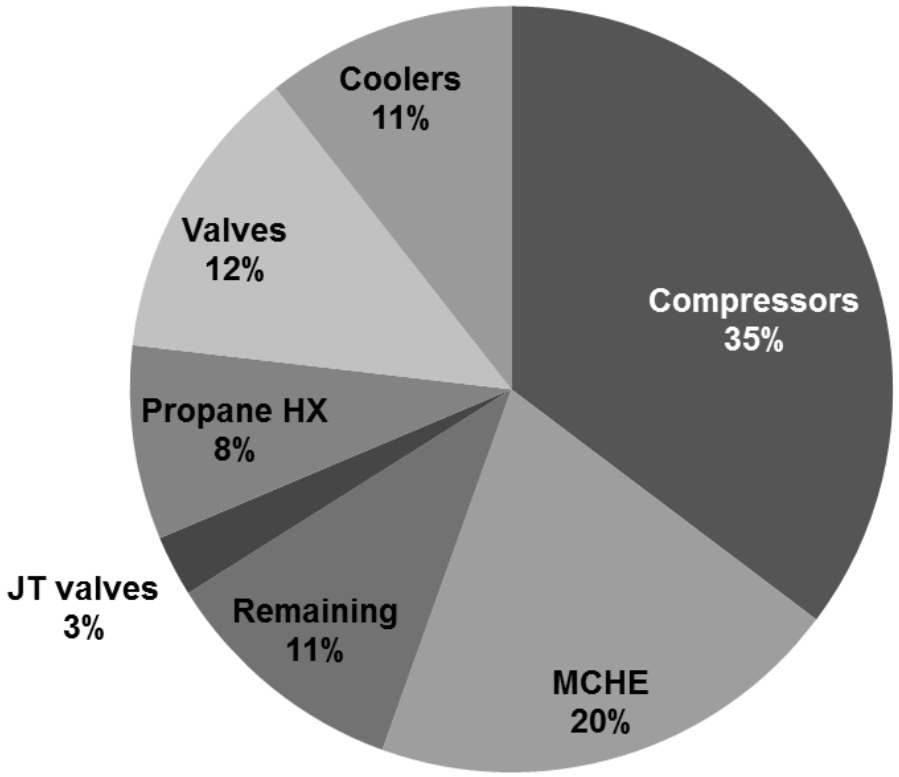

(a)

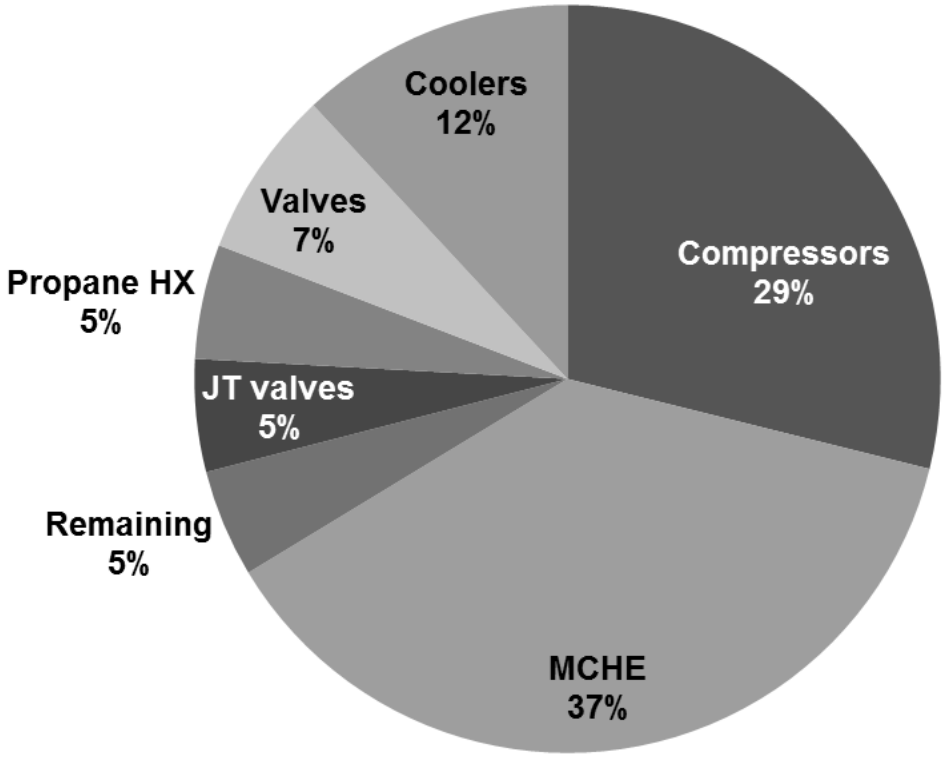

(b)

Figure 4-8 Distribution of exergy loss in the C3MR process (a) OF1 (b) OF4.

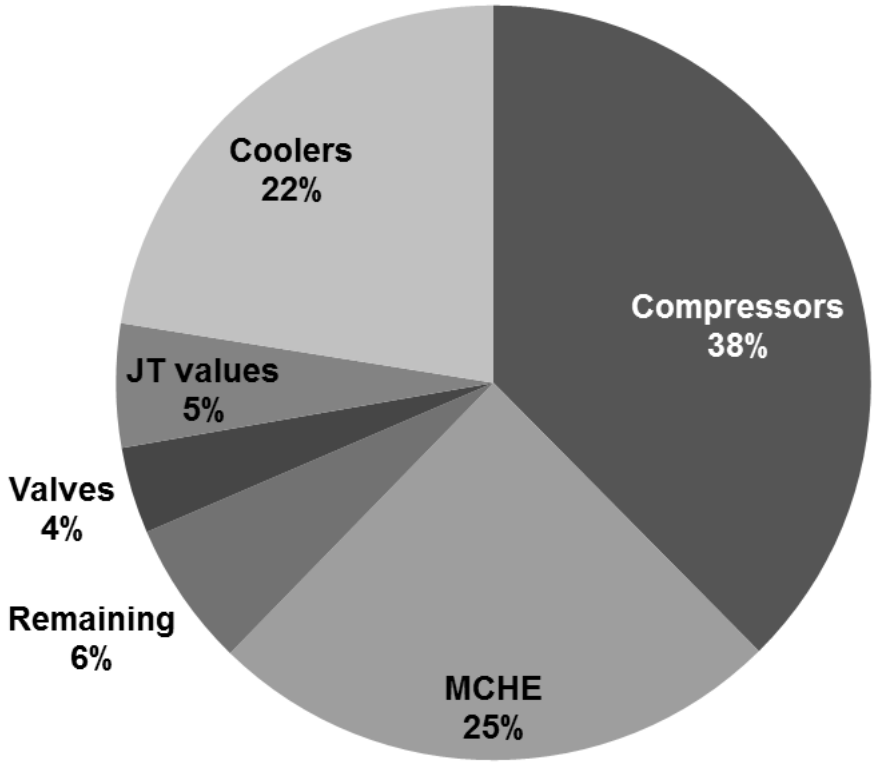

(a)

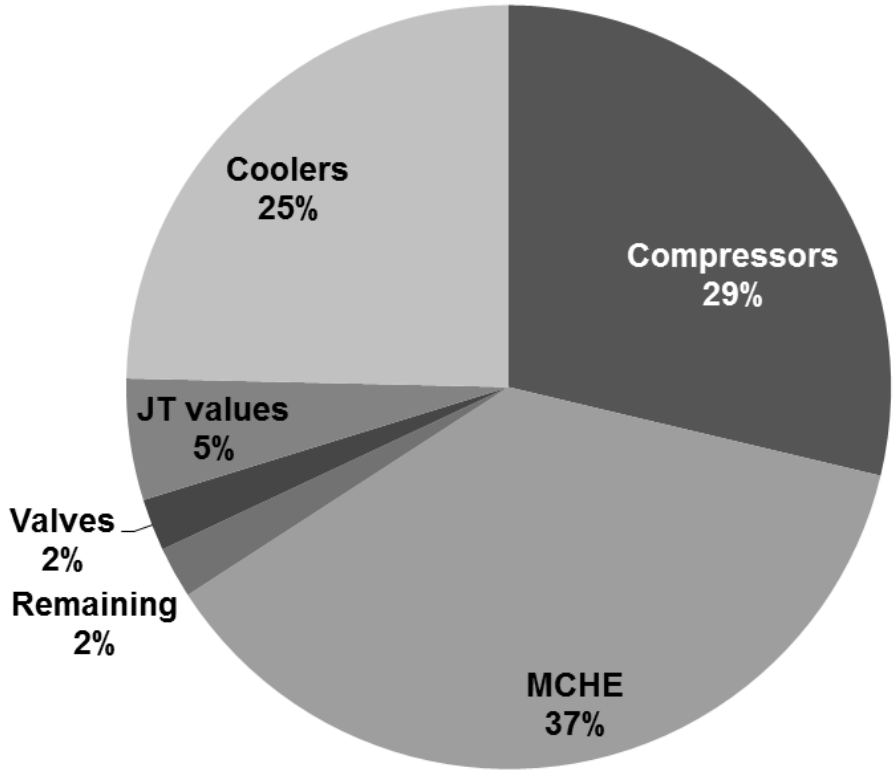

(b)

Figure 4-9 Distribution of exergy loss in the DMR process (a) OF1 (b) OF4.

4.4.3 Mixed refrigerant composition

The effect of mixed refrigerant components on process performance was investigated. The subcooling mixed refrigerant in the literature is typically comprised of methane, ethane, propane, i-butane and nitrogen, as reviewed. Table 4-4 shows the optimal refrigerant composition obtained via different objective functions for the C3MR process. Mixed refrigerant compositions bring out slight variations in the subcooling cycle. The optimal results obtained from OF4 represent the relatively worst optimum performance accompanied by the most optimal *UA* value of MCHE. It is favourable for mixed refrigerant components to have more methane but less propane. The initial composition of methane and i-butane in the mixed refrigerant stream before optimisation was 50.5% mole fraction. After optimisation, the composition of methane was increased to 55.04% mole fraction. Also, there was a decrease in the percentage composition of propane from 7.1% mole fraction to 5.17% mole fraction.

Three components of refrigerant were used in the precooling cycle of the DMR process: ethane, propane and n-butane. We allowed for more refrigerant components to be used as variables in order to show the effect of nitrogen, methane, ethane, propane, i-butane and n-butane on the process performance. As shown in Table 4-6, the optimal refrigerant mixtures in the subcooling cycle obtained from OF1 are compared with those of the baseline values. There is an absence of propane which agrees with Hatcher *et al*. (2012) and Wang *et al*. (2013).

4.5 Conclusions

The optimisation of the C3MR and DMR processes was conducted. Power consumption is taken into consideration as an objective function for energy reduction, and a new formulation of economic objective functions is developed for minimising energy consumption and

equipment size. The cost estimate for DMR was determined using the same methodology as that for C3MR. The cost optimisation considers not only power consumption, but also equipment size, as they equally contribute to the greater cost of the LNG process. The cost components considered herein included the capital costs (compressors, main heat exchangers and others) and the utility costs (water, electricity, and natural gas costs). We compared the optimal results of both the C3MR and DMR processes via four objective functions to their base cases at the same LNG production rate.

The optimal results showed similar results for both C3MR and DMR processes. The results of OF1 appear to be of greatest thermodynamic efficiency from an energy point of view. We implemented the proposed cost function as an objective function to minimise cost, shaft work and *UA*. The optimal results of cost function revealed a trade-off between shaft work and *UA*. Our findings in the optimal results of OF4 show the simultaneous improvement required for energy consumption and equipment size. In comparison to the optimal results of OF4, the formulations of OF2 and OF3 were acceptable in terms of reducing a certain amount of shaft work and *UA*. They appear to be of lower specific shaft work, although they have a relatively higher *UA* than their baseline values.

In order to identify the effects of the two variable costs (λ and β_f) on the optimal results through cost objective functions, two scenarios were proposed. In Scenario 1, the percentage of the capital cost of an LNG plant in an LNG value chain (λ) was varied, and this was found to insignificantly influence the optimal results of the cost functions. Total equipment costs (OF2 and OF4) as objective functions indicate performance improvement and *UA* value reduction. The optimal results from Scenario 2 show a trade-off between power consumption and *UA* value. OF4 could potentially reduce a certain amount of required energy and it could also reduce the size of MCHE which, in turn, provides the feasible solution of optimisation. It

is recommended to optimise the capital expenditures to increase the net profit in a liquefaction plant.

CHAPTER 5. OPERATION OPTIMISATION OF PROPANE PRECOOLED MIXED REFRIGERANT PROCESS

5.1 Introduction

In Chapter 4, process optimality was found to be dependent on both the design parameters and the objective functions used. This chapter focuses on the operational optimisation of the C3MR and C3MR-SP processes and evaluates their performances. The major differences of the C3MR-SP process are detailed in Section 3.3.2. We also intended to investigate the merits of several promising objective functions, along with a combination of critical techno-economic variables in order to achieve the optimisation goal. The optimisation results of the C3MR and C3MR-SP processes are illustrated along with a comparison with that of the literature due to lack of presented data. Further potential enhancement of the optimised process was evaluated via the exergy analysis of the individual equipment and the OPEX analysis.

5.2 Optimisation formulation

5.2.1 Assumptions

Natural gas enters the liquefaction process at a temperature of 25 ºC and a pressure of 5000 kPa. The flow rate of the feed natural gas is 3.73×10^5 kg/h (equivalent to 2.261×10^4 kmol/h). To ensure a reliable comparison is conducted, the assumptions for the case studies of the C3MR and C3MR-SP processes were made so as to be identical to those discussed in Section 3.2. The additional assumptions are listed below:

1) The utility used in the cooler is water. The temperature of the mixed refrigerant after the cooler is 30 °C.

5.2.2 Objective functions

Four objective functions are formulated for the operation optimisation. Objective function 1 (OF1) is a minimisation of total shaft work required, which is one of the most common objective functions found in the literature for both the design and operation objectives. It is represented as:

$$\min\ W_{total} = \sum_{i=1}^{n} W_i \qquad \text{Eq. 5-1}$$

where, W_{total} is the toal shaft work required; W_i is the shaft work used at compressor i.

According to the first law of thermodynamics, the shaft work and cooling duty cannot be completely converted into useful energy in actual practice. Exergy is useful for evaluating the utilities consumed in the system which, in turn, reveals the potential for the minimisation of energy consumption. However, there is a current shortage of publications in finding the most optimum conditions via the use of various objective functions, especially exergy efficiency and OPEX. Objective function 2 (OF2) is the maximisation of exergy efficiency and is described as:

$$\max\ \varepsilon_{total} = \frac{E_{LNG} - E_{NG}}{\sum_{i=1}^{n} W_i} \qquad \text{Eq. 5-2}$$

where, ε_{total} is exergy efficiency of a gas liquefaction process, E_{LNG} is the exergy of liquefied natural gas, E_{NG} is the exergy of natural gas.

The cost of the cooling duty is neglected in many papers since it is far lower than the cost of the shaft work required. However, optimising the cooling duty can also create future benefits to the overall operating cost. Objective function 3 (OF3) is a new formulation of an exergy equation based on OF2 in which the cooling duty has been added to the denominator:

$$\max\ \varepsilon_{total} = \frac{E_{LNG} - E_{NG}}{\sum_{i=1}^{n} W_i + \sum_{j=1}^{m} Q_j} \qquad \text{Eq. 5-3}$$

where, Q_j is the cooling duty required at heat exchanger j.

Objective function 4 (OF4) is a minimisation of OPEX. The fixed OPEX has been neglected and only the most critical OPEX variables have been included which are the costs of the shaft work, the cooling duty and the feed gas. This is given by:

$$\min OPEX = P_{Electricity} \sum_{i=1}^{n} W_i + P_{Water} \sum_{j=1}^{m} Q_j + P_{NG} F_{NG} \qquad \text{Eq. 5-4}$$

where, $P_{Electricity}$ is the price of electricity, P_{Water} is the price of water, and P_{NG} is the price of the feed natural gas. The prices of the electricity and the cooling water are \$10.99/GJ and \$0.40/GJ, respectively (Turton *et al*., 2009). The price of the feed natural gas is \$2/MMBtu.

5.2.3 Optimisation variables

The optimisation variables and their base-case values for the C3MR and C3MR-SP processes are listed in Table 5-1. In this study, a mixture of potential hydrocarbons and nitrogen has been used as the candid refrigerant for the mixed refrigerant cycle. The hydrocarbon mixture includes methane, ethane, propane, i-butane, and nitrogen. The zero composition for any refrigerant towards the final optimal results will indicate the infeasibility of that specific refrigerant.

Table 5-1 Optimisation variables and their base-case values for the precooling and subcooling cycles of the C3MR and C3MR-SP processes.

Variables	**Unit**	**C3MR**	**C3MR-SP**
	Precooling cycle		
Type of refrigerant		Propane	Propane
Refrigerant molar flow rate	kmol/h	36,740	38,480
Refrigerant pressure	kPa	1100	1100
Refrigerant composition			
Nitrogen	mol%	0.0	0.0
Methane	mol%	0.0	0.0
Ethane	mol%	0.0	0.0
Propane	mol%	100.0	100.0
i-Butane	mol%	0.0	0.0
Outlet pressure of C-201	kPa	268	241
Outlet pressure of C-202	kPa	528	1130
Outlet pressure of C-203	kPa	1130	1130
Outlet pressure of C-204	kPa	-	289
Outlet pressure of C-205	kPa	-	528
Mass split ratio to T-201		0.127	0.130
Mass split ratio to HX-201		0.286	0.293
Mass split ratio to HX-202		0.437	0.323
Mass split ratio to HX-203		-	0.377
Mass split ratio to HX-204		0.216	0.197
Mass split ratio to HX-205		0.221	0.141
Mass split ratio to HX-206		-	0.197
	Subcooling cycle		
Type of refrigerant		Mixed	Mixed
Refrigerant molar flow rate	kmol/h	71,000	66,610
Refrigerant pressure	kPa	2630	2630
Refrigerant composition			
Nitrogen	mol%	8.5	8.5
Methane	mol%	50.5	50.5
Ethane	mol%	33.8	33.8
Propane	mol%	7.1	7.1
i-Butane	mol%	0.1	0.1
Outlet pressure of C-301	kPa	454	454
Outlet pressure of C-302	kPa	1212	1212
Outlet pressure of C-303	kPa	2690	2690
Outlet temperature of LNG-101	°C	-87.2	-87.2
Outlet temperature of LNG-102	°C	-124.0	-124.0

5.2.4 Optimisation constraints

The dot points below detail the optimisation constraints involved:

1) The sum of the mixed refrigerant mole fraction must equal one.

$$\sum x = x_1 + x_2 + x_3 + x_4 + x_5 = 1 \qquad \text{Eq. 5-5}$$

where, x_i is the mole fraction of the mixed refrigerant flow.

2) The mixed refrigerant flowing into the compressor must be in the vapour phase. To prevent any liquid from entering the compressors, the following constraints are used.

$$\frac{F_i^V}{F_i^V + F_i^L} = 1 \qquad \text{Eq. 5-6}$$

where, F_i^V and F_i^L represent the flow rate of the refrigerant in its vapour phase and liquid phase, respectively, entering compressor *i*.

3) The minimum temperature approach (MTA) between hot and cold composite curves must be greater than "zero" in order to avoid temperature cross-over. It is theoretically desirable that the MTA should be as close to zero as possible, but this would be impractical since it would, in reality, require infinite heat exchanger area.

4) The compression ratio through the compressors is within a range of 1.5 to 4 in order to meet the commercial requirements (Finlayson, 2006).

$$1.5 < \frac{P_i^{out}}{P_i^{in}} < 4 \qquad \text{Eq. 5-7}$$

where, P_i^{out} is the outlet pressure of the compressor *i* and P_i^{in} is the inlet pressure of compressor *i*.

5) The temperature of all outlet streams in MCHE must be equivalent (Hasan *et al*., 2007).

$$\begin{aligned} T_{LNG101}^{out1} &= T_{LNG101}^{out2} = T_{LNG101}^{out3} \\ T_{LNG102}^{out1} &= T_{LNG102}^{out2} = T_{LNG102}^{out3} \\ T_{LNG103}^{out1} &= T_{LNG103}^{out2} \end{aligned} \qquad \text{Eq. 5-8}$$

where, T^{out} is the temperature of the outlet stream in MCHE for LNG.

6) All inlet streams of the mixer must remain at the same pressure.

7) The propane flow splitter divides the flow by a split ratio of:

$$0 < \frac{F_1^{out}}{F_1^{out} + F_2^{out}} < 1 \qquad \text{Eq. 5-9}$$

where, F_1^{out} and F_2^{out} represent the propane flow of the outlet streams of the splitter.

8) The outlet temperature of the cooler must be lower than that of the inlet:

$$T_j^{out} \le T_j^{in} \qquad \text{Eq. 5-10}$$

where, T_j^{out} is the outlet temperature of the cooler *j* and T_j^{in} is the inlet temperature of cooler *j*.

9) The *UA* of MCHE for the C3MR and C3MR-SP processes is specified and its value is: 13.3 MW/°C.

$$UA_{overall} = UA'_{overall} \qquad \text{Eq. 5-11}$$

where, $UA_{overall}$ and $UA'_{overall}$ represent the overall heat transfer coefficient and the area of MCHE before and after optimisation, respectively.

5.3 Results

We investigated the improvement of the efficiency of two processes: C3MR and C3MR-SP. Four different objective functions were evaluated using numerous decision variables and constraints described in Section 5.2. The optimisation methodology considers propane precooling and mixed refrigerant cycles. Alongside stream pressures and temperatures, the flow rates (and thus composition) of the mixed refrigerants are also inclusive of the optimisation variables. However, *UA* of MCHE must remain constant as this task deals with the performance optimisation of an existing plant.

Table 5-2 and Table 5-3 list the optimal results for the C3MR and C3MR-SP processes, respectively, using four different objective functions. The hot and cold composite curves

before and after the optimisations are presented in Figure 5-1 and Figure 5-2. Optimal results for both processes are compared and contrasted with literature results and are presented in Table 5-4.

5.3.1 Results of the C3MR process

The specific shaft work of the C3MR process from OF3 is found to approach the lowest energy consumption of 1469 MJ/tonne-LNG at a specified *UA* value of 13.31 MW/°C. The reduction in energy consumption results in the highest exergy efficiency of 31.41% and lowest OPEX of $125.78/tonne-LNG.

The composition curves for the C3MR process before and after optimisation are shown in Figure 5-1. OF3 involves reducing the heat load from 9.97×10^8 kJ/h to 5.88×10^8 kJ/h in MCHE while simultaneously minimising the difference between the hot and cold composite curves after optimisation. The closest approach between the composite curves is around 5.00 °C but results with a considerable temperature difference. The LMTD value for the C3MR process is 13.36 °C after optimisation. The optimal results for the C3MR process are shown in Table 5-2.

The most significant changes in the variables are noted for the mixed refrigerant compositions when the optimal values of OF3 (Table 5-2) are compared with those of the base case (Table 5-1). In the absence of propane in the optimal mixture of the OF3 refrigerant, the ethane content increases from 33.80% to 49.02% and that of i-butane increases from 0.10% to 7.84%, however the methane content decreases from 50.50% to 35.81%. In addition, lower refrigerant flow is required for the optimised process. In the base case, the flows of propane and mixed refrigerant are 36,740 kmol/h and 71,000 kmol/h, respectively; these values reduce to 31,900 kmol/h and 40,820 kmol/h after optimisation.

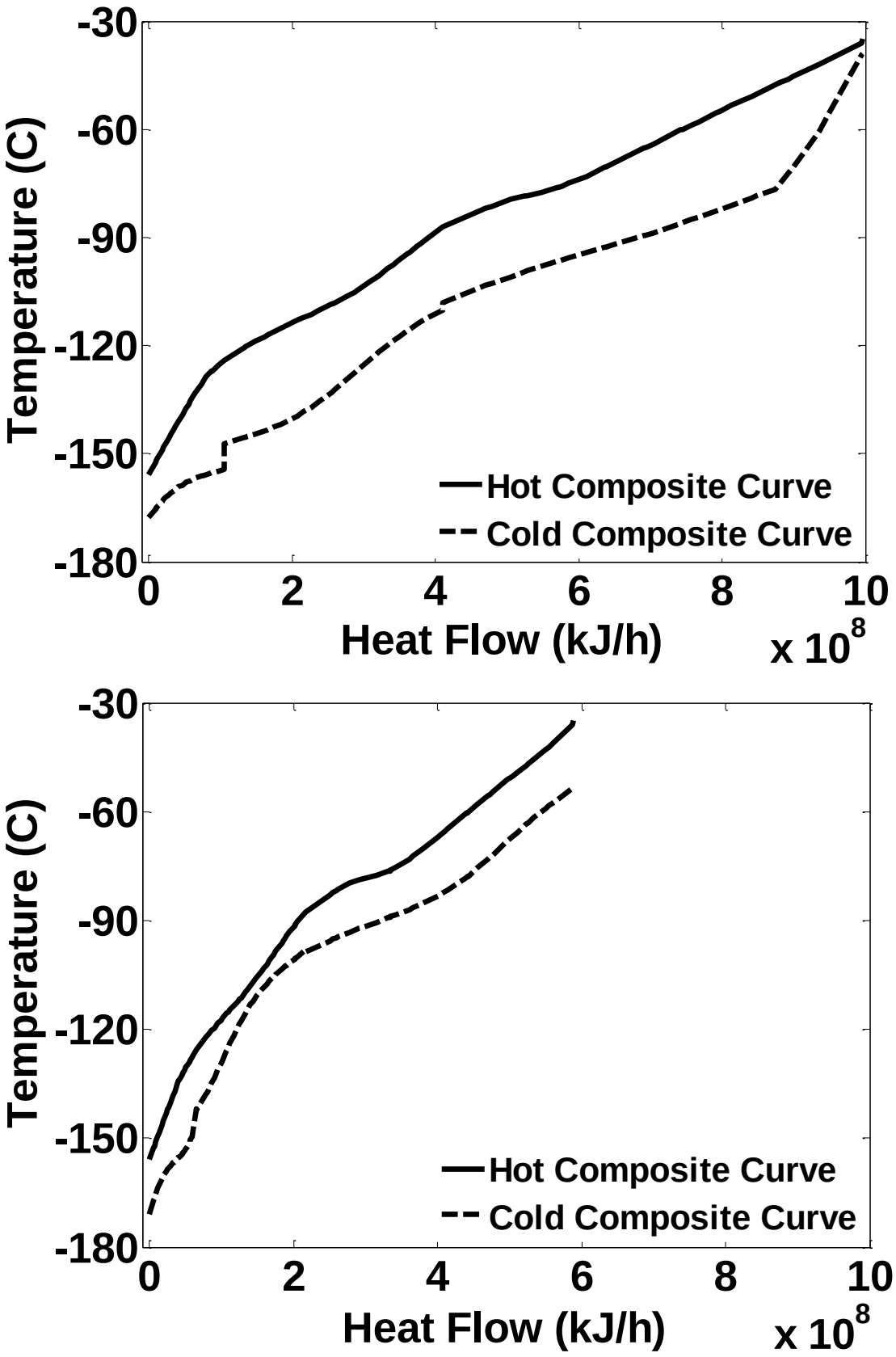

Figure 5-1 Composite curves for the C3MR process before (top) and after (bottom) optimisation.

Table 5-2 Optimal results for the C3MR process with a specified UA value of 13.31 MW/°C, using four objective functions.

Variables	Unit	OF1	OF2	OF3	OF4
Precooling refrigerant		Propane	Propane	Propane	Propane
Refrigerant flow	kmol/h	34,960	34,930	31,900	34,810
Refrigerant pressure	kPa	1081	1087	1098	1100
Subcooling refrigerant		Mixed	Mixed	Mixed	Mixed
Refrigerant flow	kmol/h	57,670	58,100	40,820	40,820
Refrigerant pressure	kPa	2629	2628	2633	2330
Refrigerant composition					
Nitrogen	mol%	8.35	8.70	7.31	8.34
Methane	mol%	47.40	47.76	35.81	36.06
Ethane	mol%	36.83	35.97	49.02	44.28
Propane	mol%	0.06	0.04	0.03	0.01
i-Butane	mol%	7.36	7.53	7.84	11.32
MCHE					
Outlet temperature of LNG-101	°C	-93.1	-89.3	-87.6	-87.2
Outlet temperature of LNG-102	°C	-117.0	-119.9	-125.6	-124.0
Energy consumption					
Total shaft work required	MW	186.4	191.0	145.0	155.5
Specific shaft work	MJ/tonne-LNG	1888	1935	1469	1575
Total cooling duty	MW	271.5	276.1	230.1	240.6
Cooling duty per unit of LNG produced	MJ/tonne-LNG	2750	2797	2331	2437
Exergy efficiency	%	24.4	23.8	31.4	29.3
Variable OPEX	$/tonne-LNG	130.56	131.09	125.78	127.00
LMTD	°C	18.23	18.26	13.36	14.14

5.3.2 Results of the C3MR-SP process

The specific shaft work obtained from OF1 is the lowest for the C3MR-SP process at a fixed *UA* value of 13.31 MW/°C. It is able to reduce the specific shaft work to 1464 MJ/tonne-LNG, thus resulting in a high exergy efficiency of 31.50% and low OPEX of $125.77/tonne-LNG. The optimal results for the C3MR-SP process are summarised in Table 5-3.

Figure 5-2 shows the composite curves for the C3MR-SP process before and after optimisation. The trends and the slopes of the two curves are similar to those of the C3MR process. However, the C3MR-SP process requires a larger heat load in MCHE than does the C3MR process before optimisation. After optimisation, the heat load of the C3MR-SP process is reduced from 9.33×10^8 kJ/h to 5.92×10^8 kJ/h. The closest temperature approach between the composite curves of the C3MR-SP process was approximately 5.36 °C with an overall LMTD of 13.72 °C.

Similar to the case of the C3MR process, the most significant changes in the optimised variables of the C3MR-SP process are associated with the mixed refrigerant composition. This is evident through comparing the optimal mixed refrigerant compositions of OF1 (Table 5-3) with those of the base case (Table 5-2): the ethane content increases from 33.80% to 48.36% and the i-butane content increases from 0.10% to 8.55%, while the methane content decreases from 50.50% to 37.00%. Moreover, the propane flow rate is reduced from 38,480 kmol/h to 35,760 kmol/h and the mixed refrigerant flow rate is reduced from 66,610 kmol/h to 40,450 kmol/h.

Table 5-3 Optimal results for the C3MR-SP process with a specified *UA* value of 13.31 MW/°C, using four objective functions.

Variables	**Unit**	**OF1**	**OF2**	**OF3**	**OF4**
Precooling refrigerant		Propane	Propane	Propane	Propane
Refrigerant flow	kmol/h	35,760	36,640	36,870	34,230
Refrigerant pressure	kPa	1083	1085	1101	1088
Subcooling refrigerant		Mixed	Mixed	Mixed	Mixed
Refrigerant flow	kmol/h	40,450	48,100	48,330	39,870
Refrigerant pressure	kPa	2376	2565	2632	2336
Refrigerant composition					
Nitrogen	mol%	5.84	9.78	10.28	8.36
Methane	mol%	37.00	42.85	43.18	35.84
Ethane	mol%	48.36	37.01	36.43	44.37
Propane	mol%	0.26	0.22	0.01	0.09
i-Butane	mol%	8.55	10.14	10.10	11.34
MCHE					
Outlet temperature of LNG-101	°C	-88.6	-93.4	-87.7	-88.2
Outlet temperature of LNG-102	°C	-125.7	-123.1	-123.7	-124.3
Energy consumption					
Total shaft work required	MW	144.5	171.2	176.8	153.9
Specific shaft work	MJ/tonne-LNG	1464	1734	1791	1559
Total cooling duty	MW	229.6	256.3	261.9	239.0
Cooling duty per unit of LNG produced	MJ/tonne-LNG	2326	2596	2653	2421
Exergy efficiency	%	31.50	26.6	25.7	29.6
Variable OPEX	$/tonne-LNG	125.77	128.85	129.50	126.86
LMTD	°C	13.18	16.38	16.16	13.92

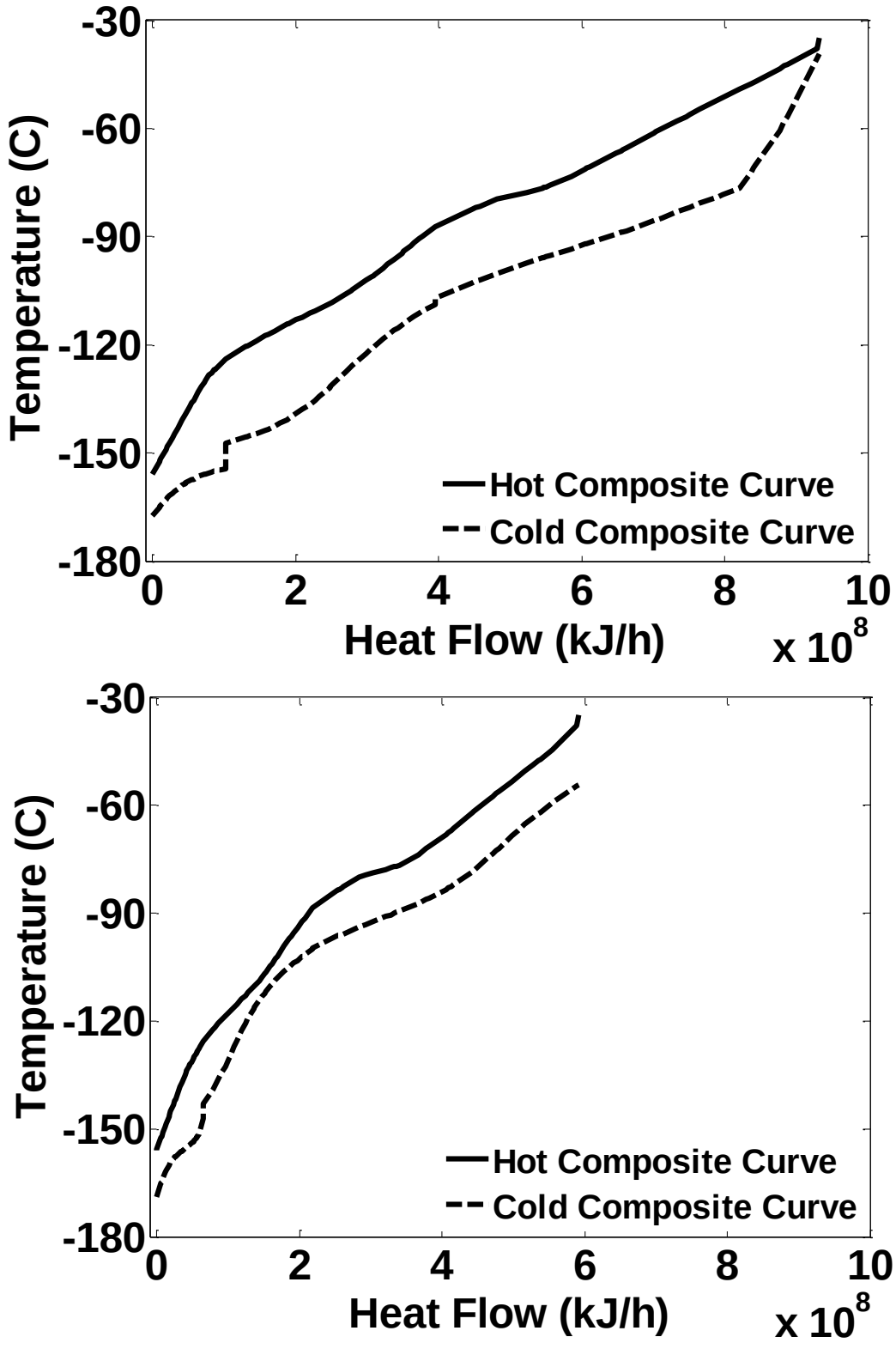

Figure 5-2 Composite curves for the C3MR-SP process before (top) and after (bottom) optimisation.

5.4 Comparison of the C3MR and C3MR-SP processes

The optimisation program can improve the process performance of the LNG plant when the feed gas flow rate and the *UA* are specified. The resulting comparison of the C3MR and C3MR-SP processes are revealed in Table 5-2 and Table 5-3. Both processes display similar levels of energy consumption, OPEX, and exergy efficiency at the given LNG production. The specific shaft work of the C3MR process is 1469 MJ/tonne-LNG and that of the C3MR-SP process is 1464 MJ/tonne-LNG at a specified *UA* value of 13.31 MW/°C. The cooling duty for the C3MR process is 2331 MJ/tonne-LNG, which is slightly higher than that of the C3MR-SP process (2326 MJ/tonne-LNG). Although C3MR-SP consumes slightly less energy than the C3MR process, it requires several additional equipment which may result in higher capital costs. Moreover, the OPEX for the C3MR and C3MR-SP processes are \$125.78/tonne-LNG and \$125.77/tonne-LNG, respectively. For the C3MR process, \$0.01/tonne-LNG in cost saving can be around \$30,000 saving per year. It is questionable, however, whether this saving is worth adding several additional unit operations in the C3MR process.

Figure 5-3 illustrates the distribution pattern of the exergy loss for the C3MR and C3MR-SP processes. The general equations for calculating the exergy loss and the exergy efficiency are provided in Section 3.6. It is evident from Figure 5-3 that the exergy distribution of the two processes is similar. All equipment of the liquefaction process reveal relatively small exergy losses. The compression system is the major source of the overall exergy losses in the process at approximately 31% for the C3MR process and 33% for the C3MR-SP process. Another source of major exergy loss is incurred by the MCHE which accounts for 28% for the C3MR process and 29% for the C3MR-SP process. It is evident that any improvements in the performance of the compressors and MCHE will consequently bring out about a significant increase in the exergy efficiency of the overall refrigeration system.

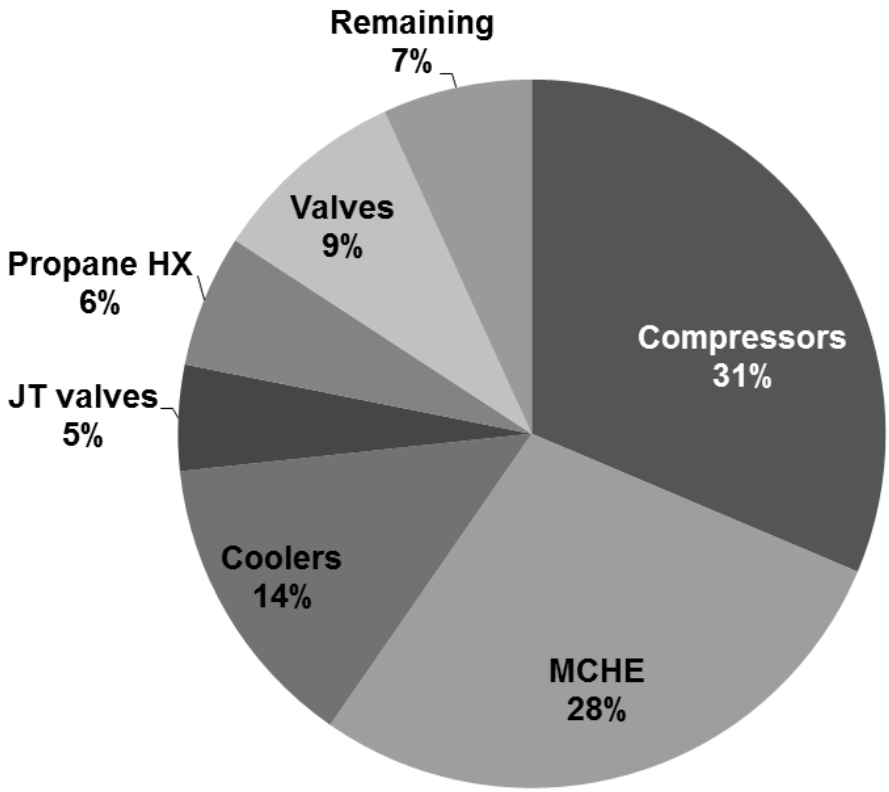

(a)

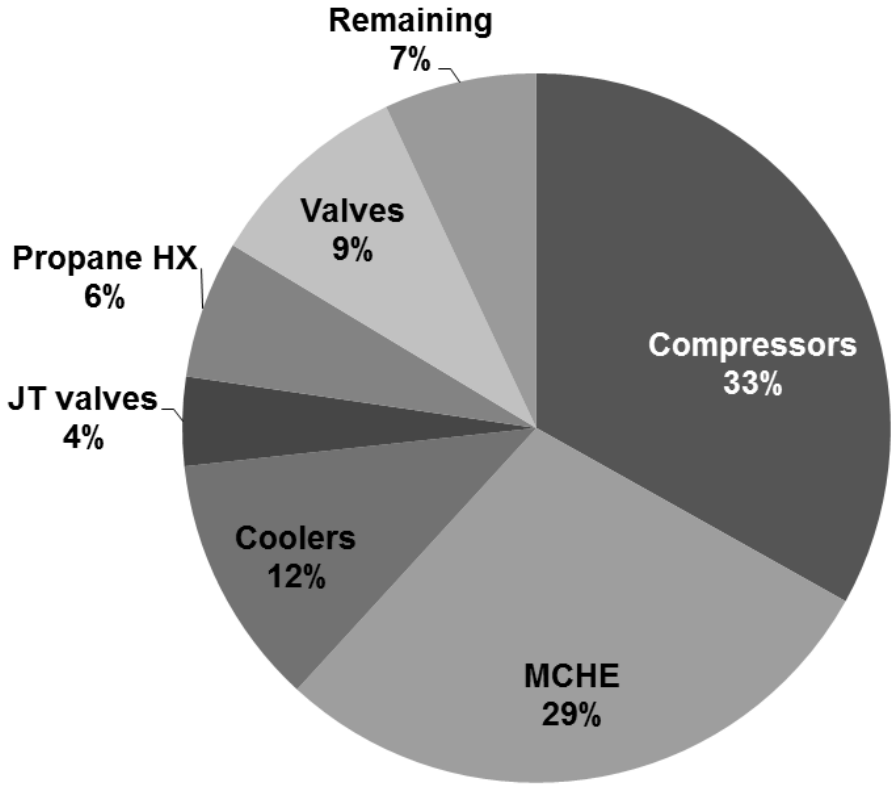

(b)

Figure 5-3 Distribution of exergy loss in the (a) C3MR process, and (b) C3MR-SP process optimisation.

It is noteworthy that although the LMTD values of MCHE for both the C3MR and C3MR-SP processes were reduced notably (from 20.81 °C to 13.36 °C for C3MR process and from 19.73 °C to 13.18 °C for C3MR-SP process), the optimal LMTD values remain relatively high. This limitation and the reasons behind it will be discussed in the following section.

5.5 Comparison of the optimal results with the literature

The optimal results of this study are comparable with those of the C3MR process obtained from the literature. The literature review results of the SMR process are presented in Table 5-4 in order to provide a broader comparison. There is a general consensus amongst the literature and this study concerning the impact of the refrigerant components and compositions on the overall liquefaction process performance. The optimal refrigerant composition of this study is in agreement with that of Hatcher *et al*. (2012): a higher ratio of methane (around 35%) and almost 50% ethane. The absence of propane is found in the optimal refrigerant composition.

The specific shaft work for this study is lower than that found in the literature including commercial PRICO, Cao *et al*. (2006), Jacobsen et al. (2013), and Khan *et al*. (2012). The specific shaft work reported by Lee *et al*. (2002), Alabdulkarem *et al*. (2011), and Mokarizadeh Haghighi Shirazi et al. (2010) are lower than our values herein from OF3 for the C3MR process and OF1 for the C3MR-SP process. However, the comparison of the specific shaft work of other studies with ours would be impractical without taking into account the factors which may have significantly affected the overall power consumption. These factors are the methane content of the feed gas, the pressure of feed gas and the LNG product, and the *UA* of MCHE.

The high portion of methane in natural gas can produce a high quality LNG product (low Wobbe Index), but subsequently causes elevated power consumption in the liquefaction

process. This is due to the lower boiling point of methane in contrast to the heavier hydrocarbons. In this study, the feed natural gas contains 96.92% of methane which is higher than that found in other literature works. Remeljej et al. (2006) used almost the same percentage of methane in natural gas as in our study.

The pressure of the feed natural gas and the LNG product are further critical parameters that affect the accuracy of our comparison. The high pressure of the natural gas not only results in lower energy consumption for liquefaction, but also increases the compactness of the LNG process, i.e. requires less area for heat transfer. In this study, natural gas is fed into the process at a pressure of 5000 kPa. In the literature, this pressure varies from 4000 kPa to 6000 kPa. In addition, the storage of the LNG product in cryogenic tanks brings about relatively lower costs at atmospheric pressure. LNG was produced at atmospheric pressure throughout the literature except for Cao et al. (2006) who used pressures of 200 kPa for their LNG product.

Moreover, the comparison of exergy efficiency reported in literature and that reported in our study may be inaccurate, as there is a non-standardised definition and equation for exergy efficiency in literature (Brodyansky et al., 1994, Bejan et al., 1996, Kotas, 1980, Szargut et al., 1988, Marmolejo-Correa et al., 2012). Several equations proposed to calculate exergy efficiency for the same process gave dissimilar results. For example, the exergy efficiency for the SMR process calculated by Khan et al. (2013a) is 50.77%. They achieved such high exergy efficiency with a high specific shaft work of 1370 MJ/tonne-LNG. However, our specific shaft work is 1046.4 MJ/tonne-LNG and exergy efficiency is 44.1%. These results are also inconsistent with the results provided by Mokarizadeh Haghighi Shirazi et al. (2010).

The most important factor influencing the power consumption is associated with the *UA* of MCHE. Aspelund *et al*. (2010) concluded that the higher the *UA* value, the better the thermal

performance of the heat exchangers for the same LNG production. It is more appropriate to compare *UA* per unit of LNG produced rather than *UA* alone due to various natural gas flow rates in literature. For our base-case, the *UA* per unit of LNG produced is 135 MJ/°C.tonne-LNG. It is much lower than those given in Aspelund *et al*. (2010), Khan *et al*. (2012), Jacobsen et al. (2013), and Khan et al. (2013a). Lee *et al*. (2002), Mokarizadeh Haghighi Shirazi et al. (2010), and Alabdulkarem *et al*. (2011) achieved lower specific shaft work than ours via OF3 for the C3MR process and OF1 for the C3MR-SP process but they did not disclose their *UA* value of the heat exchangers. Therefore comparison of our optimal shaft work with theirs is not possible as their *UA* values are unknown.

Specific shaft work and specific *UA* are both related to the natural gas flow. If either the *UA* or natural gas flow is permitted to change, it is possible to achieve improved results of optimisation. To investigate these optimisation issues, two scenarios associated with the variation of the natural gas flow for a given *UA* and the variation of *UA* at a constant flow rate of natural gas were carried out.

Scenario 1: Change of feed natural gas flow rate at fixed *UA*

In Scenario 1, MCHE of the C3MR process allows us to manipulate the natural gas flow rate from the base case flow of 3.73×10^5 kg/h to 55% of base case natural gas flow, at a fixed *UA* of 13.31 MW/°C. Figure 5-4 shows that the specific shaft work of the C3MR process decreases from 1464.1 MJ/tonne-LNG to 1361.5 MJ/tonne-LNG, as the feed natural gas flow decreases. Natural gas is supplied at a flow rate of 2.05×10^5 kg/h, accompanied by the lowest specific OPEX of $213.6/tonne-LNG and the highest exergy efficiency of 33.87%. Clearly, this may be against the process throughput.

As the feed natural gas flow is decreased, a lower refrigerant flow rate with decreased power consumption is consequently required to cool it down to the desired temperature. This results in lower LMTD for MCHE. The *UA* per unit of LNG produced increases since the natural gas flow decreases at a fixed *UA*.

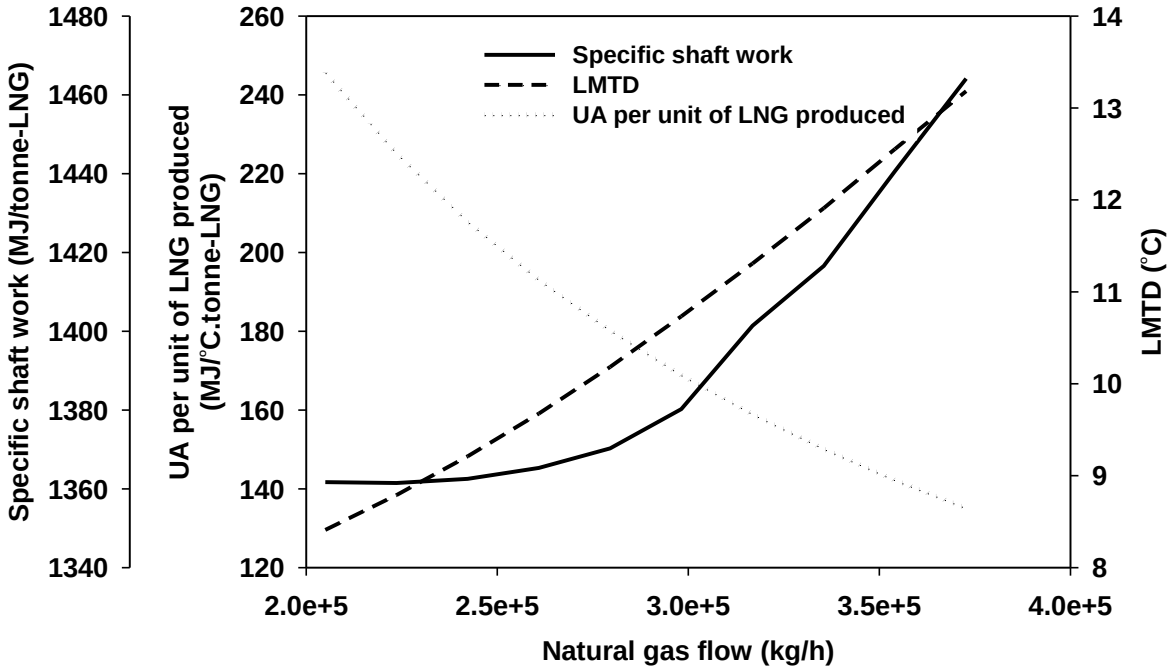

Figure 5-4 The effects of varying natural gas flow rate on the performance of the C3MR process with a *UA* value of 13.31 MW/°C.

Scenario 2: Change of *UA* at a constant flow rate of natural gas

In Scenario 2, the *UA* value of C3MR process increases from 13.31 MW/°C to 220.7 MW/°C at a constant flow rate of natural gas. Figure 5-5 shows the effect of varying *UA* on the performance of C3MR process. When the *UA* value is fixed at 13.36 °C, the specific shaft work and LMTD for C3MR process are 1469 MJ/tonne-LNG and 13.36 °C. By increasing the base case *UA* value to 220.7 MW/°C, the specific shaft work is capable of decreasing to 1046.4 MJ/tonne-LNG; the LMTD value can then reach 2.35 °C. The overall performance of MCHE is shown in Figure 5-6.

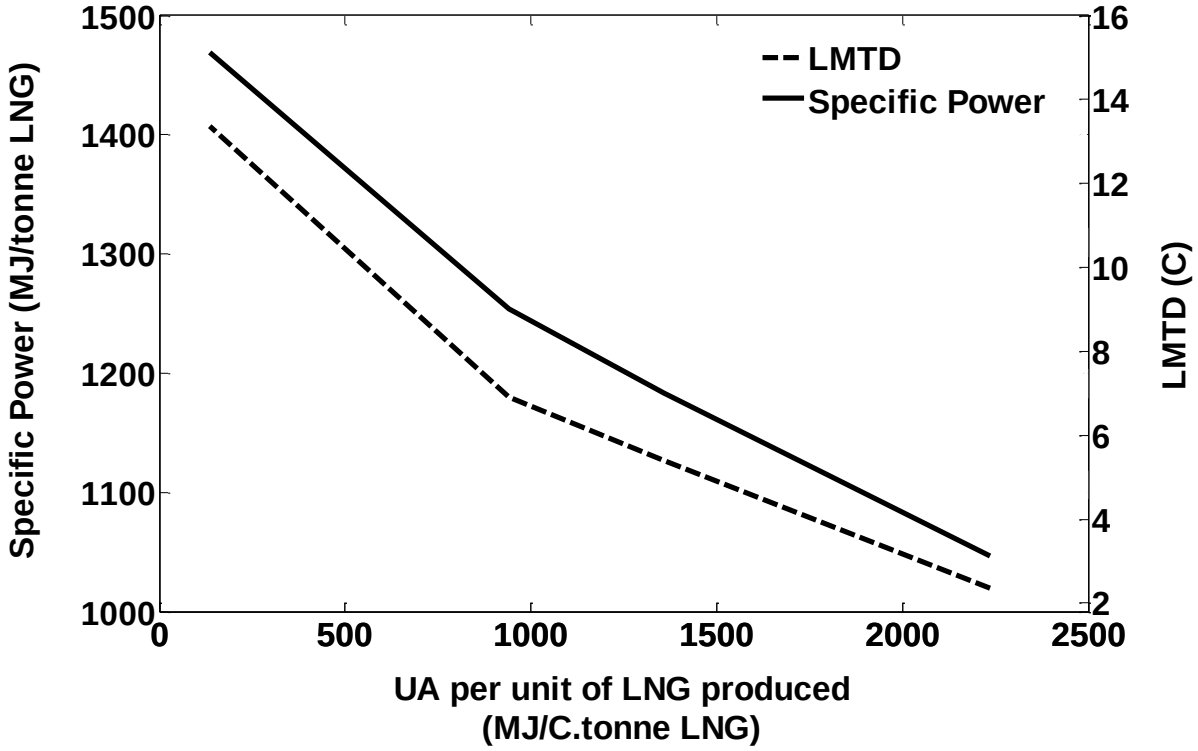

Figure 5-5 The effects of *UA* change on the performance of the C3MR process at a constant flow rate of natural gas flow.

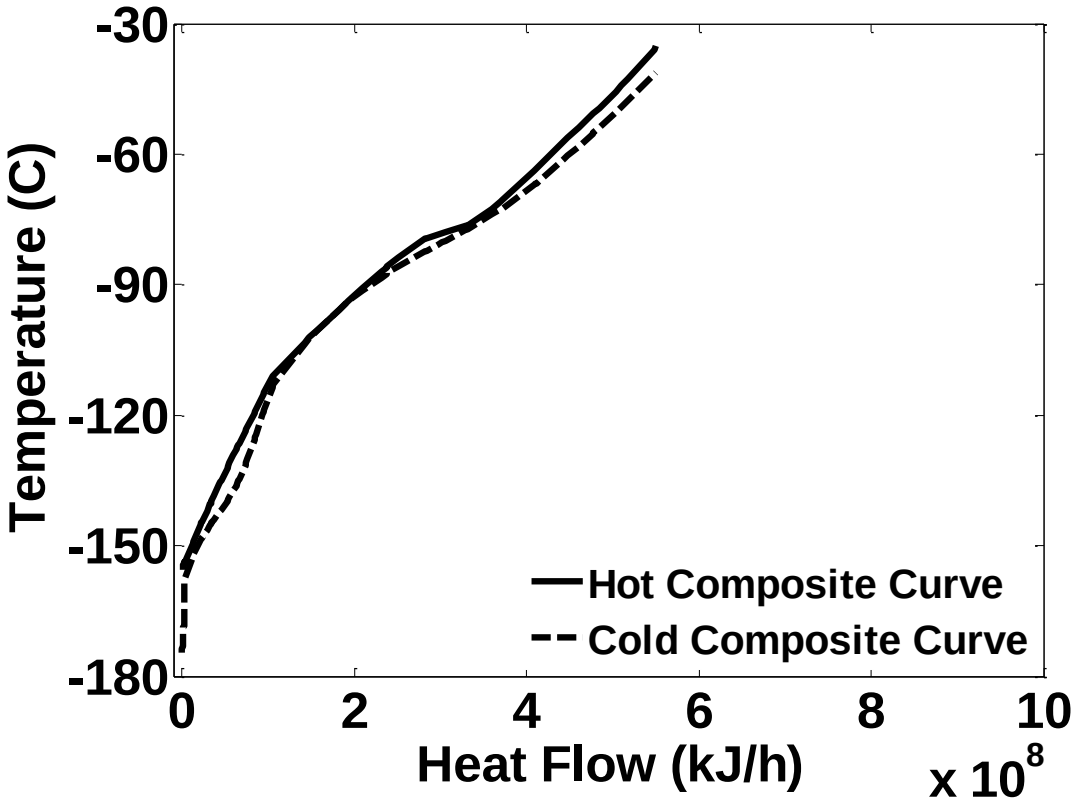

Figure 5-6 Composite curves for the C3MR process with a specific shaft work of 1046.4 MJ/tonne-LNG and *UA* value of 220.7 MW/°C.

It is apparent from Figure 5-5 that specific shaft work and LMTD vary with an increase in the *UA* of MCHE. To increase the *UA* of MCHE, the specific shaft work and LMTD must be decreased. Therefore, the optimisation solution obtained may not be the most optimal result for the given feed gas flow rate and *UA*. There is a unique optimal *UA* value which varies with the fixed *UA* for the base case. If the *UA* value is permitted to alter, significant maximisation of the energy efficiency would be possible. However, an increase in the heat exchanger area can raise the CAPEX.

Generally, this optimisation problem concerning the variation of the *UA* is relevant to the process design stage. Since, the assumption for this study is that the process has already been installed to produce a certain amount of LNG, the change in the *UA* of MCHE or feed natural gas flow is not permissible, and thus the best achievable results are those given in Table 5-2 and Table 5-3.

5.6 Conclusions

Optimisation can improve the operational performance of the C3MR and C3MR-SP processes for a given LNG production rate when the *UA* value is specified as 13.31 MW/°C. The most optimal specific shaft work for the C3MR and C3MR-SP processes are significantly close: 1469 MJ/tonne-LNG from OF3 and 1464 MJ/tonne-LNG from OF1, respectively. The exergy analysis results regarding the refrigeration system indicate that the major exergy losses are contribution of the compression system and the driving forces across the MCHE. Therefore, there is great potential for performance improvement via decreasing the temperature difference between the process and refrigerant streams in MCHE in order to reduce the shaft work in compressors.

Based on the optimisation results and exergy analysis, a sensitivity study for C3MR process was carried out to examine the impact of the natural gas flow and *UA* on energy

consumption. The optimal results from Scenario 2 show that the optimisation of the C3MR process with enormous flexibility of the *UA* can save more energy in the liquefaction process than that of Scenario 1 which allows variations in the natural gas flow rate at a fixed *UA*. In Scenario 2, the specific shaft work reduces to 1046.4 MJ/tonne-LNG while the *UA* value increases to 220.7 MW/°C. In future work, it is recommended to optimise the liquefaction processes by varying the natural gas flow rate. Any performance comparisons of specific shaft work and LMTD should consider the methane content of the feed natural gas, the pressure of the feed natural gas and LNG product, and *UA* of MCHE in order to formulate a meaningful discussion.

Table 5-4 Optimal results obtained from literature.

Parameters	Unit	Commercial PRICO	Lee *et al.* (2002)	Remeljej et al. (2006)	Aspelund *et al.* (2010) Case 1	Aspelund *et al.* (2010) Case 2	Jacobsen et al. (2013)	Cao *et al.* (2006)	Mokarizadeh Haghighi Shirazi et al. (2010)	Khan *et al.* (2012)	Khan et al. (2013a)	Alabdulkarem *et al.* (2011)	Hatcher *et al.* (2012)	Wang *et al.* (2012)	This study: OF3 for C3MR (Table 5-2)	This study: OF1 for C3MR-SP (Table 5-3)	This study: Results from sensitivity study
Process		SMR	SMR	SMR	SMR	SMR	SMR	SMR	SMR	SMR	SMR	C3MR	C3MR	C3MR	C3MR	C3MR-SP	C3MR
Natural gas																	
Temperature	°C	-	25	25	-	-	30	32	25	32	32	-	38	-	25	25	25
Pressure	kPa	-	-	5500	6000	6000	4000	5000	5500	5500	5000	-	4200	-	5000	5000	5000
Methane	mol%	-	-	96.93	95.89	95.89	89.7	82.0	82.0	91.34	91.35	85.995	81.7	90.97	96.92	96.92	96.92
LNG																	
Production	kg/h	-	-	81,360	360,000	360,000	268,600	74.95	3253	1.0	1.0	356,004	-	-	355,400	355,400	355,400
Temperature	°C	-	-163	-165	-163.7	-163.7	-157	-150.7	-161	-157	≤-157	-160	-162	-160	-161.3	-161.3	-161.3
Pressure	kPa	-	-	101.3	105	105	-	200		-	-	101.3	101.3	100	101.3	101.3	101.3
Precooling cycle																	
Refrigerant type		-	-	-	-	-	-	-	-	-	-	Propane	Propane	Propane	Propane	Propane	Propane
Refrigerant flow	kmol/h	-	-	-	-	-	-	-	-	-	-	36,490	-	-	31,900	35,760	31,410
Refrigerant pressure	kPa	-	-	-	-	-	-	-	-	-	-	1540	-	-	1098	1083	1082
Mixed refrigerant cycle																	
Refrigerant type		Mixed	Mixed	Mixed	Mixed	Mixed	Mixed	Mixed	Mixed	Mixed	Mixed	Mixed	Mixed	Mixed	Mixed	Mixed	Mixed
Refrigerant flow	kmol/h	-	104.3	12,960	55,870	53,620	60,984	60.25	483.81	0.1248	-	37,450	36,731	384.6	40,820	40,450	32,700
Refrigerant pressure	kPa	-	3400	-	3126	5237	553	2600	3950	4785	4650	4000	2689	5500	2633	2376	2308
Refrigerant composition																	
Nitrogen	mol%	-	11.0	-	10.5	15.5	-	1.0	14.2	7.82	6.77	9.0	7.3	8.0	7.31	5.84	4.90
Methane	mol%	-	27.3	-	26.9	28.8	-	40.0	29.7	23.13	24.63	36.0	36.1	46.0	35.81	37.00	33.34
Ethane	mol%	-	35.6	-	37.6	34.5	-	40.0	22.6	19.12	15.94	47.0	48.8	46.0	49.02	48.36	49.87
Propane	mol%	-	5.2	-	2.3	2.2	-	19.0	13.6	49.92	52.66	8.0	0.0	-	0.03	0.26	3.76
i-Butane	mol%	-	20.9	-	22.7	19.0	-	-	13.2	-	-	-	7.7	-	7.84	8.55	8.12
n-Butane	mol%	-	-	-	-	-	-	-	6.7	-	-	-	-	-	-	-	-
MCHE																	
UA	MW/°C.	-	-	-	376.9	48.6	55.4	-	-	0.000111	0.000142	-	-	0.09883	13.31	13.31	220.7
***UA* per unit of LNG produced**	MJ/°C.tonne-LNG	-	-	-	3769	486	742.5	-		399.3	509.7	-		-	135.0	135.0	2235.6
LMTD	°C	-	-	-	0.85	6.80	0.7	-		7.852	6.94	5.24/4.91		13.83-15.48	13.36	13.18	2.35
Energy consumption																	
Total shaft work required	MW	-	26.6	16.5	110.5	144.4	116.4	0.12923	0.987	0.0004244	0.000381	100.78	-	1.475	145.0	144.5	103.3
Specific shaft work	MJ/tonne-LNG	1485.0	1126.7	1238.4	1105.0	1444.0	1560.0	1724.2	1092.4	1527.8	1370.0	1019.11	-	-	1469.0	1464.0	1046.4
Exergy efficiency	%	-	-	-	-	-	-	-	37.1	-	50.77	-	-	-	31.4	31.5	44.1

CHAPTER 6. THE EFFECT OF FEED GAS CONDITIONS ON THE PERFORMANCE OF THE MIXED REFRIGERANT PROCESS

6.1 Introduction

This chapter focuses on the understanding, through sensitivity analysis, of the effects of upstream well conditions, including gas composition, gas flow rate, gas pressure, and gas temperature on the process performance and LNG product of the C3MR process.

Additionally, an investigation was conducted on the effect of varying feed gas conditions on the alternative configurations of the C3MR process which are: a frontend NGL recovery unit in the upstream of the LNG value chain and an NGL recovery integrated within the liquefaction unit.

6.2 Sensitivity analysis

Sensitivity analysis was carried out using the C3MR model shown in Figure 3-3 and its performance was assessed under the initial conditions and assumptions as aforementioned in Chapter 3.

6.2.1 Assumptions

The C3MR process is modelled and simulated under the same input conditions and assumptions as in Section 3.2. For the sensitivity study, the feed gas conditions vary based on the following restrictions:

1) The temperature variation of the feed gas is within the range of 10 °C and 50 °C.
2) The pressure variation of the feed gas is within the range of 3000 kPa and 5000 kPa.
3) The flow rate variation of the feed gas is within the range of ±20% of its design value.
4) The compositions of the natural gas on which the sensitivity analysis was conducted in this study are listed in Table 6-1.

5) The *UA* of MCHE is fixed at the design value of 16.39 MW/°C.

For the NGL cycle,

6) The gas splitting ratio to the bottom column stream (T-401 to C-401) is in the range of 0.4 and 0.65.

The operating conditions used for simulating NGL recovery are listed in [1]Refer to Section 3.2
[2]NG1 represents feed gas composition case 1

7) Table 6-2.

Table 6-1 Feed gas composition (in unit of mole fraction).

Feed composition	Methane	Ethane	Propane	n-butane	Nitrogen	Total
Base case[1]	96.92	2.94	0.06	0.01	0.07	100
NG1[2]	96.70	3.15	0.06	0.01	0.07	100
NG2	96.31	3.53	0.07	0.01	0.08	100
NG3	94.80	4.96	0.10	0.02	0.12	100
NG4	91.63	7.99	0.16	0.03	0.19	100
NG5	84.55	14.75	0.30	0.05	0.35	100

[1]Refer to Section 3.2

[2]NG1 represents feed gas composition case 1

Table 6-2 Column operating conditions.

Operating conditions	Value	Unit
Total number of trays	40	-
Column top stream pressure	2689	kPa
Column bottom stream pressure	2758	kPa

6.2.2 Performance equations

The following equations are used for calculating the total power consumption and variable operating cost of the C3MR process. Total shaft work (W_{Total}) is expressed by Eq. 6-1:

$$W_{Total} = \sum_{i=1}^{n} W_i \qquad \text{Eq. 6-1}$$

where, W_i is the shaft work used at compressor i

OPEX includes electricity, water, and feed natural gas. It is represented by Eq. 6-2:

$$OPEX = \frac{P_{Elec} \sum_{i=1}^{n} W_i + P_{Water} \sum_{j=1}^{m} Q_j + P_{NG} F_{NG}}{F_{LNG}} \qquad \text{Eq. 6-2}$$

where, P_{Elec} is electricity price, P_{Water} is cooling water price, P_{NG} is the price of feed natural gas.

6.3 Case 1: C3MR

6.3.1 Variation in natural gas composition only

The effect of varying the natural gas composition at a constant temperature of 25 °C and pressure of 5000 kPa was studied. It can be seen in Table 6-1 that six different compositions of natural gas were scrutinised. The mole fraction of methane in the natural gas is adjusted from its base value of 96.92% to 84.55% with 10% decrements of the component mole flow of methane; meanwhile, the mole flow of the remaining components was maintained at a constant level, as described in Table 6-1.

The results in Table 6-3 and Figure 6-1 indicate that for a given amount of feed gas, a decrease of 12.37 mol% in methane's concentration results in the reduction of the specific shaft work by 5.17%; however, this only increases the LNG production by 0.76%. This is

because methane reduction increases the molecular weight of a natural gas mixture. A feed natural gas with lower methane content and lower dew point requires less refrigeration capacity; consequently, this would potentially produce more LNG product. According to Clementino *et al*. (2014), plant operation and LNG production are also sensitive to pressure, temperature, and flow rate variation of the feed natural gas.

Table 6-3 Results for the C3MR process with varying feed gas compositions.

Variables	**Unit**	**Base case**	**NG1**	**NG2**	**NG3**	**NG4**	**NG5**
Natural gas							
Methane	%mol	96.92	96.70	96.31	94.80	91.63	84.55
Feed mass flow	kg/h	399,000	399,000	399,000	399,000	399,000	399,000
LNG production	kg/h	380,467	380,559	380,636	381,033	381,843	383,406
Mixed refrigerant							
Refrigerant flow	kmol/h	73,600	73,545	73,433	73,019	72,190	70,316
Refrigerant pressure	kPa	2630	2630	2630	2630	2630	2630
Energy consumption							
Total shaft work	MW	245.3	245.1	244.8	243.5	240.9	235.0
Specific shaft work	MJ/tonne-LNG	2321.0	2318.8	2315.0	2300.3	2270.9	2206.6
Specific OPEX	$/tonne-LNG	128.33	128.28	128.22	127.94	127.39	126.24

Three scenarios were carried out: (i) change in feed flow rate, (ii) change in feed pressure, and (iii) change in feed temperature. In each scenario, feed gas composition varies based on Table 6-1.

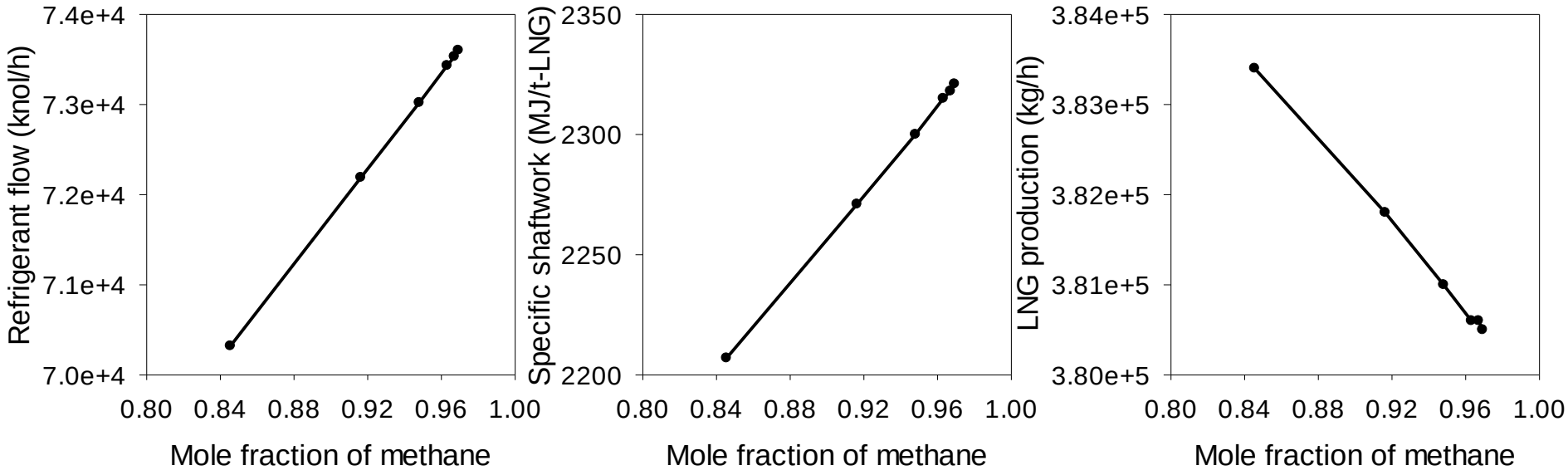

Figure 6-1 The effect of varying feed natural gas compositions on refrigerant flow, specific shaft work and LNG production (T = 25 °C and P = 5000 kPa).

6.3.2 Scenario 1: Variation in the natural gas composition and the feed flow rate

This scenario examined the variation in the natural gas composition and the feed natural gas flow rate. The results for the C3MR process with varying feed gas flow rates are shown in Table 6-4 and Figure 6-2. It is clear that a decline in the natural gas flow rate with a constant composition requires less cooling duty provided by the C3MR process at a fixed *UA*, which agrees with the findings of Wang *et al*. (2013).

Table 6-4 Results for the C3MR process with varying feed gas flow rates.

Variables	**Unit**	**Flow 1**	**Flow 2**	**Base case**	**Flow 3**	**Flow 4**
Natural gas						
Methane	%mol	96.92	96.92	96.92	96.92	96.92
Feed mass flow	kg/h	319,200	359,100	399,000	438,900	478,800
LNG production	kg/h	304,374	342,421	380,468	418,514	456,561
Mixed refrigerant						
Refrigerant flow	kmol/h	58,556	65,966	73,600	82,115	96,406
Refrigerant pressure	kPa	2630	2630	2630	2630	2630
Energy consumption						
Total shaft work	MW	195.4	220.1	245.3	272.8	315.4
Specific shaft work	MJ/tonne-LNG	2311.0	2313.6	2321.0	2346.9	2487.2
Specific OPEX	$/tonne-LNG	153.61	139.53	128.33	119.40	113.30

As natural gas flow rate decreases from 4.788×10^5 kg/h to 3.129×10^5 kg/h, the base case natural gas composition with the highest methane content brings about the maximum effect on the cooling duty. This results in the largest decrease of specific shaft work by 7.08% for the base case, alongside the smallest decrease by 1.34% for NG5. However, specific OPEX increases since natural gas flow rate decreases at a fixed *UA*. Specific OPEX for base case natural gas composition increases from $113.3/tonne-LNG to $153.6/tonne-LNG. Similar trends were observed for the four remaining feed gas compositions.

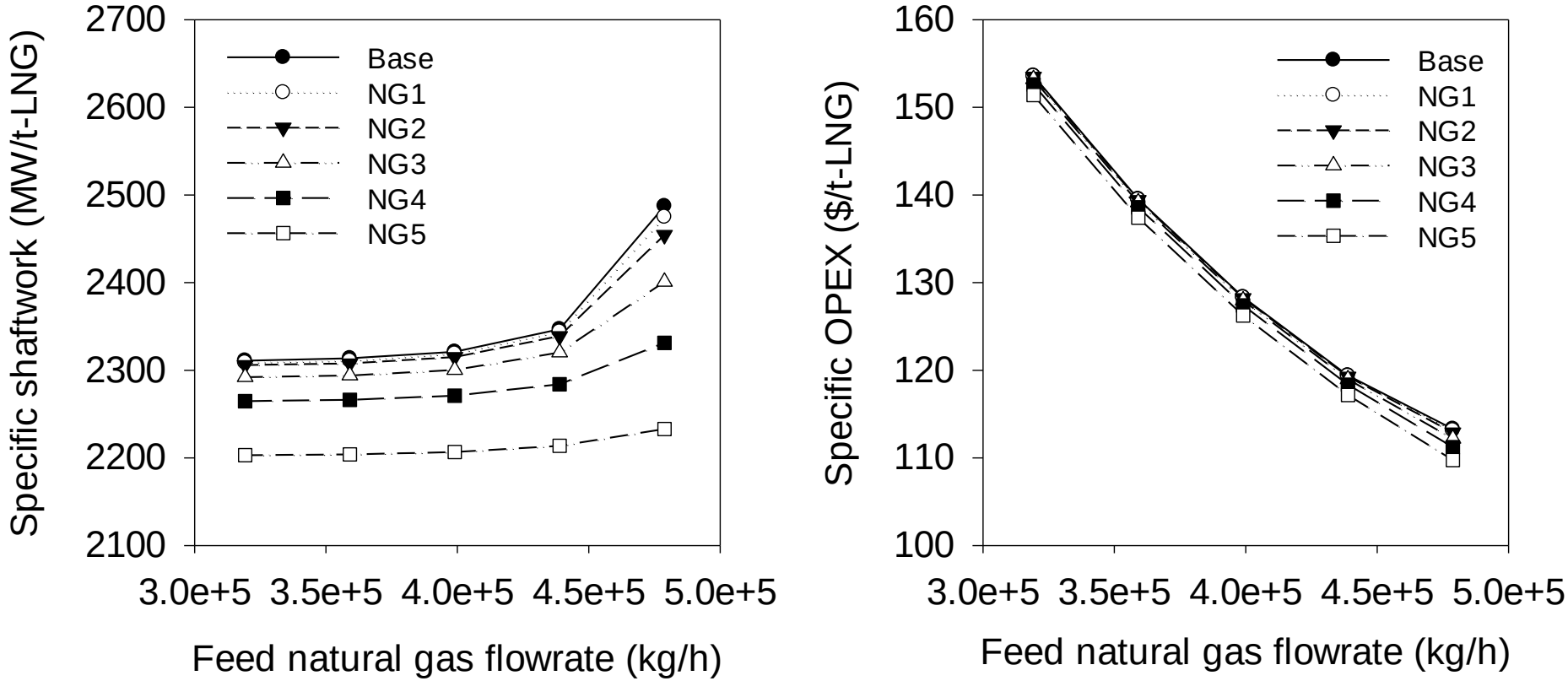

Figure 6-2 The effect of feed natural gas flow rate change on specific shaft work and specific OPEX (T = 25 °C and P = 5000 kPa).

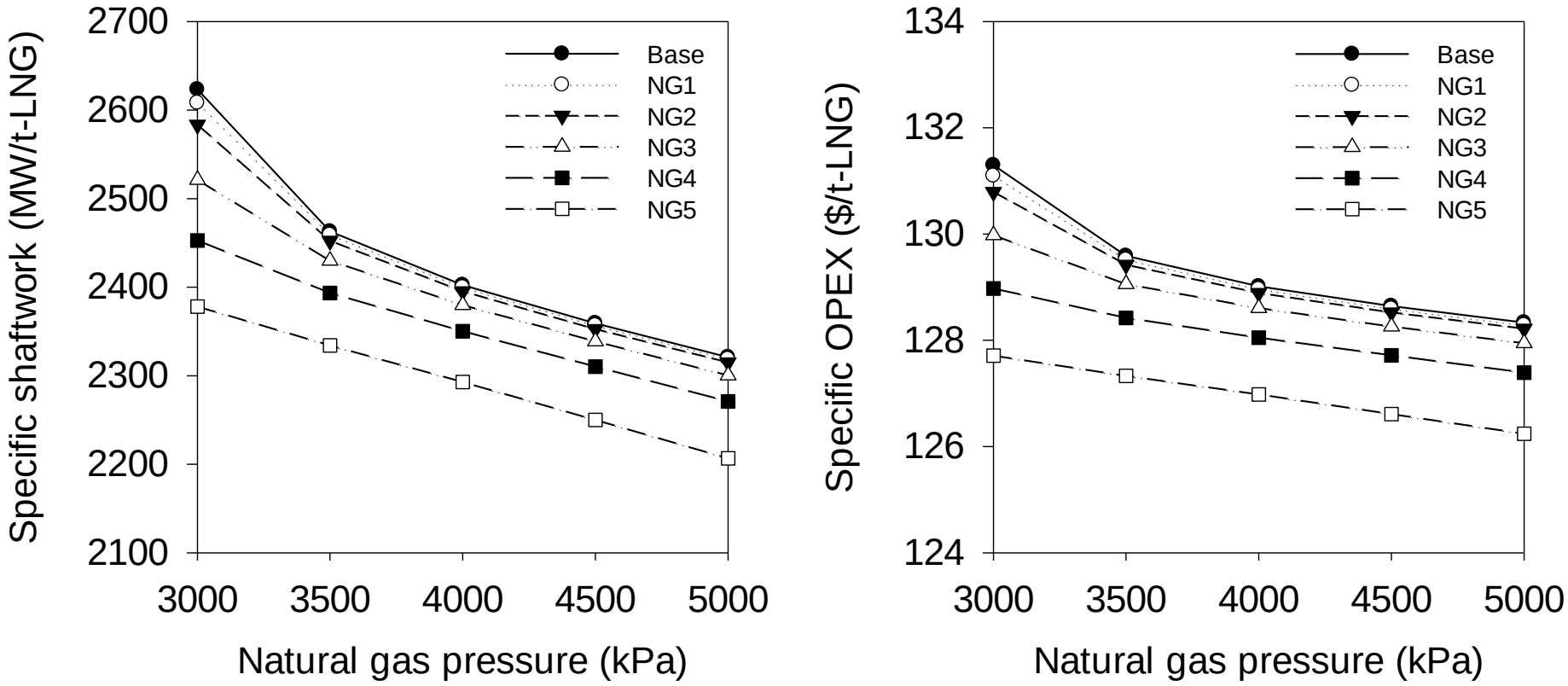

Figure 6-3 The effect of feed natural gas pressure change on specific shaft work and specific OPEX (T = 25 °C).

6.3.3 Scenario 2: Variation in the natural gas composition and the feed pressure

The feed pressure of a natural gas well declines over time. The scenario herein examines the effect of supplying natural gas with varying composition and pressure on the specific shaft work at a constant temperature of 25 °C, as shown in Figure 6-3. The reference specific shaft work is obtained at a feed pressure of 5000 kPa. It is evident from Table 6-5 and Figure 6-3 that with a reduction in the feed gas pressure, a given amount of natural gas requires higher specific shaft work to liquefy, thus resulting in higher specific OPEX.

Table 6-5 Results for the C3MR process with varying feed gas pressures.

Variables	**Unit**	**P1**	**P2**	**P3**	**P4**	**Base case**
Natural gas						
Methane	%mol	96.92	96.92	96.92	96.92	96.92
Feed mass flow	kg/h	399,000	399,000	399,000	399,000	399,000
Feed pressure	kPa	3000	3500	4000	4500	5000
LNG production	kg/h	382,311	381,854	381,392	380,932	380,468
Mixed refrigerant						
Refrigerant flow	kmol/h	58,556	65,966	73,600	82,115	96,406
Refrigerant pressure	kPa	2630	2630	2630	2630	2630
Energy consumption						
Total shaft work	MW	278.6	261.3	254.5	249.6	245.3
Specific shaft work	MJ/tonne-LNG	2623.4	2463.0	2402.4	2359.1	2321.0
Specific OPEX	$/tonne-LNG	131.3	129.6	129.0	128.6	128.3

6.3.4 Scenario 3: Variation in the natural gas composition and the feed temperature

Figure 6-4 shows the effect of the variation of natural gas temperature on specific shaft work at a constant feed pressure of 5000 kPa. The temperature variation of the natural gas is within

a range of 10 °C and 50 °C. It is evident from Figure 6-4 that temperature variation of feed natural gas has an insignificant effect on specific shaft work. At a constant pressure, the specific shaft work increases by 0.73% for the base case and 0.76% for NG5 when feed natural gas temperature is increased by 40 °C. For the base case, the natural gas contains more methane in contrast to other cases, hence causing an increased requirement for compression work in order to produce the same amount of LNG.

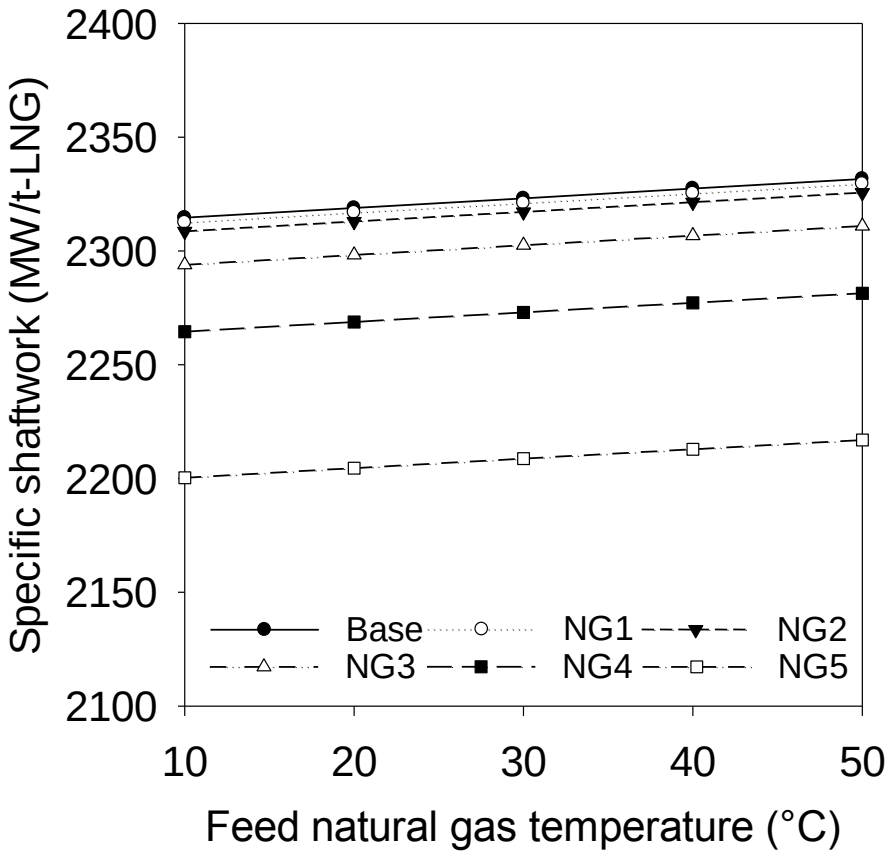

Figure 6-4 The effect of feed natural gas temperature change on specific shaft work (P = 5000 kPa).

6.4 Case 2: NGL recovery in the C3MR process

Heavier hydrocarbons are separated from natural gas in order to recover as NGL. This process brings out an improvement in energy efficiency in the production of LNG. There are two common configurations of NGL recovery and natural gas liquefaction: a frontend NGL

recovery unit in the upstream of the LNG value chain and an NGL recovery integrated within the liquefaction unit.

According to Case 1, three scenarios were carried out so as to explain the differences between the two configurations under varying feed conditions (feed flow rate and feed composition) and operating conditions (gas splitting ratio to the column bottom stream). For comparison, they are simulated using the equivalent feed gas conditions, refrigerant mixture, operating conditions, and LNG production. The aforementioned configurations employ the C3MR process and a patented NGL recovery process, studied by Mak et al. (2013), as the basis. The main difference between the two configurations is the location of the NGL recovery within the gas liquefaction plant.

Figure 6-5 shows the flow diagram of a frontend NGL recovery and C3MR process (a frontend NGL/C3MR). A portion of the vapour is condensed against the column overhead stream and the remaining gas is expanded through a turbo-expander before entering the scrub column to remove the heavier hydrocarbons. The column overhead stream is recompressed and then cooled through a refrigeration section.

C3MR consists of a precooling cycle and a subcooling cycle. The treated natural gas and MR is partially cooled to approximately -35 °C in a propane precooling cycle. The precooled MR is then separated into gaseous stream and liquid stream to provide the cooling for the natural gas in the MCHE to approximately -161 °C at atmospheric pressure. Afterwards, mixed refrigerant is completely vapourised from the outlet of the MCHE and then compressed by a series of compressors to its initial inlet conditions.

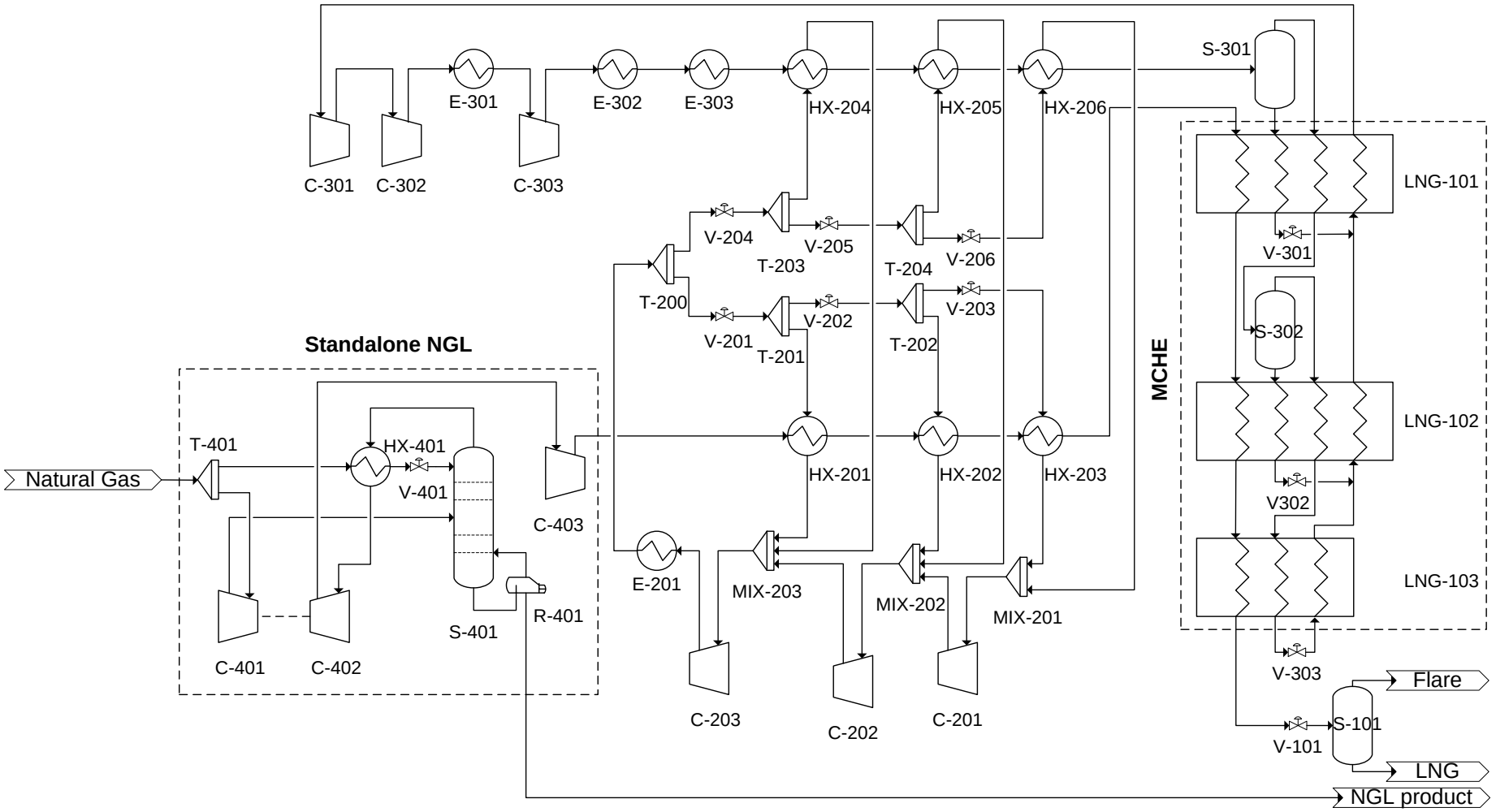

Figure 6-5 A frontend NGL recovery and C3MR process.

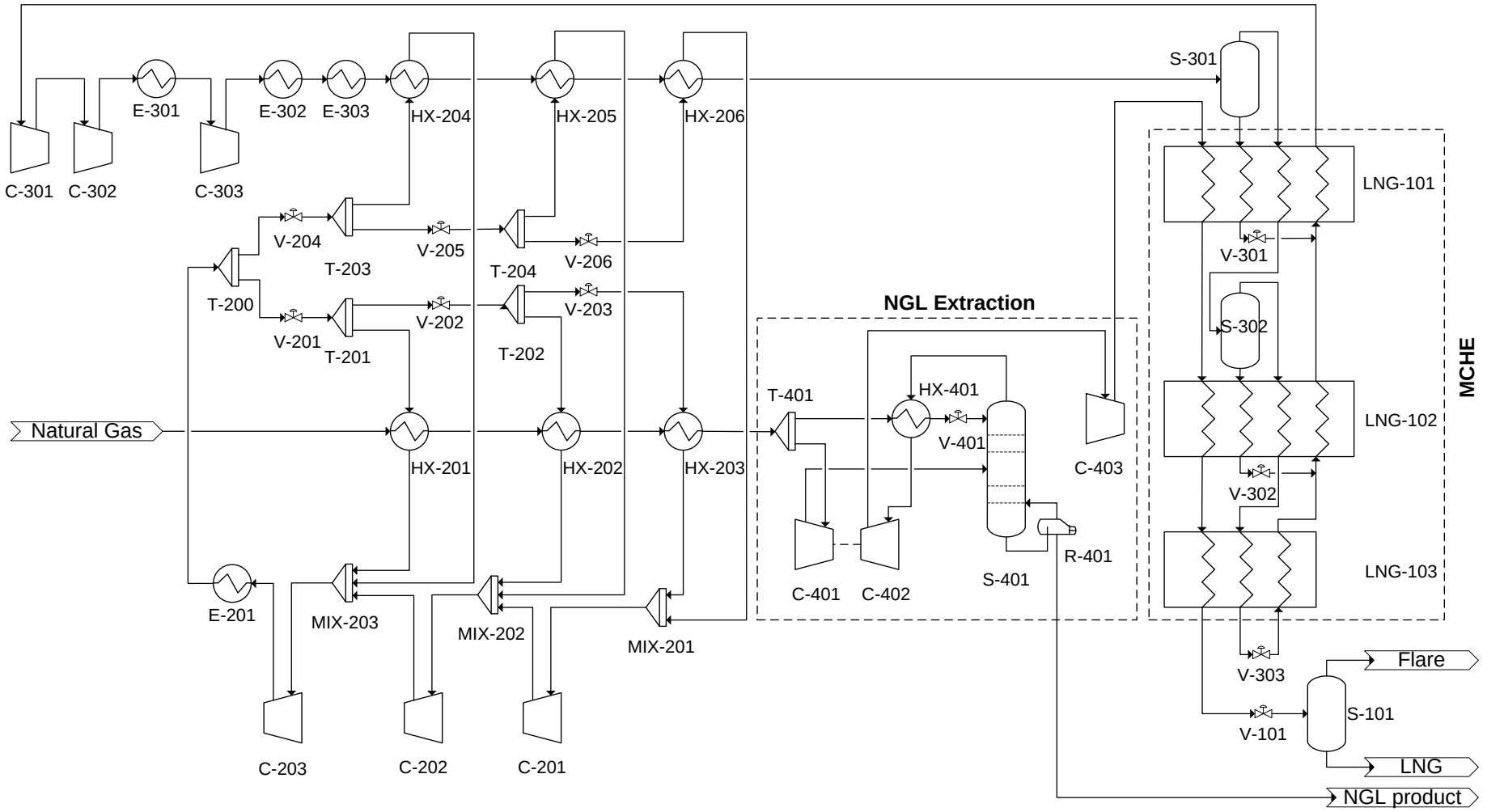

Figure 6-6 An integration of NGL recovery within the C3MR process.

Figure 6-6 shows the flow diagram of an integrated NGL recovery within the C3MR process (an integrated NGL/C3MR). It is an alternative configuration of Figure 6-5 in which NGL recovery is located at an intermediate location. Feed gas is precooled in a propane refrigerant cycle and then proceeds onto NGL recovery. The column overhead stream is liquefied and subcooled in the MCHE to produce LNG.

6.4.1 Scenario 1: Variation in the natural gas composition

Figure 6-7 shows the effect of supplying natural gas with different compositions on the specific shaft work and specific OPEX. The results for these NGL/C3MR processes are summarised in Table 6-6 and Table 6-7. Table 6-1 describes the six different compositions of natural gas used herein. The mole fraction of methane in natural gas was adjusted from its base value of 96.92% to 84.55% with 10% decrements of the component mole flow of methane, while maintaining the mole flow of the remaining components constant. For a given amount of feed gas, a decrease of 12.37mol% in the methane concentration results in the reduction of the specific shaft work by 0.175% for frontend NGL/C3MR, this is in contrast to the 0.74% increase for an integrated NGL/C3MR. However, frontend NGL/C3MR obtained 38.3% savings in specific OPEX, while 21.4% was obtained for an integrated NGL/C3MR. When the methane concentration in natural gas exceeds 95%, both processes have almost equivalent specific OPEX values. In summary, both processes are more preferable to operate with natural gas of high methane content. In contrast, an integrated NGL/C3MR is more preferable for gas with low methane content.

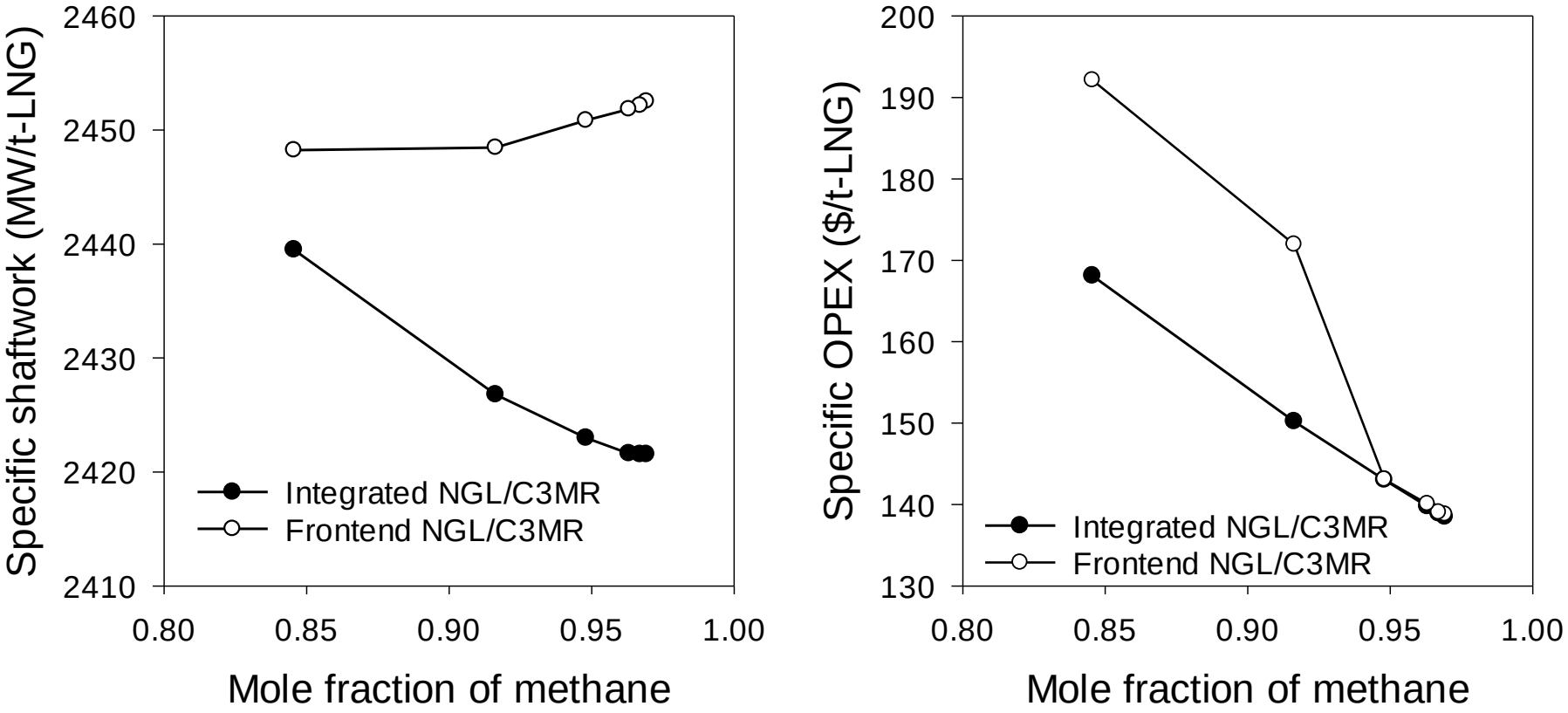

Figure 6-7 The effect of feed gas composition change on specific shaft work and specific OPEX (T = 25 °C and P = 5000 kPa).

Table 6-6 Results for a frontend NGL/C3MR process with varying feed gas composition.

Variables	Unit	Base case	NG1	NG2	NG3	NG4	NG5
Natural gas							
Methane	%mol	96.92	96.70	96.31	94.80	91.63	84.55
Feed mass flow	kg/h	399,000	399,000	399,000	399,000	399,000	399,000
LNG production	kg/h	349,889	349,172	345,854	336,755	269,010	235,903
Mixed refrigerant							
Refrigerant flow	kmol/h	68,346	68,060	67,533	55,662	52,423	45,967
Refrigerant pressure	kPa	2630	2630	2630	2630	2630	2630
Energy consumption							
Total shaft work	MW	238.4	237.8	235.5	229.3	183.0	160.4
Specific shaft work	MJ/tonne-LNG	2452.5	2452.2	2451.8	2450.9	2448.5	2448.2
Specific OPEX	$/tonne-LNG	138.81	139.03	140.09	143.09	171.95	192.12

Table 6-7 Results for an integrated NGL/C3MR process with varying feed gas composition.

Variables	Unit	Base case	NG1	NG2	NG3	NG4	NG5
Natural gas							
Methane	%mol	96.92	96.70	96.31	94.80	91.63	84.55
Feed mass flow	kg/h	399,000	399,000	399,000	399,000	399,000	399,000
LNG production	kg/h	349,913	348,542	345,922	336,155	316,524	276,358
Mixed refrigerant							
Refrigerant flow	kmol/h	68,340	68,063	67,534	65,598	61,734	53,904
Refrigerant pressure	kPa	2630	2630	2630	2630	2630	2630
Energy consumption							
Total shaft work	MW	235.4	234.4	232.7	226.3	213.4	187.3
Specific shaft work	MJ/tonne-LNG	2421.6	2421.6	2421.6	2423.0	2426.8	2439.5
Specific OPEX	$/tonne-LNG	138.49	138.92	139.76	143.02	150.20	168.10

Table 6-8 Results for a frontend NGL/C3MR process with varying feed gas flow rates.

Variables	**Unit**	**Base case**	**Flow 1**	**Flow 2**	**Flow 3**	**Flow 4**
Natural gas						
Methane	%mol	96.92	96.92	96.92	96.92	96.92
Feed mass flow	kg/h	399,000	379,050	359,100	339,150	319,200
LNG production	kg/h	349,890	332,439	314,900	297,406	279,911
Mixed refrigerant						
Refrigerant flow	kmol/h	68,347	64,844	61,361	57,929	54,514
Refrigerant pressure	kPa	2630	2630	2630	2630	2630
Energy consumption						
Total shaft work	MW	227.9	216.3	204.7	193.2	181.9
Specific shaft work	MJ/tonne-LNG	2344.5	2341.9	2339.9	2339.2	2338.2
Specific OPEX	$/tonne-LNG	137.48	143.25	149.70	156.91	165.02

Table 6-9 Results for an integrated NGL/C3MR process with varying feed gas flow rates.

Variables	**Unit**	**Base case**	**Flow 1**	**Flow 2**	**Flow 3**	**Flow 4**
Natural gas						
Methane	%mol	96.92	96.92	96.92	96.92	96.92
Feed mass flow	kg/h	399,000	379,050	359,100	339,150	319,200
LNG production	kg/h	349,913	332,461	314,921	297,426	279,930
Mixed refrigerant						
Refrigerant flow	kmol/h	68,340	64,845	61,372	57,940	54,520
Refrigerant pressure	kPa	2630	2630	2630	2630	2630
Energy consumption						
Total shaft work	MW	228.3	216.7	205.2	193.7	182.3
Specific shaft work	MJ/tonne-LNG	2349.2	2346.8	2345.3	2344.6	2344.1
Specific OPEX	$/tonne-LNG	137.53	143.30	149.75	156.96	165.08

6.4.2 Scenario 2: Variation in the feed gas flow rate

Based on the sensitivity study discussed in Section 6.3, the feed gas flow rate alternates from its base value of 3.990×10^5 kg/h to 3.129×10^5 kg/h with 5% decrements. Figure 6-8 illustrates that overall power consumption decreases with fixed *UA*, for natural gas flow rate decreases from 3.990×10^5 kg/h to 3.129×10^5 kg/h. The integrated NGL/C3MR requires a 1.26% less specific shaft work than a frontend NGL/C3MR. However, specific OPEX increases from \$138.5/tonne-LNG to \$166.0/tonne-LNG for an integrated NGL/C3MR and from \$138.8/tonne-LNG to \$166.4/tonne-LNG for a frontend NGL/C3MR given that natural gas flow rate decreases at a fixed *UA*. It is clear that this is slightly less than the specific OPEX of a frontend NGL. The decline in the natural gas flow rate with a constant composition requires a 19.9% less specific OPEX for both processes (Table 6-8 and Table 6-9).

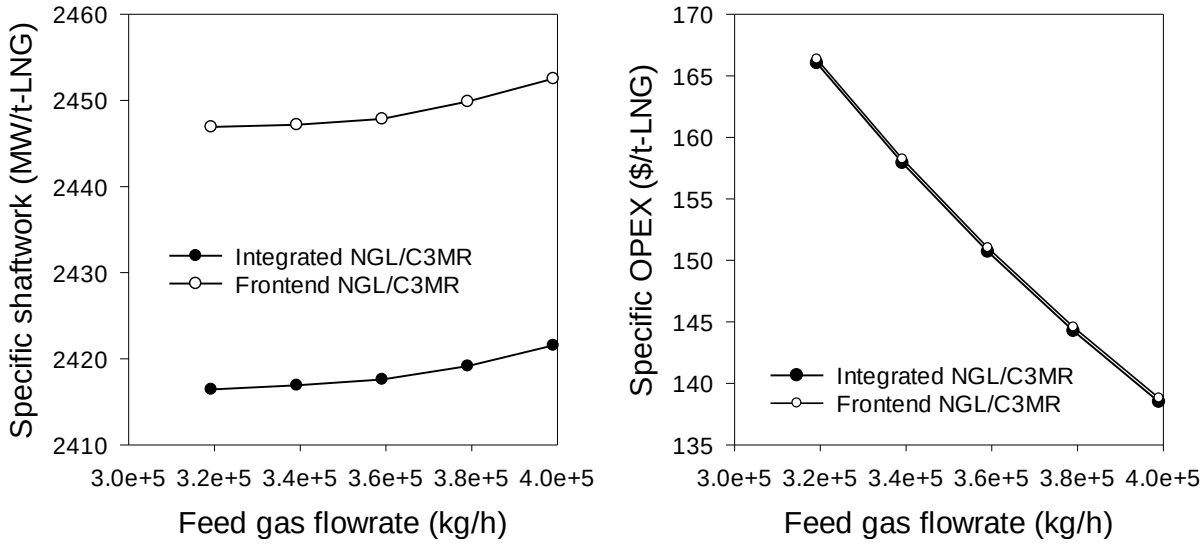

Figure 6-8 The effect of feed gas flow rate change on specific shaft work and specific OPEX (T = 25 °C and P = 5000 kPa).

6.4.3 Scenario 3: Variation in the splitting flow ratio of feed gas

Figure 6-9 shows the effect of the gas splitting ratio to the column bottom stream (T-401 to C-401) on specific shaft work and specific OPEX. This variation has a trivial effect on specific shaft work and specific OPEX for both configurations. The specific shaft work

remains constant for frontend NGL/C3MR and integrated NGL/C3MR when the splitting flow ratio increases. It is apparent that integrated NGL/C3MR provides a greater efficiency in energy consumption which is 1.25% less than that of frontend NGL/C3MR in order to produce the same amount of LNG.

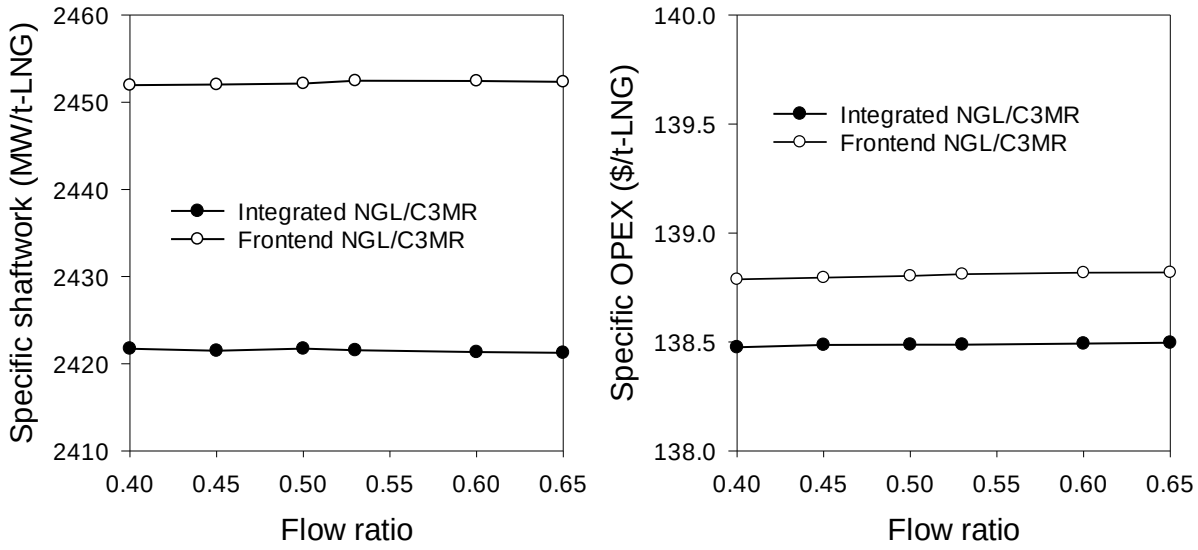

Figure 6-9 The effect of the gas splitting ratio change on specific shaft work and specific OPEX (T = 25 °C and P = 5000 kPa).

6.5 Conclusions

This chapter investigated the effects of varying the inlet natural gas conditions of an existing LNG plant (i.e. with a constant *UA* value).

In Case 1, the findings from this study were that variations in feed natural gas composition, pressure, and flow rate have more refrigeration effect than feed temperature for a given feed flow rate. With a reduction in the feed gas flow rate over time, the overall shaft work declines. However, the specific energy requirement per unit weight of LNG product increases translating into higher production costs.

In Case 2, it was revealed that variation in the feed gas compositions and flow rate have more refrigeration effect than gas splitting ratio for an NGL/C3MR plant (i.e. with a constant *UA*

value). With reduction in feed gas composition over time, the specific shaft work of a frontend NGL/C3MR declines, however the specific shaft work of an integrated NGL/C3MR increases. Nevertheless, the two processes are favourable for the removal of heavier hydrocarbons from natural gas of high methane content.

CHAPTER 7. CONCLUSIONS AND FUTURE RECOMMENDATIONS

This chapter briefly summarises the key findings of our research and also presents recommendations for future work. The detailed conclusions of our work are presented in each respective chapter.

7.1 Conclusions

This study has addressed the LNG optimisation with the aim of minimising energy consumption and cost. Our main findings have highlighted the impacts of the optimisation formulation on the LNG process. Several factors potentially affect the optimal results, which include the formulation of objective functions, the selection of the design variables, and the constraints. The adequate formulation of the objective function was found to create a significant improvement in the overall process performance.

Design optimisation determines the design variables that lead to achieving the optimal performance of an LNG process. In this study, the objectives of the design problem were to attain energy and cost savings from the LNG processes. In order to obtain the optimal results, it was suggested to consider the heat exchanger size (*UA*) and shaft work (*W*) in the objective function for the design. However, there is a trade-off between capital cost and operating cost. A formulation of an economic function was then proposed which could provide an efficient solution to resolve the conflicting objectives. The cost function is expressed in the form of *UA* and *W*. The optimal results of OF2 and OF3 illustrated that C3MR shows a decrease in specific shaft work while a relatively higher *UA* than the baseline values. The formulation of these cost functions is feasible for the given cost distribution and equipment size.

In addition, several uncertainties, such as equipment prices and equipment size, influence the coefficients of the design variables in the function. The findings from the sensitivity analysis

show that variations in equipment cost of the liquefaction plant (β_f) have an impact on the optimal results. OF4 was suggested to be the best function for design.

The total shaft work and exergy efficiency were considered the best objective functions of operation optimisation. The *UA* value of MCHE was specified at 13.31 MW/°C. Exergy efficiency as an objective function produces the most optimal result for C3MR in which the lowest specific shaft work was 1469 MJ/tonne-LNG.

Similar findings were also obtained from the operation optimisation where a conflict between heat exchanger size and shaft work existed. The heat exchanger size determines the capital cost of the LNG process, while an increase in its size allows for the reduction in energy consumption. When the *UA* value of the heat exchanger increase 13.31 MW/°C to 220.7 MW/°C at a constant flow rate of natural gas, it results in a 28% decrease in specific shaft work. These results were investigated via the sensitivity analysis. The exergy analysis reveals that a major contribution to the exergy loss is associated with both the compression system and MCHE.

As aforementioned in Section 5.5, a practical comparison of our optimal results with those of the literature should consider the factors which may significantly contribute to the power consumption. These factors are feed gas conditions (methane content, flow rate, pressure and temperature), LNG production, and *UA* of MCHE.

As the feed gas condition varies over time, an additional study presents the effects of varying the inlet natural gas conditions on the operation of a C3MR process (i.e. with a constant *UA*). It shows that the methane content of natural gas, pressure and flow rate have a greater refrigeration effect on the overall shaft work. In practice, NGL recovery processes are built in some LNG plants. By integrating an NGL recovery into the C3MR process, an integrated

NGL/C3MR is more suitable for liquefying natural gas with high methane content than a frontend NGL/C3MR. As the methane content in natural gas increases, the specific shaft work of an integrated NGL/C3MR decreases. When natural gas contains more than 95% methane, both processes show almost equivalent specific OPEX, though, the specific shaft work of a frontend NGL/C3MR increases.

7.2 Future work

The objective of optimisation is to find the best solution of a constrained optimisation problem. The optimisation problem of the LNG process is nonlinear. The optimal results should be global optima rather than local optima. However, global optima cannot be guaranteed. To find the global optimum, it is of high importance to select the appropriate starting point and optimisation algorithm for the optimisation. Initially, a number of mixed refrigerant compositions can be used as the starting points for the LNG processes. The mixed refrigerant composition is the key factor influencing the energy consumption, operating parameters and equipment size design. It may be in presence of multiple local optima, leading to the more difficult and complex to solve the optimisation problems. Secondly, the optimiser tool in Aspen HYSYS® can be used to search for global optima in the constrained region. Nevertheless, it has a limited number of optimisation algorithms as reviewed in Section 2.4.2. It is therefore recommended to formulate the global optimisation algorithm in Microsoft® VBA or MATLAB® and then interface with Aspen HYSYS®.

It is also suggested to develop a dynamic model of the C3MR process. This would aid in the analysis and verification of the predefined steady-state optimal conditions in a dynamic environment. Additionally, reliable operation of LNG processes is dependent on the effective control system design. Due to the complexity of the LNG model, it is thus desirable to propose a simple and effective control structure and analyse how this process responds to

different disturbances and choices of controlled variables. The control performance, however, must be acceptable in the early stage of the steady-state design and economics, thus ensuring the reliable operation of the LNG plant with various ambient conditions and feed composition.

REFERENCES

ALABDULKAREM, A., MORTAZAVI, A., HWANG, Y., RADERMACHER, R. & ROGERS, P. 2011. Optimization of propane pre-cooled mixed refrigerant LNG plant. *Applied Thermal Engineering,* 31**,** 1091-1098.

ASPELUND, A., GUNDERSEN, T., MYKLEBUST, J., NOWAK, M. P. & TOMASGARD, A. 2010. An optimization-simulation model for a simple LNG process. *Computers & Chemical Engineering,* 34**,** 1606-1617.

ASPENTECH 2004. Aspen HYSYS® Operations Guide.

AVIDAN, A. A., GARDNER, R. E., NELSON, D. & BORRELI, E. N. 1997. LNG links remote supplies and markets. *Oil & Gas Journal.* Houston.

BARCLAY, M., DENTON, N. & WHEELER, F. 2005. Selecting Offshore LNG Processes. *LNG Journal***,** 34-36.

BARNÉS, F. J. & KING, C. J. 1974. Synthesis of cascade refrigeration and liquefaction systems. *Industrial and Engineering Chemistry: Process Design and Development,* 13**,** 421-433.

BAUCK JENSEN, J. & SKOGESTAD, S. 2009. Single-cycle mixed-fluid LNG process Part II: Optimal operation. *In:* HASSAN, E. A., REKLAITIS, G. V. R., MAHMOUD M. EL-HALWAGIA2 - HASSAN E. ALFADALA, G. V. R. R. & MAHMOUD, M. E.-H. (eds.) *Proceedings of the 1st Annual Gas Processing Symposium.* Amsterdam: Elsevier.

BEJAN, A., TSATSARONIS, G. & MORAN, M. J. 1996. *Thermal Design and Optimization,* Wiley.

BP 2017. BP Energy Outlook.

BRODYANSKY, V. M., SORIN, M. V. & GOFF, P. L. 1994. *The Efficiency of Industrial Processes: Exergy Analysis and Optimization*, Elsevier.

BRONFENBRENNER, J. C., PHILLARELLA, M. & SOLOMON, J. 2009. Selecting a suitable process. *Review the process technology options available for the liquefaction of natural gas.* USA: Air Products and Chemicals, Inc.

CAO, W.-S., LU, X.-S., LIN, W.-S. & GU, A.-Z. 2006. Parameter comparison of two small-scale natural gas liquefaction processes in skid-mounted packages. *Applied Thermal Engineering,* 26**,** 898-904.

CASTILLO, L. & DORAO, C. A. 2012. Consensual decision-making model based on game theory for LNG processes. *Energy Conversion and Management,* 64**,** 387-396.

CASTILLO, L. & DORAO, C. A. 2013a. On the conceptual design of pre-cooling stage of LNG plants using propane or an ethane/propane mixture. *Energy Conversion and Management,* 65**,** 140-146.

CASTILLO, L., MAJZOUB DAHOUK, M., DI SCIPIO, S. & DORAO, C. A. 2013b. Conceptual analysis of the precooling stage for LNG processes. *Energy Conversion and Management,* 66**,** 41-47.

ÇENGEL, Y. A. & BOLES, M. A. 2011. *Thermodynamics: An Engineering Approach,* New York, McGraw-Hill.

ÇENGEL, Y. A. & BOLES, M. A. 2011. *Thermodynamics : an engineering approach,* New York, NY, McGraw-Hill.

CHENG, W. B. & MAH, R. S. H. 1980. Interactive synthesis of cascade refrigeration systems. *Industrial & Engineering Chemistry Process Design and Development,* 19**,** 410-420.

CLEMENTINO, P., HANDAYA, S. A. & SUTRASNO, K. 2014. Thermodynamic Analysis for Liquefaction of Natural Gas Using the C3-MR Refrigeration Process. *International Journal of Chemical Engineering and Applications,* 5.

DEPARTMENT OF RESOURCES, ENERGY AND TOURISM. 2011. *Australian Liquefied Natural Gas* [Online]. Australian Government. Available: http://www.ret.gov.au/resources/upstream_petroleum/australian_liquefied_natural_gas/ [Accessed].

FINLAYSON, B. A. 2006. *Introduction to chemical engineering computing,* Hoboken, N.J., Wiley-Interscience.

FINN, A. J., TOMLINSON, H. L. & JOHNSON, G. L. April 1999. Developments in natural gas liquefaction. *Hydrocarbon Processing***,** 47-59.

FOUNTAIN, P. S. 2011. *Apparatus and method for optimizing a liquefied natural gas facility*. 11/708,957.

GETU, M., MAHADZIR, S., LONG, N. V. D. & LEE, M. 2013. Techno-economic analysis of potential natural gas liquid (NGL) recovery processes under variations of feed compositions. *Chemical Engineering Research and Design,* 91**,** 1272-1283.

HASAN, M. M. F., KARIMI, I. A., ALFADALA, H. & GROOTJANS, H. 2007. Modeling and simulation of main cryogenic heat exchanger in a base-load liquefied naturk gas plant. *In:* PLESU, V. & AGACHI, P. S. (eds.) *17th European symposium on computer aided process engineering.* Elsevier.

HASAN, M. M. F., KARIMI, I. A. & ALFADALA, H. E. 2009a. Optimizing Compressor Operations in an LNG Plant. *In:* HASSAN, E. A., REKLAITIS, G. V. R., MAHMOUD M. EL-HALWAGIA2 - HASSAN E. ALFADALA, G. V. R. R. & MAHMOUD, M. E.-H. (eds.) *Proceedings of the 1st Annual Gas Processing Symposium.* Amsterdam: Elsevier.

HASAN, M. M. F., KARIMI, I. A., ALFADALA, H. E. & GROOTJANS, H. 2009b. Operational modeling of multistream heat exchangers with phase changes. *AIChE Journal,* 55**,** 150-171.

HATCHER, P., KHALILPOUR, R. & ABBAS, A. 2012. Optimisation of LNG mixed-refrigerant processes considering operation and design objectives. *Computers & Chemical Engineering,* 41**,** 123-133.

HIRSCHHAUSEN, C. V., NEUMANN, A., RUESTER, D.-W.-I. S. & AUERSWALD, D. 2008. Advice on the Opportunity to Set up an Action Plan for the Promotion of

LNG Chain Investments Dresden: Dresden University of Technology

HUMPHREY, G. 2011. Current State & Outlook for the LNG Industry. Rice Global Engineering & Construction Forum.

HWANG, J.-H., ROH, M.-I. & LEE, K.-Y. 2013. Determination of the optimal operating conditions of the dual mixed refrigerant cycle for the LNG FPSO topside liquefaction process. *Computers & Chemical Engineering,* 49**,** 25-36.

JACOBSEN, M. G. & SKOGESTAD, S. 2013. Active constraint regions for a natural gas liquefaction process. *Journal of Natural Gas Science and Engineering,* 10**,** 8-13.

JAGER, M. D. & KAART, S. 2009. Method and apparatus for cooling a hydrocarbon stream. Google Patents.

JENSEN & JAMES, T. 2004. *The Development of a Global LNG Market. Is It Likely? If so, When?*, Oxford Institute for Energy Studies.

JENSEN, J. B. & SKOGESTAD, S. 2006. Optimal operation of a simple LNG process. *Proceedings Adchem***,** 241-247.

JENSEN, J. B. & SKOGESTAD, S. 2007a. Optimal operation of simple refrigeration cycles: Part I: Degrees of freedom and optimality of sub-cooling. *Computers & chemical engineering,* 31**,** 712-721.

JENSEN, J. B. & SKOGESTAD, S. 2007b. Optimal operation of simple refrigeration cycles: Part II: Selection of controlled variables. *Computers & Chemical Engineering,* 31**,** 1590-1601.

JENSEN, J. B. & SKOGESTAD, S. 2008. Problems with Specifying ΔTmin in the Design of Processes with Heat Exchangers. *Industrial & Engineering Chemistry Research,* 47**,** 3071-3075.

JENSEN, J. B. & SKOGESTAD, S. 2009a. Single-cycle mixed-fluid LNG process Part I: Optimal design. *1st Annual Gas Processing Symposium***,** 10-12.

JENSEN, J. B. & SKOGESTAD, S. 2009b. Single-cycle mixed-fluid LNG process Part II: Optimal operation. *1st Annual Gas Processing Symposium***,** 10-12.

KHAN, M. S., CHANIAGO, Y. D., GETU, M. & LEE, M. 2014. Energy saving opportunities in integrated NGL/LNG schemes exploiting: Thermal-coupling common-utilities and process knowledge. *Chemical Engineering and Processing: Process Intensification,* 82**,** 54-64.

KHAN, M. S. & LEE, M. 2013a. Design optimization of single mixed refrigerant natural gas liquefaction process using the particle swarm paradigm with nonlinear constraints. *Energy,* 49**,** 146-155.

KHAN, M. S., LEE, S. & LEE, M. 2012. Optimization of single mixed refrigerant natural gas liquefaction plant with nonlinear programming. *Asia-Pacific Journal of Chemical Engineering,* 7**,** S62-S70.

KHAN, M. S., LEE, S., RANGAIAH, G. P. & LEE, M. 2013b. Knowledge based decision making method for the selection of mixed refrigerant systems for energy efficient LNG processes. *Applied Energy,* 111**,** 1018-1031.

KIDNAY, A. J. & PARRISH, W. R. 2006. *Fundamentals of Natural Gas Processing,* CRC Press.

KLINKENBIJL, J. M., DILLON, M. L. & HEYMAN, M. C. 1999. Gas Pre-Treatment and their Impact on Liquefaction Processes. *GPA Nashville TE meeting.* Amsterdam: Shell Internantional Oil Products Research & Technology Centre.

KOTAS, T. J. 1980. Exergy criteria of performance for thermal plant: Second of two papers on exergy techniques in thermal plant analysis. *International Journal of Heat and Fluid Flow,* 2**,** 147-163.

LEE, G. C., SMITH, R. & ZHU, X. X. 2002. Optimal Synthesis of Mixed-Refrigerant Systems for Low-Temperature Processes. *Industrial & Engineering Chemistry Research,* 41**,** 5016-5028.

LIM, W., CHOI, K. & MOON, I. 2012. Current Status and Perspectives of Liquefied Natural Gas (LNG) Plant Design. *Industrial & Engineering Chemistry Research,* 52**,** 3065-3088.

MAK, J. & GRAHAM, C. 2013. Configurations and methods of integrated ngl recovery and lng liquefaction. Google Patents.

MARMOLEJO-CORREA, D. & GUNDERSEN, T. 2012. A comparison of exergy efficiency definitions with focus on low temperature processes. *Energy,* 44**,** 477-489.

MOKARIZADEH HAGHIGHI SHIRAZI, M. & MOWLA, D. 2010. Energy optimization for liquefaction process of natural gas in peak shaving plant. *Energy,* 35**,** 2878-2885.

MOKHATAB, S., MAK, J. Y., VALAPPIL, J. V. & WOOD, D. A. 2013. *Handbook of Liquefied Natural Gas,* Elsevier Science.

MOKHATAB, S. & POE, W. A. 2012. *Handbook of Natural Gas Transmission and Processing,* Elsevier Science.

NARAYANAN, K. V. 2004. *A Textbook Of Chemical Engineering Thermodynamics,* Prentice-Hall of India.

NOGAL, F. D., KIM, J.-K., PERRY, S. & SMITH, R. 2008. Optimal Design of Mixed Refrigerant Cycles. *Industrial & Engineering Chemistry Research,* 47**,** 8724-8740.

PARADOWSKI, H., BAMBA, M. & BLADANET, C. 2004. Propane Pecooling Cycles for Increased LNG Train Capacity. *14th International Conference and Exhibition on Liquefied Natural Gas.*

PARK, J. H., KHAN, M. S., ANDIKA, R., GETU, M., BAHADORI, A. & LEE, M. 2014. Techno-economic evaluation of a novel NGL recovery scheme with nine patented schemes for offshore applications. *Journal of Natural Gas Science and Engineering*.

REMELJEJ, C. W. & HOADLEY, A. F. A. 2006. An exergy analysis of small-scale liquefied natural gas (LNG) liquefaction processes. *Energy,* 31**,** 2005-2019.

SHAH, N., RANGAIAH, G. P. & HOADLEY, A. 2009. Multi-Objective Optimization: Techniques and Applications in Chemical Engineering. *In:* RANGAIAH, G. P. (ed.). World Scientific Publishing Company, Incorporated.

SHAH, N. M. & RANGAIAH, G. P. 2007. Multi-objective optimization of the dual independent expander gas-phase refrigeration process for LNG. *AIChE annual meeting.* Salt Lake City, UT, USA.

SHIRAZI, M. M. H. & MOWLA, D. 2010. Energy optimization for liquefaction process of natural gas in peak shaving plant. *Energy,* 35**,** 2878-2885.

SHUKRI, T. 2004. LNG Technology Selection. *Hydrocarbon Engineering.*

SMAAL, A. 2003. Liquefaction Plants: Development of Technology and Innovation, Working Committee Contribution. *22nd World Gas Conference.* Tokyo.

SUSAN, L. & SAKMAR, J. 2010. Environmental Sustainability and the Role of LNG in a Carbon Constrained World. *In:* BENYAHIA, F. & ELJACK, F. T. (eds.) *Proceedings of the 2nd Annual Gas Processing Symposium.* USA: Elsevier.

SZARGUT, J., MORRIS, D. R. & STEWARD, F. R. 1988. *Exergy analysis of thermal, chemical, and metallurgical processes,* Hemisphere Publishing Corporation.

TARIQ, S. & WHEELER, F. 2004. *LNG technology selection,* Farnham, ROYAUME-UNI, Palladian Publications.

TURTON, R., BAILIE, R. C. & WHITING, W. B. 2009. *Analysis, synthesis, and design of chemical processes,* Prentice Hall.

TUSIANI, M. D. & SHEARER, G. 2007. *Lng: A Nontechnical Guide,* PennWell Corporation.

VAIDYARAMAN, S. & MARANAS, C. D. 1999. Optimal synthesis of refrigeration cycles and selection of refrigerants. *AIChE Journal,* 45**,** 997-1017.

VAIDYARAMAN, S. & MARANAS, C. D. 2002. Synthesis of Mixed Refrigerant Cascade Cycles. *Chemical Engineering Communications,* 189**,** 1057-1078.

VENKATARATHNAM, G. 2008. *Cryogenic Mixed Refrigerant Processes,* Springer.

VENKATARATHNAM, G. 2010. *Cryogenic Mixed Refrigerant Processes,* Springer.

VINK, K. J. & NAGELVOORT, R. K. 1998. Comparison of Baseload Liquefaction Processes. *LNG12.*

WAHL, P. E., LØVSETH, S. W. & MØLNVIK, M. J. 2013. Optimization of a simple LNG process using sequential quadratic programming. *Computers & Chemical Engineering,* 56**,** 27-36.

WANG, M., KHALILPOUR, R. & ABBAS, A. 2013. Operation optimization of propane precooled mixed refrigerant processes. *Journal of Natural Gas Science and Engineering,* 15**,** 93-105.

WANG, M., ZHANG, J. & XU, Q. 2012. Optimal design and operation of a C3MR refrigeration system for natural gas liquefaction. *Computers & Chemical Engineering,* 39**,** 84-95.

WANG, M., ZHANG, J., XU, Q. & LI, K. 2011. Thermodynamic-Analysis-Based Energy Consumption Minimization for Natural Gas Liquefaction. *Industrial & Engineering Chemistry Research,* 50**,** 12630-12640.

WINNICK, J. 1997. *Chemical engineering thermodynamics : an introduction to thermodynamics for undergraduate engineering students,* New York, Wiley.

YIN, Q. S., LI, H. Y., FAN, Q. H. & JIA, L. X. 2008. ECONOMIC ANALYSIS OF MIXED-REFRIGERANT CYCLE AND NITROGEN EXPANDER CYCLE IN SMALL SCALE NATURAL GAS LIQUEFIER. *AIP Conference Proceedings,* 985**,** 1159-1165.

APPENDIX A LIST OF GLOBAL LNG PLANTS

Location	Start-up	Trains	Train Capacity (MTPA)	Liquefaction Technology	Project
Abu Dhabi	1977	2	1.7	AP-C3MR™	Das Island I Trains 1-2
	1994	1	2.6	AP-C3MR™	Das Island II Trains 3
Algeria	1977	6	1.3	AP-C3MR™	Arzew GL1Z
	1981	6	1.4	AP-C3MR™	Arzew GL2Z
	2014	1	4.7	AP-C3MR/SplitMR®	Arzew GL3Z
	2013	1	4.5	AP-C3MR/SplitMR®	Skikda
Angola	2012	1	5.2	ConocoPhillips Optimised Cascade®	Angola LNG
Australia	1989	3	2.5	AP-C3MR™	NWS
	1989	2	2.5	AP-C3MR™	North West Shelf T1&2
	1994	1	2.5	AP-C3MR™	North West Shelf T3
	2004	1	4.6	AP-C3MR™	North West Shelf T4
	2005	1	3.7	ConocoPhillips Optimised Cascade®	Darwin LNG
	2008	1	4.6	AP-C3MR™	North West Shelf T5
	2014	2	4.25	ConocoPhillips Optimised Cascade®	Queensland Curtis LNG
	2015	2	3.9	ConocoPhillips Optimised Cascade®	Gladestone LNG
	2016	3	5	AP-C3MR/SplitMR®	Gorgon LNG T1-3
	2017	2	4.2	AP-C3MR/SplitMR®	Ichthys
	2017	2	4.45	ConocoPhillips Optimised Cascade®	Wheatstone LNG
Brunei	1972	5	1.3	AP-C3MR™	Brunei LNG T1-5
Egypt	2004	1	5	AP-C3MR/SplitMR®	SEGAS
	2005	2	3.6	ConocoPhillips Optimised Cascade®	Egyptian LNG
Equatorial Guinea	2007	1	3.7	ConocoPhillips Optimised Cascade®	Equatorial Guinea LNG
Indonesia	1977	7	2.6	AP-C3MR™	Bontang
	1999	1	3	AP-C3MR™	Bontang
	1978	6	2	AP-C3MR™	Arun
	2009	3	3.8	AP-C3MR/SplitMR®	Tangguh LNG
	2015	1	2.1	AP-C3MR™	Donggi
Malaysia	1982	3	2.5	AP-C3MR™	Satu

	1995	3	2.8	AP-C3MR™	Dua
	2003	2	3.8	AP-C3MR™	Tiga
	2016	1	3.6	AP-C3MR™	Petronas 9
Nigeria	1999	3	3.2	AP-C3MR™	Bonny Island
	2005	3	3.7	AP-C3MR™	Bonny Island
Norway	2007	1	4.2	Linde MFC®	Snøhvit LNG
Oman	2000	3	3.3	AP-C3MR™	Oman LNG
Papau New Guinea	2014	2	3.3	AP-C3MR™	PNG LNG T1&2
Peru	2010	1	4	AP-C3MR/SplitMR®	Peru LNG
Qatar	1996	3	3.3	AP-C3MR™	Qatargas
	2009	4	7.8	AP-X®	Qatargas
	1999	2	3.3	AP-C3MR™	Rasgas
	2004	3	4.7	AP-C3MR/SplitMR®	Rasgas
	2009	2	7.8	AP-X®	Rasgas
Russia	2009	1	4.6	Shell® DMR	Sakhalin 2 (T1)
	2009	1	4.8	Shell® DMR	Sakhalin 2 (T2)
Trinidad and Tobago	1999	1	3	ConocoPhillips Optimised Cascade®	Atlantic LNG
	2002	2	3.3	ConocoPhillips Optimised Cascade®	Atlantic LNG
	2005	1	5.2	ConocoPhillips Optimised Cascade®	Atlantic LNG
Russia	2018	3	5.5	AP-C3MR™	Yamal
United States	1969	1	1.5	ConocoPhillips Optimised Cascade®	Kenai LNG
	2016	2	4.5	ConocoPhillips Optimised Cascade®	Sabine Pass Liquefaction T1&2
	2017	2	4.5	ConocoPhillips Optimised Cascade®	Sabine Pass Liquefaction T3&4
	2019	1	4.5	ConocoPhillips Optimised Cascade®	Sabine Pass Liquefaction T5
	2017	1	5.25	AP-C3MR™	Cove Point
	2018	3	4.4	AP-C3MR™	Freeport
	2018	3	4.4	AP-C3MR/SplitMR®	Cameron
	2018	2	4.5	ConocoPhillips Optimised Cascade®	Corpus Christi LNG
Yemen	2009	2	3.4	AP-C3MR/SplitMR®	Bal-Haf

APPENDIX B CAPITAL COST ESTIMATION

Appendix B presents the detailed derivation of the preliminary cost equations in Section 4.2.2. Capital investment of main equipment in Table 0-1 (Yin et al., 2008).

Table 0-1 Capital cost distribution of an LNG plant's main equipment.

Item	**Million RMB**	β_f **(%)**
Cold box (including pipeline, heat exchangers)	2.30	37.70
Compression system	1.50	24.59
Instrument and control system	1.40	22.95
Assistant equipment	0.70	11.48
Mixed refrigerant confection system	0.20	3.28
Sum	6.1	100

Scaling factor method

The capital cost of the cold box can be estimated via the scaling factor method. The equivalent cost of the cold box for a 3 MTPA (million tonne per annum) plant can be found via Eq 0-1.

$$Cost_a = \left(\frac{Size_a}{Size_b} \right)^y Cost_b \qquad \text{Eq. 0-1}$$

where, $Cost_a$ and $Cost_b$ are the equivalent capital costs of the cold box for an estimated plant capacity and that of the reference unit, respectively; $Size_a$ and $Size_b$ are the size of the cold box for an estimated plant and that of the reference unit, respectively; y is the scaling exponent.

The total capital investment (*TCI*) is estimated via Eq.0-2.

$$TCI = \sum_{f=1}^{m} C_f \left(\frac{X}{X_0} \right) \quad \text{Eq. 0-2}$$

where, *TCI* is total capital investments ($), *X* is the estimated plant capacity (MTPA), X_0 is the basis reference of plant capacity (MTPA), C_f is the equipment cost of an LNG plant for equipment type *f* ($).

Thus, the individual equipment cost (Eq.0-3) is derived from Eq.0-2. This equation is also used in Eq. 4-2.

$$C_f = \alpha_f \left(\frac{X}{X_0} \right) TCI_0 \quad \text{Eq. 0-3}$$

where, TCI_0 is a baseline value for the total capital investment of an LNG plant , α_f is the percentage of the equipment cost of an LNG value chain which is expressed in Eq. 0-4.

$$\alpha_f = \lambda \beta_f \quad \text{Eq. 0-4}$$

where, λ is the percentage of the capital cost of an LNG plant over the total cost of an LNG value chain, β_f is the percentage of the component cost of an LNG plant over the total capital cost of an LNG plant, β_f values are shown in Table 0-1.

Capital cost

Assume total capital investment (TCI_0) of an LNG plant is $3 billion for a train capacity of 3 MTPA.

$$C_{MCHE} = \left(\alpha_1 \frac{\sum_{t=1}^{k} UA_t}{UA_0} \right) \left(\frac{X}{X_0} \right) TCI_0 \quad \text{Eq. 0-5}$$

$$TCI = \left(\alpha_1 \frac{UA}{UA_0} + \alpha_2 \frac{W}{W_0} + \alpha_3 + \alpha_4 \right) \left(\frac{x}{3} \right) TCI_0 \qquad \text{Eq. 0-6}$$

Assume the λ value is 25%,

$C_f = 0.25 TCI_0 \times \beta_f$

According to the β_f values in Table 0-1, the capital cost of the cold box ($C_{coldbox}$) is

$C_{coldbox} = 0.25 TCI_0 \times 0.377$, thus $\alpha_1 = 0.09425$

The capital cost of the compressors ($C_{compressor}$) is

$C_{compressor} = 0.25 TCI_0 \times 0.2459$, thus $\alpha_2 = 0.061475$

The capital cost of the utility system ($C_{utility}$) is

$C_{utility} = TCI_0 \times (25\% - 9.425\% - 6.1475\%)$, thus $\alpha_3 = 0.094275$

The capital cost of others in the LNG value chain (C_{others}) is

$C_{others} = TCI_0 \times (1 - 0.25)$, thus $\alpha_4 = 0.75$

Given that the major costs of an LNG plant are the energy consumption in the process operation and the purchased equipment, and according to the capital cost distribution of main equipment for mixed refrigerant cycles given by Yin *et al*. (2008) in Table 0-1, Eq.0-5 can be formulated as a function of *UA* and reference UA_0 as the following:

$$TCI = \left(0.09425 \frac{UA}{UA_0} + 0.061475 \frac{W}{W_0} + 0.094275 + 0.75 \right) \left(\frac{x}{3} \right) TCI_0 \qquad \text{Eq. 0-7}$$

The equation for the capital cost of MCHE (C_{MCHE}) is defined as a function of reference UA_0 value written as below:

where, UA_t is the overall heat transfer coefficient and area at MCHE$_t$ in this study (MW/°C), UA_0 is the reference value for MCHE obtained from the patent given by Jager et al. (2009), α_1 is the ratio of the capital cost of the cold box to the capital cost of the LNG value chain.

The derivation of the capital cost equation for the compressors (C_{comp}) is similar to the above. It is a function of the operating variable of W:

$$C_{comp} = \left(\alpha_2 \frac{\sum_{i=1}^{n} W_i}{W_0} \right) \left(\frac{X}{X_0} \right) TCI_0 \qquad \text{Eq. 0-8}$$

where, W_0 is the referenced shaft work obtained from the patent given by Jager et al. (2009), α_2 is the ratio of the capital cost of the compressors to the capital cost of the LNG value chain.

Then, the new equation for the total capital investment consisting of the key operating variable (W) and the design variable (the overall UA of MCHE) is represented below as:

$$TCI = \left(\alpha_1 \frac{\sum_{t=1}^{k} UA_t}{UA_0} + \alpha_2 \frac{\sum_{i=1}^{n} W_i}{W_0} + \alpha_3 + \alpha_4 + \alpha_5 + \alpha_6 \right) \left(\frac{X}{X_0} \right) TCI_0 \qquad \text{Eq. 0-9}$$

where, TCI is the total capital investment ($), α_3, α_4, α_5, and α_6 are the proportion of the capital cost of the instrument and control system, assistant equipment, construction engineering, and mixed refrigerant confection system in an LNG value chain, respectively.

The train capacity and equipment size can be scaled based on the reference data in Table 0-2. Substitute them into Eq. 0-10,

$$TCI = \left(0.09425 \frac{UA}{73.022} + 0.061475 \frac{W}{264.063} + 0.844275 \right) \left(\frac{x}{3} \right) TCI_{BaseCase} \qquad \text{Eq. 0-10}$$

The *TCI* is expressed as a unit of $billions:

$$TCI = \left(0.001291UA + 0.0002328W + 0.844275\right)\left(\frac{x}{3}\right)TCI_{BaseCase} \quad \text{Eq. 0-11}$$

Convert into $million:

$$TCI = \left(1.291UA + 0.2328W + 844.275\right)\left(\frac{x}{3}\right)TCI_{BaseCase} \quad \text{Eq. 0-12}$$

The areas of MCHE is 13.33MW/°C. Thus, the total annualised cost (*TAC*) is formulated below as:

$$TAC = 0.1TCI + C_{NG} + C_{UT} \quad \text{Eq. 0-13}$$

where, *TCI* is the total capital investments ($), *0.1TCI* is the depreciation cost ($/yr), C_{RM} is the capital cost of the raw materials ($/yr), C_{UT} is the capital cost of the utility ($/yr), *HPA* is 8760 hours per annum.

Table 0-2 MCHE areas and compressor duty at a certain LNG production.

	Unit	**Reference***
UA of MCHE cold bundle	MW/°C	13.082
UA of MCHE warm bundle	MW/°C	59.940
Overall *UA*	MW/°C	73.022
Molar flow of feed gas	kmol/h	62964
Precooling compressor duty	MW	86.863
Mixed refrigerant compressor duty	MW	177.2
Total compressor duty	MW	264.063

* Refer to Patent US 2009/0241593 A1

The capital cost of natural gas

$$C_{NG} = m_{NG} P_{NG} HPA \qquad \text{Eq. 0-14}$$

The capital cost of the utility

$$C_{UT} = P_{Electricity} W_s HPA + P_{cooling} QHPA \qquad \text{Eq. 0-15}$$

Therefore, the specific annual cost of the 3 MTPA C3MR process is given by

$$\text{Aunnual cost per tonne LNG} = \frac{\left(0.1TCI + C_{NG} + C_{UT}\right)}{x} \qquad \text{Eq. 0-16}$$

$$= \frac{1}{x}\left(0.1 \times \left(1.291UA + 0.2328W + 844.275\right)\left(\frac{x}{3}\right) TCI_{BaseCase} + m_{NG} P_{NG} HPA + P_{Electricity} W_s HPA + P_{cooling} QHPA \right)$$